

**PALAEOENVIRONMENTS
OF THE ESTCOURT FORMATION (BEAUFORT GROUP),
KWAZULU-NATAL.**

Dawn Green

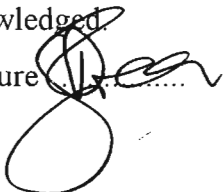
Department of Geology and Applied Geology,
University of Natal
Durban 4001

Submitted in partial fulfilment of the requirements for the degree of Masters in the
Department of Geology and Applied Geology of the University of Natal, 1997.

Declaration

I declare that this is my own unaided work except where referenced or suitably
acknowledged.

Signature



Date

26/3/98

ABSTRACT

At present the Karoo Basin covers approximately 20 000km². It is a large intracratonic basin which, from Carboniferous to Jurassic times, was infilled with a succession of sediments ranging from glacial deposits to those deposited in warm, equable conditions. The Beaufort Group forms part of this succession, and was deposited in a terrestrial, river dominated environment. The dominant lithologies exposed in the Estcourt region in the KwaZulu Natal Midlands belong to the lower and middle Beaufort divided by the Permo-Triassic boundary. The Permo-Triassic palaeoenvironment in this region is reconstructed using sedimentary profiles combined with the study of the fossil remains discovered in the area, including plant, body, and trace fossils.

The lower Beaufort sediments in this region belong to the Estcourt Formation, and the Middle Beaufort sediments to the Belmont Formation. The Estcourt Formation is dominated by a succession of alternating sandstones, siltstones and mudstones, which are interpreted as representing sediments deposited in a fluvial-floodplain environment, which can be divided into two sub-environments. The first is dominated by sediments that were deposited by meandering rivers on a semi-arid floodplain, and the second sub-environment is represented by those sediments deposited in lacustrine environments. Both of these sub-environments are closely linked and alternate in the rock record indicating many episodes of transgressive-regressive lacustrine episodes. The Estcourt Formation can be closely correlated with the lower Beaufort sediments mapped in other regions of the Karoo Basin, indicating similar climatic and environmental controls throughout the Karoo Basin of southern Africa.

The Estcourt Formation also contains a wide variety of body and trace fossils. The Permo-Triassic boundary can be traced along the western border of Estcourt by using the distribution pattern of the two mammal-like reptiles *Dicynodon* and *Lystrosaurus*. There is evidence of an overlap in the distribution between these two mammal-like reptiles, which together with palaeoflora evidence, indicates that *Lystrosaurus* evolved during the Late Permian and not Early Triassic as previously thought. The first Triassic sediments are represented in the Estcourt region by a series of maroon shales which can be correlated with the Palingkloof Member.

CONTENTS

	Page
Abstract	1
1 INTRODUCTION	4
1.1 Overview of project	4
1.2 The Karoo Supergroup	4
1.3 The Beaufort Group	5
2. THE SEDIMENTOLOGY OF THE BEAUFORT GROUP AROUND ESTCOURT	9
2.1 Location of study sections	9
2.2 Facies description and interpretation	14
2.2.1. Fluvial-floodplain facies association	14
2.2.2. Discussion of fluvial-floodplain facies associations	23
2.2.3. Lacustrine facies association	25
2.2.4. Interpretation and discussion of lacustrine facies association	29
3. THE VERTEBRATE PALAEOLOGY OF THE PERMO-TRIASSIC BEAUFORT SEDIMENTS OF THE ESTCOURT REGION	38
3.1 Introduction	38
3.1.1. The fossil assemblage of Estcourt	38
3.1.2. Work history	38
3.2 Record of therapsid fossils discovered in the Estcourt region	39
3.3 Discussion	45
4. PALAEOFLOTA OF THE PERMO-TRIASSIC BEAUFORT SEDIMENTS OF THE ESTCOURT REGION	47
4.1 Introduction	47
4.2 Description of fossil flora	47
4.3 Discussion	49
5. FOSSILISED INSECT IMPRESSIONS	52
6. PALAEOICHOLOGY OF THE PERMO-TRIASSIC BEAUFORT SEDIMENTS IN THE ESTCOURT REGION	54
6.1 Palaeoichnology of the Estcourt sediments (excluding tetrapod trackways)	54
6.1.1. Marginal lacustrine palaeoichnology	55

6.1.2. Basinal lacustrine palaeoichnology	55
6.1.3. Floodplain palaeoichnology	61
6.1.4. Miscellaneous ichnofossils	61
6.1.5. Discussion	61
6.2. Vertebrate tetrapod trackways	62
6.2.1. Introduction	62
6.2.2. Detailed description of trackways	63
6.2.3. Trackway comparison	95
6.2.4. Discussion	98
7. MORPHOLOGY OF MAMMAL-LIKE REPTILE TUSKS	104
7.1. Introduction	104
7.2. Analytical results	105
7.3. Development of teeth in mammals	105
7.4. Discussion	106
8. PALAEOENVIRONMENTAL RECONSTRUCTION	108
9. CONCLUSIONS	111
10. APPENDICES	113
Key to appendices 1 - 4	114
Appendix 1	115
Appendix 2	122
Appendix 3	147
Appendix 4	154
Appendix 5	159
Appendix 6	163
Appendix 7	165
11. ACKNOWLEDGMENTS	181
12. REFERENCES	182

1. INTRODUCTION

1.1 Overview of Project

In 1991, Mr. David Green contacted Professor T. Mason of the University of Natal, in connection with fossils located on his farm Rensburgspruit, in the KwaZulu-Natal Midlands. This contact sparked off interest in the fossils and sedimentary rocks of the regions surrounding Estcourt, and in 1992 led to the author carrying out a detailed sedimentological investigation. The results of this study are reported here. The strata of this region in the KwaZulu-Natal Midlands, are of Permo-Triassic age and form part of the Beaufort Group. The Beaufort Group has been the subject of intense investigation in the southern and eastern parts of the Karoo Basin, with little work reported from the northern Karoo basin (Smith, 1990a). The aim of this project is to reconstruct the Permo-Triassic palaeoenvironment using the sedimentary profiles to ascertain the type of depositional environment, and the fossil remains to reconstruct the palaeoecology of the region. This thesis therefore fills an important gap in the depositional history of the Beaufort Group, and gives a more complete view of the palaeoenvironments in the Karoo Basin during Beaufort times.

1.2 The Karoo Supergroup

The Beaufort Group forms part of the thick continental deposits comprising the Karoo Supergroup (Yemane et al, 1989). Deposition of the Karoo Supergroup spans roughly 100 million years from Late Carboniferous (300 Ma) through to Early Jurassic (180 Ma) (Johnson *et al.*, 1996; Yemane *et al.*, 1989; Smith, 1990a).

The intracratonic Karoo Basin of southern Africa contains the most complete stratigraphic record of the Karoo Supergroup (Smith et al, 1993), and forms the richest collecting grounds for mammal-like reptiles in the world (Smith, 1990a). The Karoo succession encompasses the Dwyka, Ecca, Beaufort Groups, and the Molteno, Elliot, and Clarens Formations, topped by volcanics of the Drakensberg Group. Sedimentary environments range from glacial, marine, fluvial, lacustrine, and aeolian (Yemane et al, 1989). Climate changed through the 100 million years of basin infilling from the period of glaciation

encompassing the Dwyka Group, through to the cool climatic conditions of the Ecca, becoming semi-arid during Beaufort deposition. Progressive aridification occurred during Elliot Formation deposition giving way to dune sand-dominated system of the Clarens Formation (Smith, 1990a). The maximum cumulative thickness of the Karoo Supergroup varies between 7 and 10km in the type Karoo foreland basin, but is much thinner to the north and northwest (Yemane et al, 1989).

1.3 The Beaufort Group

The sedimentary rocks outcropping in the Estcourt region form part of the Beaufort Group which spans the Permo-Triassic boundary. In this region the Beaufort Group is stratigraphically divided into the Estcourt and Belmont Formations. The corresponding vertebrate biozones are the *Dicynodon* Assemblage zone, and the *Lystrosaurus* Assemblage zone respectively (Rubidge, 1995). The stratigraphic divisions for the various authors are summarised in Table 1.1.

In the main Karoo Basin the Beaufort Group is exposed over an area of some 145 000km², with thicknesses exceeding 3000m (Smith, 1990a); Yemane et al reports a maximum thickness of 3233m in the type Karoo Basin of South Africa, thinning towards the north and east. The Beaufort Group has been divided into the lower, middle and upper Beaufort Groups. The Lower Beaufort Group is part of the Adelaide Subgroup, and the Middle and Upper Beaufort Groups are part of the Tarkastad Subgroup (SACS, 1980). The lower Beaufort Group is represented in KwaZulu-Natal by the Estcourt Formation, the middle, by the Belmont Formation, and the upper by the Otterburn Formation.

Continental deposition during the lower Beaufort (Late Permian) apparently occurred over several hundred thousands of square kilometres in southern and central Africa (Yemane and Kelts, 1990), with thicknesses of lower Beaufort Group sediments ranging from 10m in Angola to 1000m in the type Karoo Basin (Yemane and Kelts, 1990). It is a monotonous succession of terrestrial deposits consisting of alternating siltstones, mudstones and sandstones (Smith, 1993a; and le Roux, 1992).

PERIOD	Smith ¹ (1990)						Visser and Dukas ² (1979)		Le Roux ³ (1992)		
	GROUP	SUBGROUP	FORMATION			VERTEBRATE BIOZONE	BIOZONE	STRATIGRAPHIC UNIT	SE AND CENTRAL KAROO		SW KAROO
			SW	SE	E						
CLASSIC 50 Ma - TRIASSIC	Beaufort	Middle Upper		Burgersdorp	Otterburn	Kannemeyeria- Diademodon	Lystrosaurus	Katberg	Katberg		
			Tarkastad	Katberg	Belmont	Lystrosaurus- Thrinaxodon					
		Lower	Adelaide	Balfour	Estcourt	Dicynodon- Whaitsia	Daptocephalus	Elandsberg M.	Balfour	Palingkloof Elandsberg	
				Teekloof	Middleton	Tropidostoma- Endothiodon	Cistecephalus	Barberskrans M.		Barberskrans	
								Boesmanskop M.		Boesmanskop	
						Ferndale M.	Ferndale				
						Oudeberg M.	Oudeberg				
			Abrahamskraal	Koonap	Pristerognathus- Diictodon	Middleton Formation	Middleton		Teekloof		
				Dinocephalian	Koonap					Abrahamskraal	

Table 1.1 The Stratigraphy and Biostratigraphy of the Beaufort Group.

1. Smith, 1990(a) - The stratigraphy of the Karoo Supergroup.
2. Visser and Dukas, 1979 - Lithostratigraphy and biostratigraphy of the Beaufort Group in the southern and central Karoo.
3. Le Roux, 1992 - The stratigraphy of the Beaufort Group between Graaf-Reinet and Richmond.

However, despite the overall lithological similarities of these deposits, detailed correlation between sequences is difficult because of rapid facies changes from lacustrine to floodplain-fluvial depositional environments (Yemane and Kelts, 1990; Yemane *et al*, 1989). For example, lower Beaufort sequences are dominantly lacustrine in the eastern part of the type Karoo Basin in KwaZulu-Natal (Hobday, 1978 and Yemane *et al*, 1989), whilst lower Beaufort sequences from the Cape Province are described as flood plain deposits (Smith, 1990b), and those from north-western KwaZulu-Natal as fluvial (Botha and Linstrom, 1978).

The middle Beaufort (early Triassic) is dominated by a fluvial channel sandstone wedge (the Katberg sandstone Formation) which thins northwards from 1000m in the foreland basin along the southern coast to less than 100m in northern KwaZulu-Natal (Hobday, 1978), where it is known as the Belmont Formation. The Katberg Formation sandstone was deposited by swiftly flowing, low sinuosity, ephemeral braided streams (Hiller and Stavrakis, 1984).

The upper Beaufort (middle Triassic) returns to the floodplain deposits of meandering streams (Hiller and Stavrakis, 1984). It is represented by the Burgersdorp Formation in the south, and the Otterburn Formation in the east.

The Beaufort basin fluctuated markedly in outline, with a progressive reduction in size accompanied by segmentation into a series of shallow lakes (Hobday, 1978). Initial influx was mainly along the southwestern margin, where a prograding alluvial floodplain developed (Hobday, 1978). According to Smith (1990a) deposition of the Beaufort Group was influenced by three tectonically controlled troughs within the main Karoo Basin;

- a. East-west trending southern Karoo trough.
- b. North-northeast trending eastern Karoo trough.
- c. Northern Karoo trough.

The southern Karoo trough shows a transition from low to high sinuosity river deposits of the Abrahamskraal Formation, through to the floodplain dominated sedimentation of the

Teekloof Formation. The eastern Karoo trough traverses the Eastern Cape, and consists of shallow lacustrine facies which give way to fluvial deposits and finally the braided channel sequence of the Katberg Formation. Above the Katberg Formation, sedimentation was again dominated by floodplain processes.

The northern Karoo trough contains deposits on average only 500m thick. These deposits correlate biostratigraphically with the upper Beaufort deposits of the southern Karoo trough. The succession begins with deltaic-lacustrine sedimentation, and is overlain by braided stream deposits of the Belmont sandstone, and finally the Otterburn Formation floodplain deposits.

2. SEDIMENTOLOGY OF THE BEAUFORT GROUP AROUND ESTCOURT.

2.1 Location of study sections

The Beaufort Group of the Estcourt region comprises the Estcourt and Belmont Formations, and forms part of the northern Karoo basin (Fig. 2.1).

Botha and Linstrom (1978) carried out a sedimentological investigation of the Estcourt area and concluded that the Estcourt Formation had no direct correlative in the Eastern Cape and the Free State. However, in this investigation, it will be shown that the Estcourt Formation is typical of the Upper Permian deposits throughout southern Africa, and shows the typical fluvio-lacustrine characteristics seen elsewhere.

Areas west and east of Estcourt were investigated to create an overall picture of the palaeoenvironment during Permo-Triassic times. The areas west of Estcourt are only mentioned briefly in section three in connection with the fossil assemblage of Estcourt, as they represent the typical meandering river and floodplain deposits of the Lower Beaufort Group described by authors working in other areas of the Karoo Basin, these include Smith (1980, 1990a, 1990b, 1993a, 1993b); Stear (1978, 1980); Turner (1986); Hiller and Stavrakis (1984) and Hobday (1978).

Four detailed logs were mapped on the farm Rensburgspruit, situated 10km east of Estcourt (Fig. 2.2). These logs are discussed in detail due to the high percentage of lacustrine deposits. The four profiles are stratigraphically continuous, and join to form a sequence of sediments representing alternating lacustrine and fluvial conditions that prevailed during Late Permian times. The profiles occur in order of the Bedstead log, followed by the Kudu stream log, which in turn is followed by the Shoreline log. The Fossil dam log is thought to be the lateral equivalent of the Shoreline log. This discussion will involve only the sedimentology of these areas as the palaeontology will be discussed later in detail.

Therefore although no detailed interpretation will be made as to the age of the sediments, it will be shown later that they are of Late Permian age.

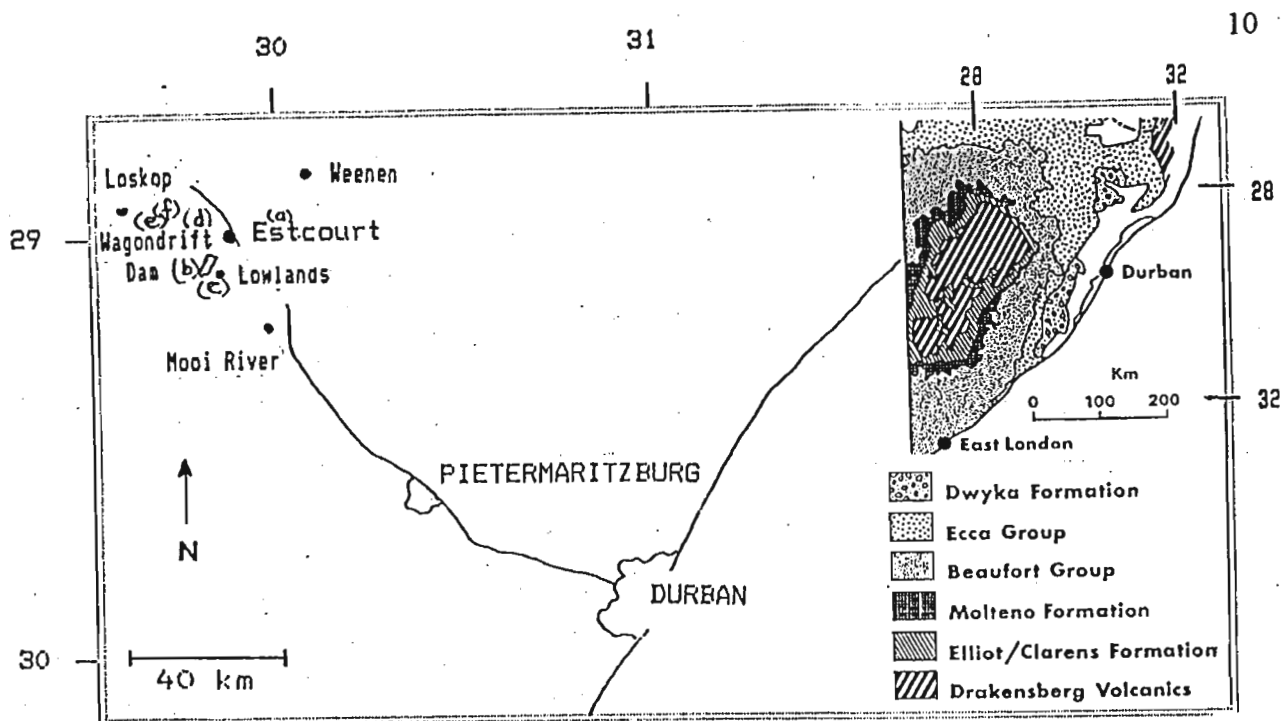


Figure 2.1 Locality map of Estcourt and surrounding areas. Insert - Generalised geological map of the Karoo Basin (Smith, 1990a)

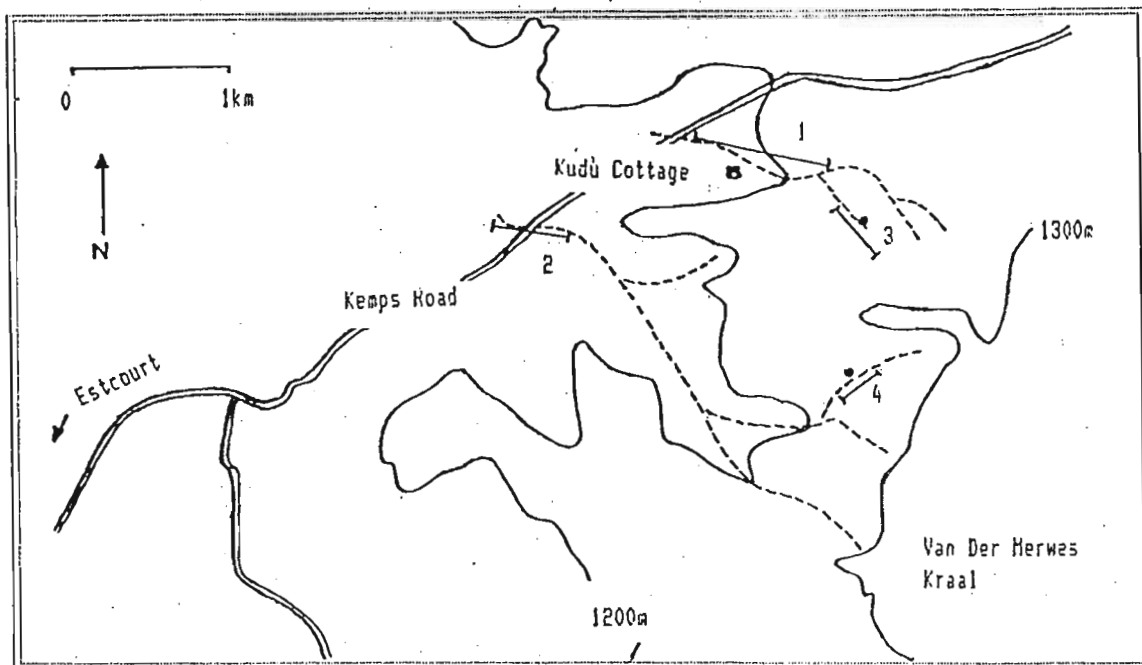


Figure 2.2 Simplified map showing location of sedimentary logs mapped on the farm Rensburgspruit.

Location - marked (a) on figure 2.1. (From South Africa 1:50 000 2829DD Frere)

1. Kudu stream log.
2. Bedstead log.
3. Shoreline log - o represents shoreline exposure at 13.m mark on profile.

Latitude and longitude position - S 28° 58' 00.6" E 29° 59' 13.1"

4. Fossil dam log - o represents position of fossil dam excavation at 10m mark on profile.

Latitude and longitude position - S 28° 58' 37.2" E 29° 59' 16.7"

These sequences are interpreted as floodplain deposits, and represent two sub-environments of deposition - that is fluvial-floodplain and lacustrine. Each sub-environment is divided into several facies for interpretation and discussion purposes. These facies are common to all four of the profiles which will be shown to represent a meandering river system flowing across a semi-arid floodplain, with transgressive-regressive lacustrine phases (Fig. 2.3 and Fig. 2.4).

The Bedstead log represents rapid alternations of marginal lacustrine deposits, and meandering-floodplain deposits. The lacustrine facies represented in the Bedstead log include Lithofacies G, H, and K, and the floodplain facies represented include Lithofacies A, C and D.

The Kudu sequence can be divided into four separate sections, with two of the sections representing lacustrine deposits, separated by two sections of fluvial deposits. The lacustrine sequences are thought to consist of the sediments logged from the 0m mark to the 17m mark, and from the 40m mark to the 54m mark. The remaining sections are fluvial in nature.

The deposits of the Shoreline log are dominantly fluvial-floodplain in nature, with only a small incursion of marginal lacustrine sediments. This matches up with the environmental trend of the Kudu stream succession, whose upper reaches are totally fluvial.

As previously stated, the Fossil dam log is thought to represent the lateral equivalent of the Shoreline log, however it is dominated by lacustrine sediments representing a lateral change in the environment of deposition.

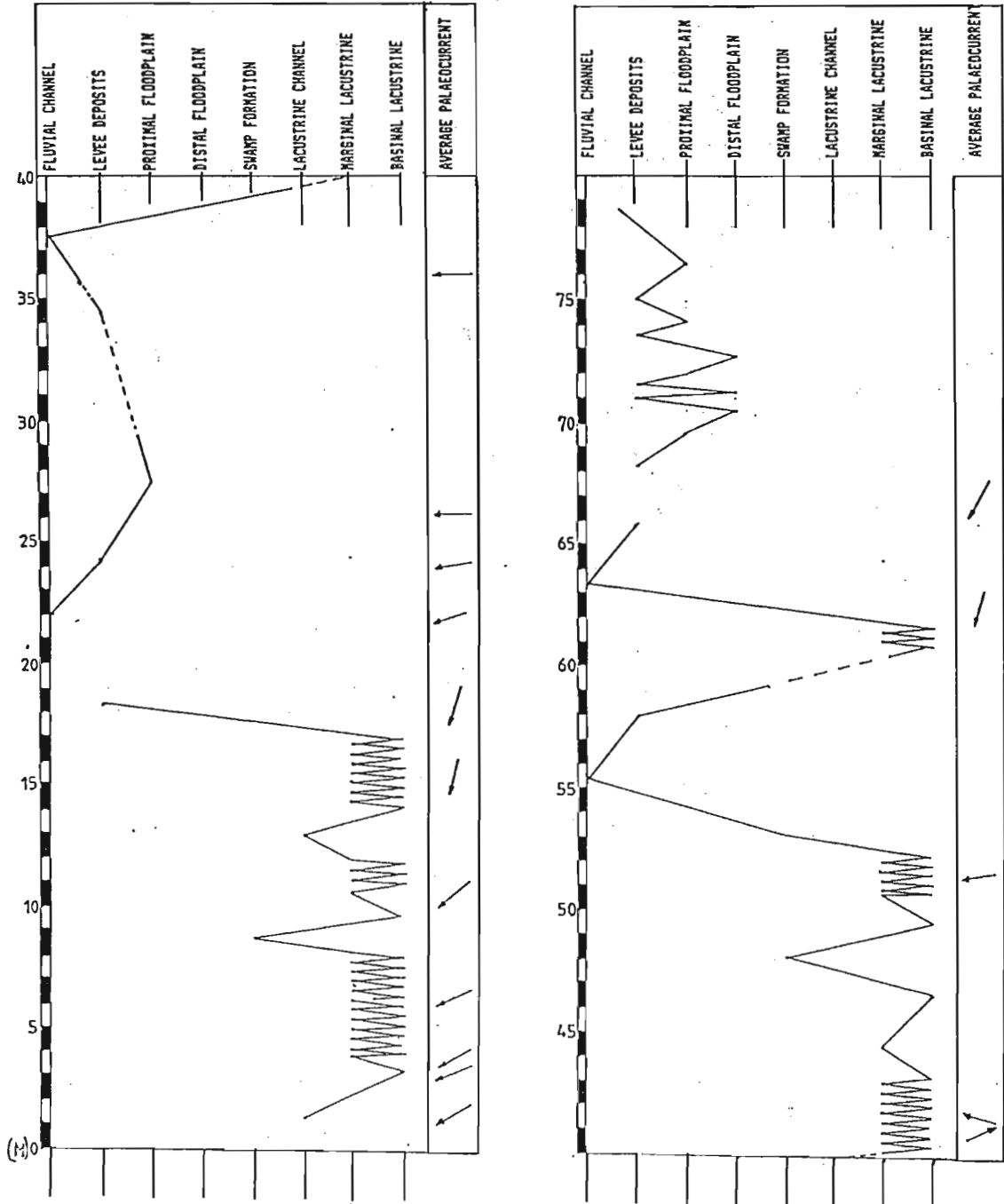


Figure 2.3 Graphical representation of transgressive-regressive lacustrine and fluvial cycles interpreted from the Kudu Stream log mapped east of Estcourt.

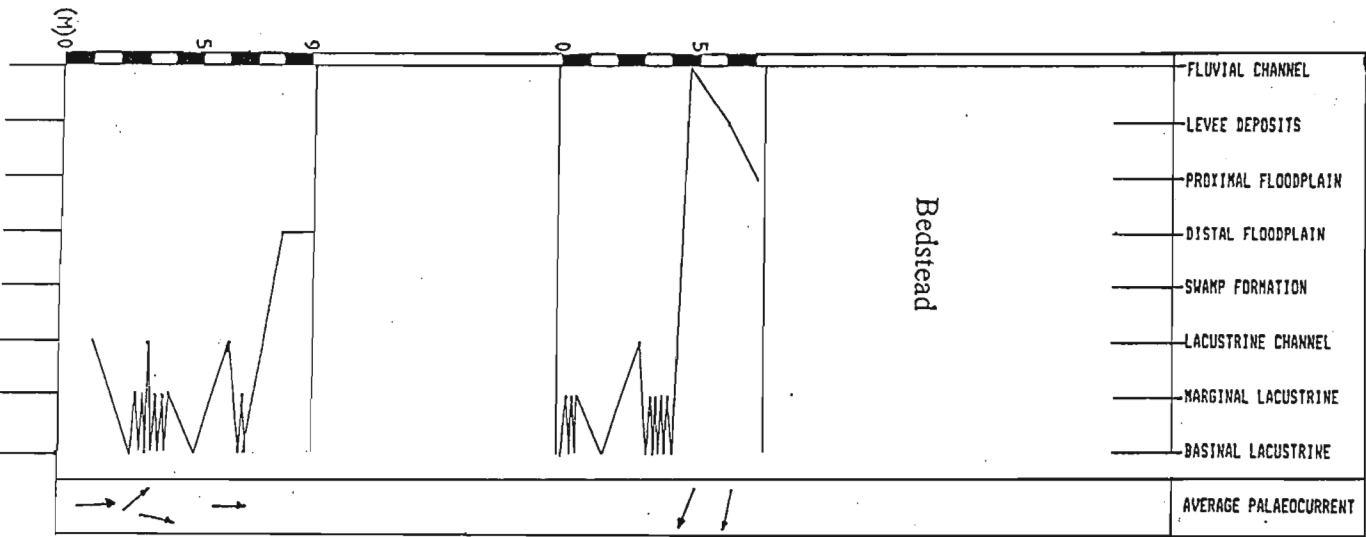
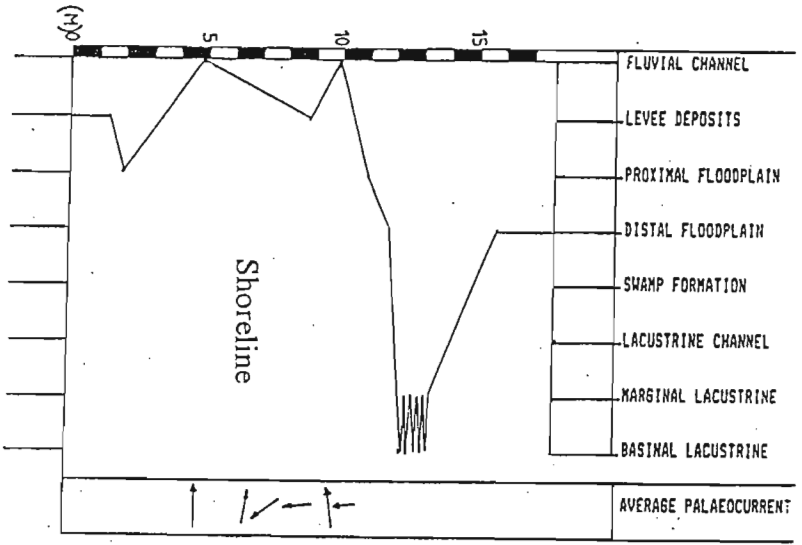
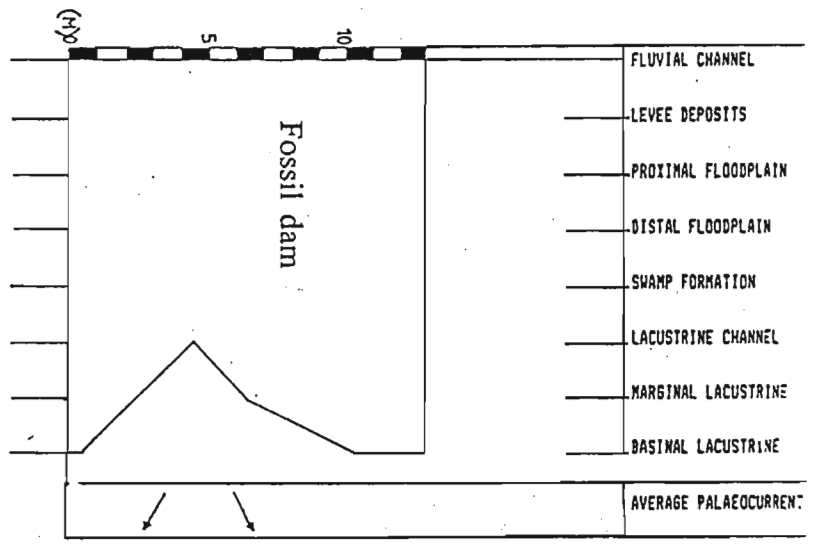


Figure 2.4 Graphical representation of transgressive-regressive lacustrine and fluvial cycles interpreted from the Bedstead, Shoreline and Fossil Dam logs mapped east of Estcourt.

2.2. Lithofacies description and interpretation

The facies described can be classified as lithofacies, which is defined by Miall (1984), as "a rock unit defined on the basis of its distinctive lithologic features, including composition, grain size, bedding characteristics and sedimentary structures." The facies (Table 2.1) are discussed in an environmental context, as each facies represents an individual depositional event which was influenced by the environment at the time of deposition. This allows one to reconstruct the palaeoenvironment.

Fluvial-floodplain facies association	Depositional environment
Lithofacies A - Cross-bedded sandstone	Channel-fill
Lithofacies B - Ripple-cross laminated sandstone	Channel-fill
Lithofacies C - Laminated siltstone and mudstone	Distal floodplain
Lithofacies D - Massive siltstone and mudstone	Proximal floodplain
Lithofacies E - Palaeosols	Overbank soils
Lithofacies F - Tabular thin sandstone bodies	Crevasse splay
Lacustrine facies association	Depositional environment
Lithofacies G - Ripple-cross laminated sandstone	Marginal lacustrine - shoreline
Lithofacies H - Finely laminated siltstone	Basinal lacustrine
Lithofacies I - Cross-bedded sandstone	Deltaic lacustrine
Lithofacies J - Organic-rich mudrocks	Marginal lacustrine - swamp formation
Lithofacies K - Finely laminated mudstone	Basinal lacustrine

Table 2.1. Summary of facies associations found to occur in the Estcourt region.

2.2.1. Fluvial-floodplain lithofacies association.

The fluvial-floodplain sequences are divided into six lithofacies -

- Lithofacies A - Cross-bedded sandstone.
- Lithofacies B - Ripple cross-laminated sandstone.
- Lithofacies C - Laminated siltstone and mudstone.
- Lithofacies D - Massive siltstone and siltstone.
- lithofacies E - Palaeosols.
- Lithofacies F - Tabular thin sandstone bodies.

Lithofacies A - Cross-bedded sandstone.

This lithofacies is mainly composed of thick units of trough cross-bedded sandstone. Also included are minor micro-trough cross-bedding, and planar cross-bedding. The units can reach 3m in thickness and are based by clay pebble lag conglomerates. The troughs are often found in association with rippled sandstone, and the base of the individual troughs often contain rip-up clasts of mudrock. Colour ranges from brown to grey.

Interpretation: Trough cross-bedded sandstones of Lithofacies A comprise most of the channel deposits and are interpreted as the result of the migration of dunes with sinuous crests, or sandwaves with a more lingoid form (Collinson, 1978). Where the foresets are rippled implies that flow separation occurred at high-stage discharge (Turner, 1986). In the logged successions, Lithofacies A commonly overlies Facies B.

Zones of calcretisation are usually only reported from the mudstones of floodplain deposits. Turner (1986); Hobday (1978); Smith (1980); and Visser and Dukas (1979), all report calcareous nodules and zones of calcretisation to occur in their floodplain mudstones. However most of the calcretisation that occurs in these sequences is associated with the channel sandstones. The calcretised areas take the shape of large rounded nodules which have weathered brown and, although their boundaries are well defined, the sedimentary structures of the surrounding sediments pass through them uninterrupted. Stear (1978), found similar calcareous pods in the channel sandstones of the Adelaide Subgroup near Beaufort West. He termed them marls and also found them to occur particularly in the trough cross-bedded units.

Lithofacies B - Ripple cross-laminated sandstone

This facies comprises either light brown or light grey, fine to medium grained sandstone. The units can reach thicknesses of 3.5m, and commonly show a fining of grain size towards the top of the unit, sometimes based by massive sandstone. This facies can contain ovoid

sandstone pebbles, and is often micaceous and bioturbated. Where the ripples fill troughs, their current orientation is often different to that of the troughs. The units can be found to intercalate with thin beds of laminated muds and silts, and often contain fragments of fossilised leaves (Fig. 2.5). This facies also includes climbing-ripple cross lamination.



Fig. 2.5 Fossilised *Glossopteris* leaf casts in a channel-fill massive sandstone. Location - 0m mark on Bedstead log (Appendix 1). Hammer is 31cm long.

Interpretation: According to Collinson (1978), ripple cross-laminated sandstone commonly forms quite substantial parts of coarse in-channel deposits, and usually occurs towards the top of a channel fill sequence. Collinson (1978), also found these deposits to be typically micaceous and carbonaceous, as is also seen in the above Lithofacies B.

The association of Lithofacies A and Lithofacies B could therefore be interpreted as representing a reduction in the scale of sedimentary structures in a vertical point bar

sequence (Hiller and Stavrakis, 1984), indicating upwardly decreasing depth and flow velocity (Turner, 1986).

Where the rippled units grade into horizontal lamination can be attributed to the micaceous nature of the sediments. According to Collinson (1978), laminated sandstone often occurs towards the top of a coarse rippled member. Due to the micaceous nature of the sediments, and the decreased flow velocity, the presence of imbricated platy minerals forms a traction carpet that inhibits the formation of ripples resulting in horizontal lamination.

Where Lithofacies B forms thick units above the multistoried channel sandstones is interpreted as a gradual vertical transition from upper point bar deposits into inner-bank levee deposits. Where this occurs, Lithofacies B is often associated, and alternates, with Lithofacies C and D.

Smith (1990b), also found levee sediments to be characterised by the abundance of disarticulated fossil bones, especially vertebrate skulls. In this case however, only a single occurrence of vertebrate remains occurred in a levee siltstone, and is probably due to the small scale of the exposures logged up the stream bed.

Lithofacies C - Laminated siltstone and mudstone.

This lithofacies is composed of dark grey, fissile siltstone that is micaceous. The siltstone commonly grades upwards to a laminated mudstone. This facies commonly shows colour banding due to grain size differences, with both light and dark grey banding in the mudstones, and grey and green colour banding in the siltstones. The siltstone units contain fragmented fossil plant material, and are often found as discontinuous units in sandstone units. In one instance a laminated siltstone unit contains disarticulated fossil vertebrate remains. The units can reach 1m thickness.

Interpretation: The thin units of laminated mudstone are interpreted as distal floodplain deposits and are the result of suspension deposition from ponded water (Smith, 1980).

In the Kudu stream profile, there is a thick unit of laminated mudstone (76m mark). The mudstone is laminated on a centimetre scale, with individual layers showing an internal structure of horizontal lamination topped by ripple cross-lamination. The top of this unit contains calcrete concretions, and the unit is topped by a continuous layer of calcretisation, which is most probably a marginal lacustrine carbonate horizon indicating a long period of slow drying of the lake (pers.com. R. Smith). Plant fragments commonly separate the individual layers of the mudstone; this together with the presence of concretions excludes a lacustrine environment. These mudstone layers are interpreted as the distal equivalents of crevasse splay events. The internal structure of horizontal lamination followed by ripple cross-lamination represents decreased velocity in a single flood event. The successive layers represent separate flood events and are separated by plant remains, which are interpreted as being transported vegetation from the channel banks left stranded on the crevasse splay surface after the flood subsided (pers. com. R. Smith). This particular mudstone unit is therefore interpreted as being deposited in a proximal floodbasin environment.

Only a single occurrence of calcrete formation in mudstone is recorded, and occurs at the top of the Kudu stream succession (77m mark). Turner (1986), found calcareous nodules to tend to occur at discrete horizons within Overbank mudstones, and interprets them to have formed at shallow depths in pedocal-type soils.

Smith (1980), also reports calcareous concretions to have formed in palaeosol zones on periodically inundated floodplains. Smith (1990b), reports horizons of calcareous glaebules to commonly occur in proximal floodbasin sequences, and are the result of multiple cycles of wetting and drying on a warm semi-arid floodplain. According to Smith, they are an indication of a arid climate, as the prerequisite for their formation are hot, arid conditions. The absence, in this case, of overlying palaeosol horizons is explained by Smith, who states that on inundation of the floodplain, the palaeosol would be subjected to scour, resulting in a low preservation potential of the upper palaeosol horizons.

Lithofacies D - Massive siltstone and siltstone.

This lithofacies does not contain palaeosols. It is composed of fining upward sequences composed of dark grey mudstone and siltstone. Some of the units contain lenticular sandstone beds, and in one instance small chert-like concretions were observed. Lithofacies D mostly occurs, in the top 10m of the Kudu stream succession, as thin units no thicker than 70cm. The units often contain fragments of fossilised plant material, yet do not form palaeosol horizons. The mudstone units are darker than the siltstone units due to the higher organic content.

Interpretation: These deposits are interpreted as waning flood deposits that accumulated on the proximal floodplains. Each fining-upward cycle is interpreted as a single flood event deposited by unconfined laminar flow (pers. com. R. Smith).

Lithofacies E - Palaeosols.

The palaeosols are those fine grained sediments that contain fossilised plant root moulds and casts in their original attitude, ie. in situ. Examples of the most complete palaeosol profiles are described :-

Palaeosol 1 : This palaeosol occurs at about the 20m mark of the Kudu stream profile. The base of the palaeosol is taken as the rippled sandstone which grades up into a horizontally laminated siltstone. The siltstone loses its structure towards the top of the unit due to pedoturbation by roots. The root casts are large and penetrate the sediment vertically. The siltstone is grey and shows bioturbation. This rooted horizon is topped by silty mudstone which has weathered orange; where not weathered it appears olive green in colour. This unit appears massive and contains hashed plant material, plus vertical and horizontal burrowing. The profile ends with massive mudstone that also contains hashed plant remains.

Palaeosol 2: The second palaeosol profile occurs at the 67m mark of the Kudu stream

profile. The palaeosol has formed at the top of a trough cross-bedded sandstone unit, which fines upwards to form the soil profile. The sandstone grades into a massive, silty mudstone layer that forms the root horizon of the palaeosol as it is traversed by fossilised root remains. The profile ends with a mudstone that contains large, clear impressions of *Glossopteris* leaves.

Palaeosol 3: The third profile starts at the 69m mark of the Kudu stream profile, with a finely laminated, grey siltstone, containing small, spherical calcrete concretions and bone fragments. As the siltstone grades upwards into a silty mudstone, the lamination are destroyed by colonisation of fossilised roots. These are covered by a thin layer of fossilised roots, again, mainly *Glossopteris* leaves. The profile continues with the formation of a second palaeosol in an olive green mudstone. The mudstone contains large, thick fossilised roots that penetrate vertically, and is topped by a second mudstone layer which is grey in colour. This second mudstone has a planar base and contains fragmented fossilised plant remains.

Palaeosol 4: This palaeosol occurs at the 11m mark, topping a thin crevasse splay sandstone, of the Shoreline profile. It is based by a root horizon, which is topped by a calcareous concretionary layer, which has a gradational base and a sharp upper surface. This concretionary layer contains fossilised bones, ganoid scales and fossilised plant fragments (Fig. 2.6 and Fig. 2.7). The surface of the layer appears to be rippled, and shows evidence of vertebrate trackways.

Interpretation: The deposits of Lithofacies B are often pedogenically modified. Smith (1990b), defines a palaeosol as " a buried landscape of the past that is no longer undergoing pedogenic modification". According to Turner (1993), " pedogenesis manifests itself in the destruction of primary sedimentary structures, presence of burrowing and bioturbation, diffuse colour mottling, rootlets, and other typical soil structures and fabrics".



Fig. 2.6. Fossilised vertebrate bones in the concretionary layer of palaeosol 4, of the Shoreline profile (11m mark).



Fig. 2.7. Fossilised bone fragments and ganoid scales scattered throughout the concretionary layer of palaeosol 4, Shoreline profile (11m mark). Scale in centimetres.

The above three soils described are characterised mainly by the presence of vertical root casts and an overlying layer of fossilised leaf material. There is minor bioturbation, and in only one instance the presence of calcareous concretions. This is an indication that the palaeosols are immature and the floodplain surface was not exposed for long enough periods to undergo mature pedogenic modification.

These palaeosols are thought to be the equivalent of Smith's (1990b), levee palaeosols. However the above soils are less well developed and immature examples. Smith's levee palaeosols are characteristically weakly horizonated and contain no clearly defined calcic horizon, only smooth-surfaced glaebules. They consist of drab grey siltstone with claystone-lined burrows and root casts interpreted as the preserved portion of the surficial A horizon, and pass downwards into a more clearly defined horizon of calcareous glaebules and rhizcretions interpreted as calcic B horizon. Only in one area is this entire profile evident (described palaeosol profile 3). Only horizon A evident in the other two examples. The immature nature of these palaeosol profiles is most likely due to their close proximity to a river that was subject to regular overbank flooding (Smith, 1990b).

The soil profiles are usually found in association with overlying massive mudstones. Massive mudstones are the result of deposition in slack water areas from suspension deposition of overbank fines in the low lying areas of the flood basin (Turner, 1986). Since the palaeosol sediments are found mostly overlying channel deposits, it is thought that the above facies occur in sequences that represent an upward transition from channel deposits, up into levee deposits (with palaeosol formation of the levee siltstones), into proximal floodbasin deposits represented by the massive mudstones.

The fourth described palaeosol shows characteristics in common with Smith's (1990b) proximal floodbasin palaeosols, which are often found in association with crevasse splay sandstones. Smith states that the calcareous concretionary sheets possibly formed just above the ground water table, by capillary rise, and may thus be regarded as indicative of pedogenic maturity achieved within a 7000yr time span. It is also suggested that they formed under a semi-arid climate regime with a mean annual moisture deficiency.

Lithofacies F - Tabular thin sandstone bodies.

A further minor facies in the four sequences is horizontally laminated sandstones, with no obvious fining-upward trend. These sandstones are similar to Smith's (1980), description of crevasse splay deposits. The units are thin, and the bases sharp with low relief. They are also generally unfossiliferous, with only the occasional bone fragment. These sandstones are thus interpreted as representing deposits from streams which flowed, during flood, down the meanderbelt slope and into the flood basin (Smith, 1980).

2.2.2. Discussion of fluvial-floodplain lithofacies

Various authors working on the Lower Beaufort sediments describe the commonly fluvial sediments as being typified by fining upwards sequences composed of sandstone, siltstone and mudstone. These sediments are interpreted as the deposits of low and high sinuosity meandering rivers flowing across a semi-arid alluvial plain.

These deposits can be divided into channel deposits, represented by the channel sandstones, and the interchannel or floodplain deposits, represented by the finer sediments.

The channel sandstones of the Lower Beaufort Group are characterised by various combinations of trough cross-bedding, ripple cross-lamination, planar cross-bedding and horizontal lamination (Stear, 1978; and Turner, 1986). They are commonly based by lag conglomerates and seldom form thick sequences. The internal structure represents lateral accretion in a point bar sequence, with an upward decrease in sedimentary structure size and grain size. Overlying the channel sandstones are interchannel deposits.

These deposits can be divided into four facies (Smith, 1980) including :-

1. Levee deposits - comprising alternating beds of mudstone, siltstone and sandstone,
2. Crevasse splay deposits - comprising horizontally laminated sandstone,
3. Proximal flood basin deposits - consisting of mudstone and siltstone, and,
4. Distal flood basin deposits - comprising laminated mudstone.

All of the above facies are recorded in the floodplain facies of the Lower Beaufort Group throughout southern Africa.

The six fluvial-floodplain lithofacies of the measured sections occur as fining upward sequences, and are characterised by calcretisation, green and brown colouring, palaeosol formation, and thick units of channel sandstones.

A typical facies profile includes a basal lag conglomerate, followed by trough cross-bedded sandstone, ripple cross-laminated sandstone, and fining into siltstone and mudstone with occasional palaeosol formation. Variations in this sequence includes an absence of either the trough cross-bedded, or rippled sandstone components. This sequence of sediments can be interpreted as a typically fluvial floodplain sequence when compared to the Beaufort sediments logged in other areas.

The channel sandstones of the Shoreline sequence show a more complicated series of structures than recorded in the previous sequences. These channel sandstones are structured mainly by trough cross-bedding, with subordinate ripple cross-lamination, planar lamination, climbing-ripple cross-lamination, and horizontal lamination. One of the sandstone units shows an internal sequence of structures from trough cross-bedding, to horizontal lamination, to ripple cross-lamination, and ending with planar cross-lamination. This is a similar sequence to that quoted by Turner (1981) for channel sandstones. Markov chain analysis (Turner, 1981) shows that the two most common sequences of structures in Beaufort channel sandstones are : (1) Cross-bedding - horizontal lamination - ripple cross-lamination; and (2) horizontal lamination - cross-bedding - ripple cross-lamination.

Hiller and Stavrakis (1984), found that the Balfour (Lower Beaufort) sediments of the Eastern Cape Province are typified by alternating layers of grey, fine grained sandstone and greenish-grey or blueish-grey mudstones and shales, commonly arranged into fining upwards cycles. They found the most common sedimentary structures of the sandstones to be trough cross-bedding and ripple cross-lamination, representing a typical reduction in the scale of sedimentary structures in a vertical point bar sequence.

The meanderbelt facies of Turner (1986), is also characterised by erosively based fining-upward sequences, comprising intraformational clasts overlain by sandstones, siltstone and mudstone. The sandstones are characterised by an abundance of cross-bedding overlain by abundant horizontal lamination of upper phase plane bed origin, and ripple cross-lamination. He interpreted this as being consistent with flood flows of decreasing depth and flow intensity, but with a dominance of high-velocity, shallow upper regime flows, a condition seldom encountered in most meandering fluvial systems.

Hobday (1978) found the fluvial sediments of the eastern Karoo basin, to be characterised by overlapping lenticular units based by a lag conglomerate, followed by trough cross-bedded sandstone, plane-bedded and /or microtrough and ripple-drift cross-laminated sandstone, topped by maroon or green siltstone or mudstone. He interprets these sediments as the deposits of high sinuosity, mixed-load, low gradient streams of aggrading alluvial plains.

The above examples all share characteristics in common with the fluvial-floodplain sequences mapped in the Estcourt region. Other characteristics in common are the presence of concretions, palaeosol formation, and the abundant fossil flora and faunas. These characteristics indicate a common palaeoenvironment during Lower Beaufort times throughout southern Africa, that is, they represent terrestrial deposits by meandering rivers that flowed across an aggrading alluvial plain. The presence of calcareous concretions and palaeosols indicates a semi-arid palaeoclimate that was warm to hot, with strongly seasonal rainfall (Smith, 1993b).

2.2.3 Lacustrine Lithofacies Association

The lacustrine sequences of the four profiles can be divided into 5 lithofacies -

Lithofacies G - Ripple cross-laminated sandstone.

Lithofacies H - Finely laminated siltstones.

Lithofacies I - Cross-bedded sandstone.

Lithofacies J - Organic-rich mudrocks.

Lithofacies K - Finely laminated mudstone.

Due to the complicated facies associations of the lacustrine facies, they shall be interpreted together at the end of the facies descriptions.

Lithofacies G - Ripple cross-laminated sandstone

The sandstones of this lithofacies are comprised of light grey, fine to medium grained, sandstone. The main occurrence of this facies is as the top half of siltstone and sandstone couplets. These upward coarsening couplets occur throughout most of the profiles. The couplets are laminated on a millimetre scale, and occasionally on a centimetre scale. The rippled surface of the sandstone layers almost always shows invertebrate burrowing (Fig.2.8 and Fig. 2.9). The ripples are symmetrical and parallel, and of small scale with amplitudes never greater than 1cm.

This facies also occurs as minor units composed of entirely ripple cross-laminated sandstone. These units are less than 0.5m in thickness.

The couplet units are commonly interrupted by single lenticular beds of rippled sandstone. These layers are seldom thicker than 10cm, and commonly have pebbles and rip-up clasts at their base. The surface of these layers also show bioturbation. These layers commonly "pinch-and-swell" throughout the surrounding sediments.

Lithofacies H - Finely laminated siltstones.

These siltstones are dark grey in colour and horizontally laminated on a millimetre scale. The lithofacies occurs as single units, or as single layers alternating with lithofacies G, forming couplets. Some of the single unit siltstones show bioturbation. The siltstone units often contain lenticular sandstone layers, and occasionally shows sediment deformation. The base of the couplets, ie. the siltstone layer, is sharply defined.

Lithofacies I - Cross-bedded sandstone

This lithofacies consists of cross-bedded sandstone units no thicker than 1.5m. Cross-bedding includes planar, trough and micro-trough units. This lithofacies also includes the minor occurrence of hummocky cross-bedded sandstone. The planar units are single storied and composed of medium to coarse grained sandstone. The trough cross-bedded units are mostly small scour troughs, and there is a single occurrence of a stacked trough unit which has an erosional base and is most likely a fluvial sandstone. The micro-trough units are also thin and most likely represent channel sandstones.

The hummocky cross stratified sandstone is represented by two units of fine-grained sandstone that show variations in sedimentary structures throughout the unit. The first unit has layers of massive siltstone, and the second unit grades from a rippled sandstone, to hummocky cross-stratification, to horizontally laminated sandstone and again back to hummocky lamination. The first unit is greyish-brown in colour and the second unit light grey in colour.

Lithofacies J - Organic-rich mudrocks.

There are three occurrences of coal formation, all of which occur in the Kudu stream profile. The thickness of the coal bands range from 40cm to 10cm. They are low grade coals with a high silt content. Plant fragments seen include *Glossopteris* and *Calamities*. Silt filled, vertical burrows are also present. In all the cases the coal is associated with finely laminated mudstone and silty mudstone, plus massive mudstone. The associated fines also often contain plant material and root horizons indicating palaeosol formation.

Lithofacies K - Finely laminated mudstone.

This lithofacies is composed of dark grey mudstone that is horizontally laminated on a millimetre scale and contains lenticular sandstone layers that are ripple cross-laminated. It contains no fossils and shows no indications of bioturbation.

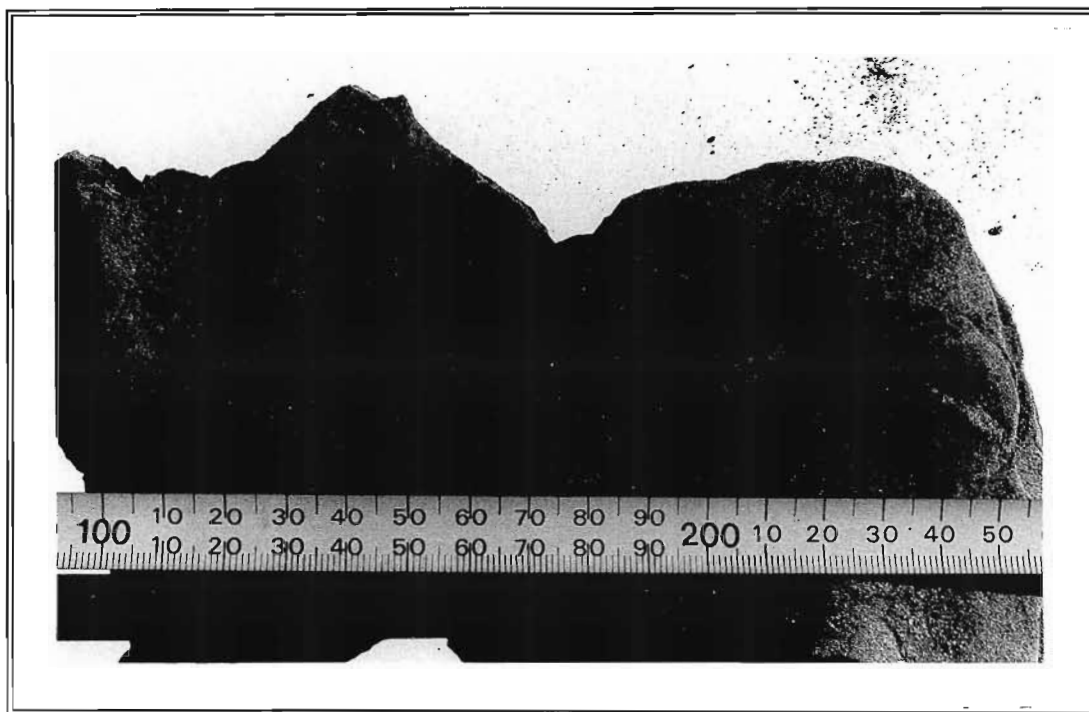


Fig. 2.8 Invertebrate burrowing on sandstone layer of couplets. Location - 5m mark of the Kudu stream profile. Scale in centimetres.

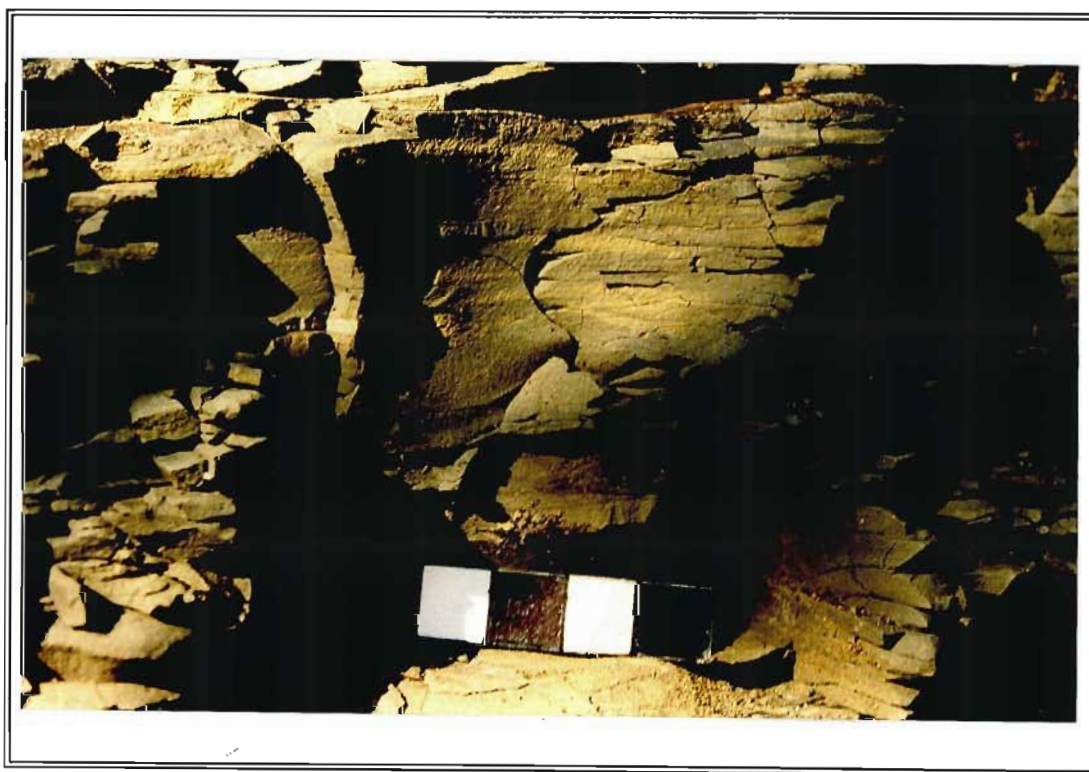


Fig. 2.9 Section of couplets showing dominance of basinal fines. Location - 12.5m mark on Shoreline profile. Scale is 5cm long.

2.2.4 Interpretation and discussion of lacustrine Lithofacies association.

The Lower Beaufort (Late Permian) sediments of the Karoo basin are predominantly the result of deposition by meandering river channels on an alluvial plain. These deposits are discussed at length, and are the main focus of Lower Beaufort sedimentology. However, an important section of this sedimentology are those deposits resulting from lake formation. Lacustrine deposits are mostly only briefly mentioned in passing, and yet form an important part of palaeoenvironmental interpretation.

The above described lithofacies show characteristics that point to a lacustrine depositional environment. They are comprised mostly of sandstone, with the only fines found in the sequence being associated with coal formation or basinal lacustrine conditions. Overbank floodplain deposits, however, are predominantly argillaceous rocks composed of fining upward sequences of subordinate sandstone, siltstone and mudstone (Smith, 1980). A overbank-floodplain environment is therefore excluded mainly due to the absence of any typical overbank deposits.

Yemane and Kelts (1990), review of Lower Beaufort palaeoenvironments show that lacustrine systems were widespread in the subcontinent, from southern to central Africa. In the type-Karoo basin, Lower Beaufort lacustrine conditions attributed to prograding alluvial deposits, and are commonly overprinted by fluvial processes. Whereas in the north, lacustrine sedimentation underwent minor fluvial influence (Yemane and Kelts, 1990). The result, is that the lacustrine deposits of the type-Karoo basin are thin, and form a very minor part of the sedimentary succession. Thus lacustrine sequences are seldom recorded and discussed from the type-Karoo basin. Yet, as Yemane and Kelts (1990), point out, lake deposits are significant for understanding the palaeogeography of the period.

Ancient lacustrine deposits may be divided into offshore and nearshore facies (Allen and Collinson, 1978). The offshore facies include thinly bedded graded silts and muds deposited from turbidity currents. The nearshore facies include wave rippled, horizontal, and low angle cross-stratified sandstones deposited in small beach zones, cross stratified

sandstones representing distributary channels and mouth bars, and lignites and silts deposited in interdistributary bays and ponds (Picard and High, 1979).

The dominant facies association of the logged lacustrine sediments is that between Lithofacies G and H, which occur together forming silt and sand couplets. Each couplet is composed of a base of dark grey siltstone, topped by ripple cross-laminated, bioturbated, light grey sandstone. These couplets are similar in composition to Picard and High's (1979) varve sequences of ancient lacustrine deposits, however occur on a larger scale representing "rythmites" (pers.com. R. Smith). Picard and High's (1979) varve sequences are described as being composed of light and dark grey couplets which often tend to coarsen upwards. The couplets represent allocyclic sequences, i.e. sequences that result from external changes such as climate, tectonic activity, or sea and lake level changes.

The couplets described for the four mapped profiles are similar in nature to those described from the Triassic Lockatong Formation of New Jersey (Picard and High, 1979). These varves consist of clastic cycles that coarsen upwards from black, fissile shale, to dark grey, silty, carbonate-rich claystone and lenses of fine, limy sandstones. The pattern records progressive decreases in precipitation with the lake becoming shallow, agitated, and the bottom better oxygenated. They represent, therefore, varves formed in response to transgressive and regressive cycles. The thickness of these varves is on a sub-millimetre scale.

It is thought that these silt/sand couplets also represent transgressive-regressive cycles. The silt component of the couplets is represented by Facies H. These deposits are dark grey in colour, and contain no evidence of bioturbation or fossil remains of any kind. This is also true of the siltstone component of the couplets, even where the sandstone component above and below the siltstone is extremely bioturbated. This absence of fossil fauna and bioturbation suggests deposition in anoxic bottom waters (Yemane *et al.*, 1989). This, together with the fine nature of the laminations of these deposits suggests deposition below wave base (Yemane *et al.*, 1989) in an offshore lacustrine environment.

Many lakes are rippled in their shallow water sands, with nearshore lacustrine facies consisting of wave rippled sandstones which were deposited in small beach zones (Allen and Collinson, 1978; Picard and High, 1979), for example, the littoral clastic facies of the Oligocene of the eastern Ebro Basin, Spain, consist of wave rippled sandstone with thin interbedded mudstones (Allen and Collinson, 1978). The fact that the ripples of the sandstone surfaces are of short wavelength (generally less than 10cm) and of mini ripple type (small amplitudes), plus the abundance of bioturbation indicates deposition in very shallow water depths (Allen and Collinson, 1978). Lithofacies G is therefore interpreted as representing marginal lacustrine deposits.

Occasionally, the rippled sandstones show random palaeocurrent directions, with no specific trend. According to Picard and High (1979) random ripple orientations only occur within 1m of the lake shoreline. This would imply shallow conditions. In the case of the Shoreline rippled sandstone unit, the random palaeocurrent directions are accompanied by the presence of ladderback ripples (Fig. 2.10), vertebrate trampling (Fig. 2.11), and single vertebrate footprints, verifying the shallow depth of deposition of these sediments.

The rythmites represented in the logged profiles are therefore thought to represent an interfingering of offshore and nearshore facies - transgressive-regressive cycles. This could occur due to a seasonal drying up of the lake resulting in the shoreline sandstones transgressing over the laminated silts of deeper water. Often, these couplet units show an overall upward coarsening trend, as the sandstone component of the couplets increases, indicating an increasing dominance of marginal lacustrine deposits. Allen and Collinson (1978), found that a typical vertical sequence of Permo-Triassic lacustrine sequences is a coarsening upwards sequence representing the gradual progradation of fluvial channels into the lake.

These rythmite sequences alternate with thicker units of only siltstone or sandstone. Their characteristics are the same as those of their couplet equivalent, and are therefore thought to represent periods of lake stability, with the siltstone units representing layers of basinal sediment, and the sandstone units representing stacked marginal sediments. The siltstone



Fig. 2.10 Ladderback ripples on a marginal lacustrine sandstone. Location - 13.5m mark on Shoreline profile. Scale is 5cm long.

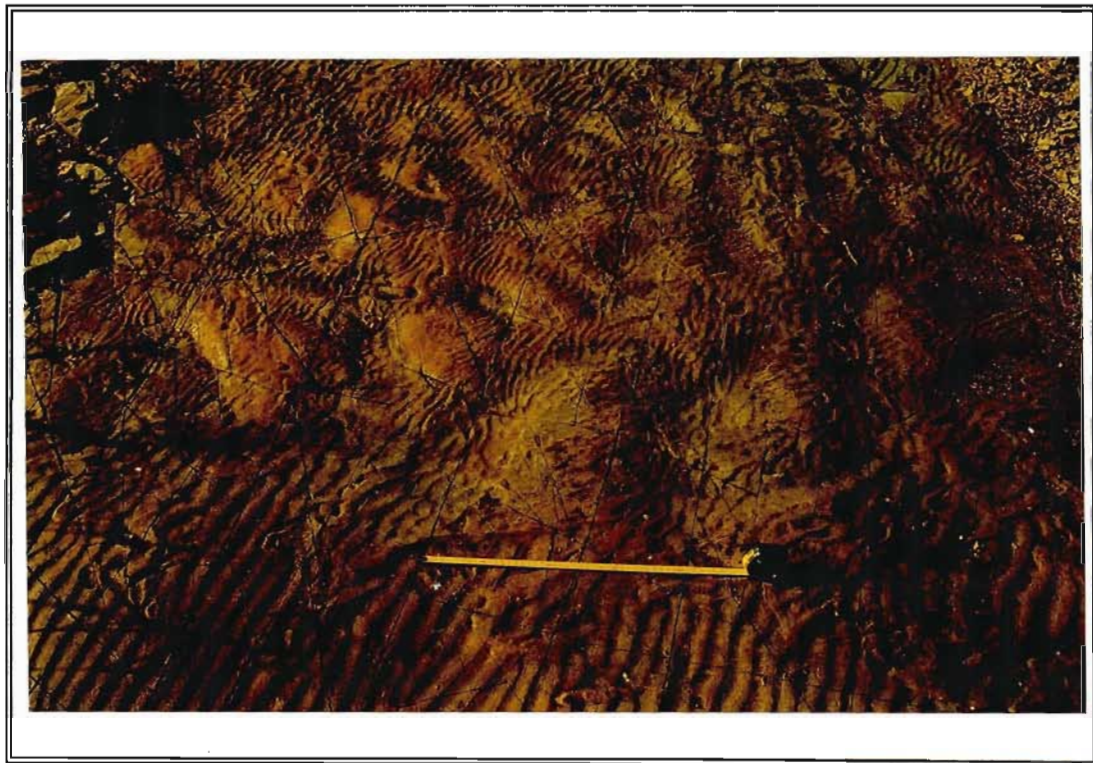


Fig. 2.11 Vertebrate trampling across marginal lacustrine sandstone. Location - 13.5m mark on Shoreline profile. Scale is 50cm long.

units, do however, contain lenticular bands of sandstone indicating shoreline incursions. Where the bands are conglomeratic in nature, is representative of coarser beach zones, storm deposits, and are the thicker and coarser grained equivalents of the rippled sandstone component of the couplets.

Since no detailed correlation can be made with type-Karoo basin lacustrine deposits, a direct comparison of the above lacustrine facies is made with Yemane *et al's* (1989) lacustrine facies from the Lower Beaufort rocks of Mt. Chombe, along the northwestern shore of Lake Malawi. Five major lithofacies were distinguished, including :-

Facies A - Finely laminated mudstones and muddy siltstones.

Facies B - Massive, muddy siltstones and siltstones.

Facies C - Thinly bedded, horizontally stratified siltstones.

Facies D - Cross stratified and flaser bedded siltstones and sandstones.

Facies E - Massive and cross-bedded, coarse grained sandstones with small scale channels and intraformational pebble layers.

All of the above facies can be correlated with the lacustrine facies of the mapped sections.

Yemane *et al's* Facies A can be correlated with lacustrine Lithofacies K. This facies comprises dark grey, parallel to wavy laminated mudstones and siltstones. The normal grading of the individual mudstone layers suggests deposition from suspension, and is most likely the result of "turbidity-like" density underflows which are most likely seasonal and occur when the lake is at its fullest, ie. in the rainy season. In Yemane *et al's*, Facies A, there is no indication of bioturbation, suggesting anoxic bottom waters. However in the studied lithofacies K, an oxygenated environment is envisaged, as the surface of the individual beds are often traversed by invertebrate and vertebrate trackways (Fig. 2.12), and fish trails. Both facies were deposited in offshore lacustrine environments.

There is no direct correlation with Yemane *et al. 's*, Facies B.

The laminated siltstones of Lithofacies H can be correlated with Yemane *et al's* Facies C, which is composed of grey to green horizontally and wavy laminated siltstones. The beds vary from a few to 30cm in thickness, and have sharp lower boundaries. These siltstones show no bioturbation, and are graded, and are therefore interpreted as deposits from turbidity currents in offshore lacustrine environments.

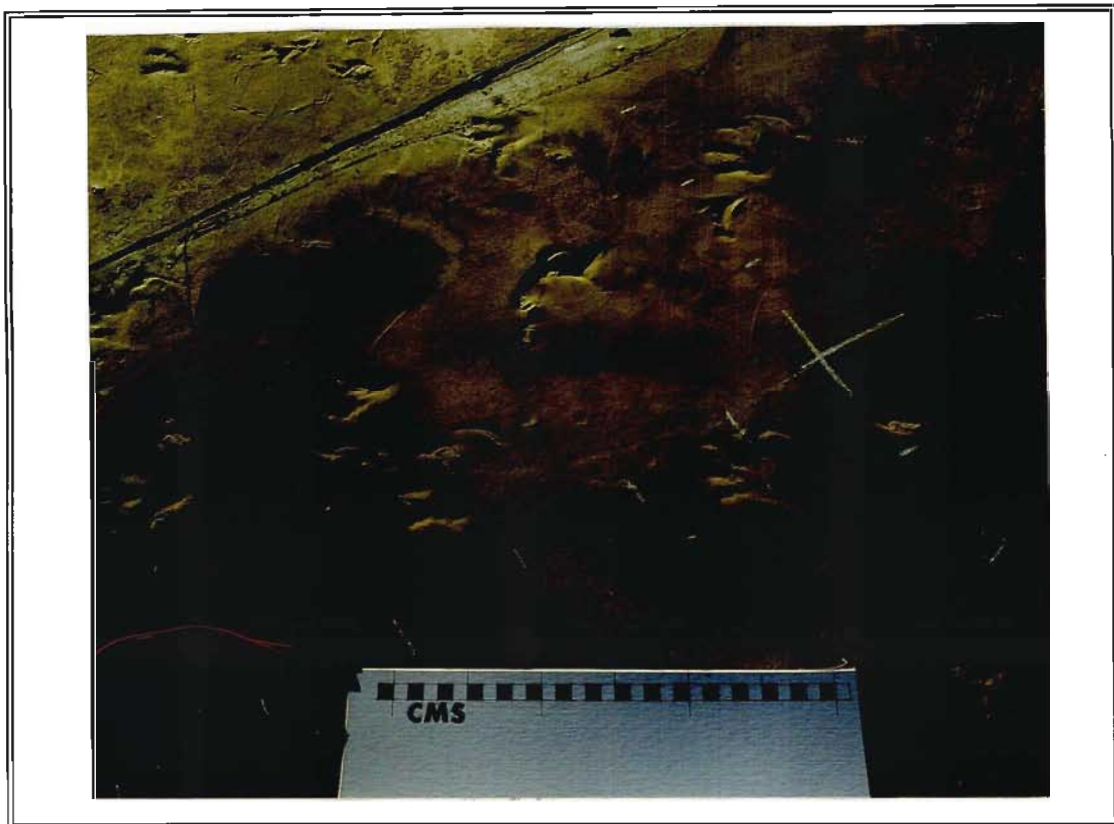


Fig. 2.12 Vertebrate trackways traversing shallow, basinal lacustrine deposits. Location - 10m mark on Fossil Dam log. Chalk marks represent 10cm intervals.

However the lacustrine siltstones of the Bedstead profile are bioturbated indicating oxygenated bottom waters and thus a shallower lacustrine environment than that envisaged for the Kudu stream profile silts. Smith (1980) also describes bioturbated, horizontally laminated siltstones as forming part of levee deposits. However, the non-erosive bases, and the close association with marginal lacustrine sands excludes a levee environment interpretation. Also, levee silts and muds are fossil rich, and show evidence of sub-aerial exposure such as pedogenesis and concretion formation. The siltstones of the above Facies

B shows no evidence of sub-aerial exposure and are therefore interpreted as being deposited in a basinal lacustrine environment.

Yemane *et al's* (1989) Facies D can be compared as the equivalent of Lithofacies G of the above sequences. It is composed of silts and sands that are internally structured by parallel lamination, and ripple cross-lamination. The ripples observed are symmetrical, straight crested, parallel and occasionally bifurcated. Both represent marginal lacustrine facies.

Due to the close association of Lithofacies G, H, and I, Facies I of the Estcourt profiles is interpreted as a lacustrine deposit, and not a meandering channel deposit. It is the experience of the author, that the floodplain channel sandstones of the Estcourt region are characteristically composed of stacked troughs. The only planar cross-bedding seen is in association with the braided channel deposits of the Belmont sandstone. This together with the fact that planar cross bedding is rare in meandering river systems (Miall, 1977), leads to the conclusion that the sediments of Lithofacies I were deposited in a lacustrine-delta environment, at the lacustrine-fluvial interface. This interpretation is made by comparing Lithofacies I with Yemane *et al.'s* (1989), lacustrine Facies E. Both characteristically comprise medium to coarse grained sandstones which are mostly planar cross bedded, with minor trough cross-bedding. Erosional contacts are common in both facies. This plus the abundance of cross bedding is interpreted as indicating strong bottom currents. Therefore a marginal lacustrine environment probably connected to lacustrine delta is envisaged.

Yemane *et al.'s* (1989) Facies D and E are also used to interpret the sandstone sequence mapped in the Fossil dam profile. At first glance the Fossil dam log appears to represent an upward fining fluvial sequence. However on closer inspection it becomes apparent that this sequence is lacustrine in nature, and represents a transgressive lacustrine event resulting in the fining upward trend.

The sandstones of the Fossil dam profile is dominated by massive bedding, with planar cross-bedding, and ripple cross-lamination. The uppermost sandstone unit is topped by a rippled sandstone that grades into a siltstone that contains calcretised boulders. This

succession would suggest a channel sandstone passing up into levee deposits typical of floodplain deposits. Therefore ideally, the above sequence should be interpreted in a fluvial context. However, based on Yemane *et al.*'s (1989) lacustrine facies, a lacustrine interpretation of this sequence is proposed. The ripple cross-laminated siltstones and sandstones of the Fossil dam profile are similar to those described in Yemane *et al.*'s, Facies D, which are interpreted as deposits of a marginal lake environment, and the cross-bedded sandstone units are almost identical to those described in Yemane *et al.*'s, Facies E. Yemane *et al.* (1989) describes Facies E as characteristically comprising buff to yellowish coloured, medium to coarse grained sandstones, which are interbedded with centimetre thick dark mudstones. The beds are mostly planar cross-bedded, but a few beds with small trough cross-bedding were observed. Erosional contacts are common. The same characteristics are seen in the sandstone units of the Fossil dam log. These deposits are interpreted as being marginal lacustrine, probably connected to lacustrine delta.

Yemane, *et al.* (1989) carries the interpretation further. In their lacustrine succession, there is an coarse clastic body composed of facies association DE, which is bounded by basinal lacustrine muds and silts. They interpret this succession as being part of a barrier system probably connected to a river mouth. This same interpretation is proposed for the above sediments, with the sandstone unit forming part of the barrier, which would therefore explain the calcretisation in the siltstone. These barrier sands were then covered by basinal fines in a lacustrine transgressive event.

Lithofacies J of the Estcourt profiles is the result of marginal swamp formation, and plant colonisation as the lake regressed. There are three occurrences of the formation of coal. Coals are the result of prolific plant growth in a high water table environment (Collinson, 1978). In the lacustrine context, it represents periods where the lake dried up enough to promote plant growth, and the formation of swamps, and therefore also represents a regressive lacustrine event.

The "hummocky" cross-stratified sandstone is also interpreted as a marginal lacustrine deposit. These deposits are the result of a reworking of sediment by storm waves, below

the wave base line.

Thus, the Late Permian lakes of the Estcourt region can be described as ephemeral features that underwent many phases of transgression and regression. This indicates that deposition in the lakes was controlled by seasonal climatic factors, such as rainfall. The lacustrine facies of the described profiles indicate the presence of both shallow, well oxygenated lakes, and deeper, anoxic lakes.

The Fossil dam profile lake shows a trace fossil and faunal assemblage that indicates a shallow lake. The presence of fossilised plant mats, and vertebrate trackways traversing the basinal muds, suggests a shallow lake environment. According to Picard and High (1979), not all plant remains indicate nearshore conditions. Apart from the problem of transported or drifted matter, plants may grow far out into the lake if the water is shallow enough. The shallow nature of the lake is further evidenced by a set of vertebrate footprints indicating a very small animal, or juvenile, which would indicate a water depth of no more than 10cm. However not all the layers are traversed by vertebrate footprints, which likely indicates greater lake depths. However even though the lake was shallow, it never fully dried up as the surfaces never show desiccation features.

Smith (1990a) reports shallow lacustrine facies from the Eastern Cape. These facies comprise horizontally laminated mudstones, wave- and current-rippled siltstones and thin discontinuous sandstone units. He also reports lacustrine deposition from the Triassic, northern Beaufort facies represented by varve-like laminated muds.

Hobday (1978) recognised that lacustrine conditions prevailed in the lower Beaufort of the eastern Karoo Basin, as did Yemane *et al.*, (1989) who also state that lower Beaufort sequences are dominantly lacustrine in the eastern part of the type Karoo Basin in KwaZulu-Natal.

All lakes are ephemeral features on the land, and are gradually converted into fluvial plains as the lake fills (Picard and High, 1979). Thus the above lacustrine successions give way to fluvial-floodplain sedimentation.

3. THE VERTEBRATE PALAEOLOGY OF THE PERMO-TRIASSIC BEAUFORT SEDIMENTS OF THE ESTCOURT REGION.

3.1 Introduction

3.1.1 The fossil assemblage of Estcourt

The sediments of the Estcourt region form part of the Lower and Middle Beaufort Group, which spans the Permian - Triassic time period. The terrestrial palaeoecology of this age was dominated by mammal-like reptiles, or therapsids. The mammal-like reptiles originated during the Early Permian, in the Kungurian (Maxwell, 1992) and survived late into the Triassic. The Late Permian and Early Triassic sediments of the Estcourt area, contain an abundance of fossilised therapsid remains, and indicate a biological palaeoenvironment dominated by the lives of these creatures. The Estcourt sediments also host a wide variety of fossilised plant remains, together with insect and amphibian fossils, indicating a rich and diverse ecology during Permo-Triassic times.

The fossil assemblage of the Estcourt sediments is dominated by the remains of two herbivorous therapsids - *Lystrosaurus* and *Dicynodon*. These therapsids belong to the dicynodont genus of the anomodont therapsid family. Only a single piece of fossil evidence was found indicating the presence of therapsid carnivores.

3.1.2. Work history

Botha and Linstrom (1978) found the sediments of the Upper Permian Estcourt sediments to be "plentiful" in vertebrate remains. This was found to be the case, when the fossil collecting started in 1992. It soon became apparent that the fossil assemblage included more than only vertebrate remains, with the sediments yielding traces of invertebrates, amphibians, fish, insects, and a rich plant life. In 1993, a dam excavation also revealed many surfaces traversed by vertebrate trackways.

The main aim of the search for fossil vertebrate remains, was to trace the Permo-Triassic boundary, representing the largest extinction event in geological history.

However the largest part of the palaeontological investigation centres around the vertebrate trackways discovered east of Estcourt. Due to their low preservation potential, fossilised trackways are scarce in the geological record. It was therefore a rare find to discover layer upon layer of these tracks, and afforded a great opportunity to study the locomotive patterns of the creatures that formed them, most likely, the mammal-like reptiles.

3.2 Record of therapsid fossils discovered in the Permo-Triassic sediments of Estcourt.

Most of the vertebrate fossil remains recorded around Estcourt, were discovered in the sediments that pass along the western border of the town. The areas of investigation include Loskop, Draycott, Moorleigh, Ennersdale, De Hoek, and Lowlands. The areas are discussed separately.

Lowlands fossil site - The Lowlands fossil site incorporates the areas south and west of Wagondrift Dam, along the western border of Estcourt (Fig. 3.1). The areas just south of Wagondrift Dam comprises two farms, the one owned by Mr. McFie, and its neighbour owned by Mr. Moor. The area west of the dam forms the Moor Park nature reserve.

Four skulls were discovered at the Moor Park locality. All four were discovered in the ditch next to the reserve road, in a horizon of maroon siltstone representing overbank, fluvial deposits. This maroon layer is stratigraphically continuous with the maroon layer seen on the Lowlands farms, south of Wagondrift Dam. The skulls were identified as all belonging to the dicynodont *Lystrosaurus*.

The fossil bones of this area are mostly perimineralised with calcareous nodular material. Three of the skulls were found with articulating lower jaws, dorsal side up, with only slight dorsal flattening of the skull. The fourth skull was found within a calcareous concretion

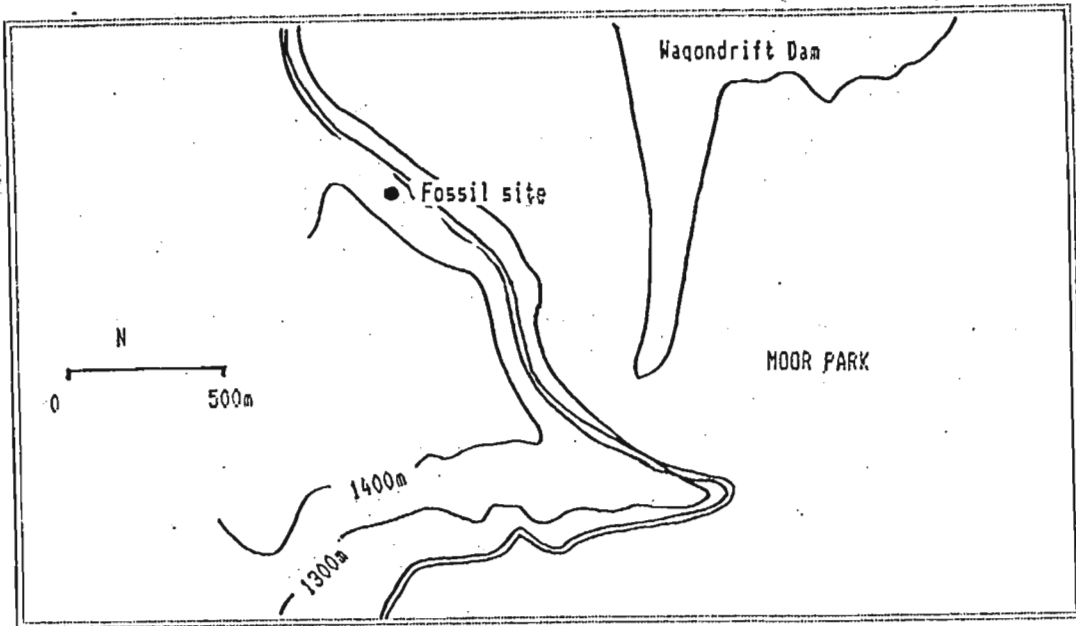


Figure 3.1 Simplified map showing location of skulls found at Moor Park site. Location - marked (b) on Fig. 2.1 (From South Africa 1:50 000 2929BB Estcourt, 1978)

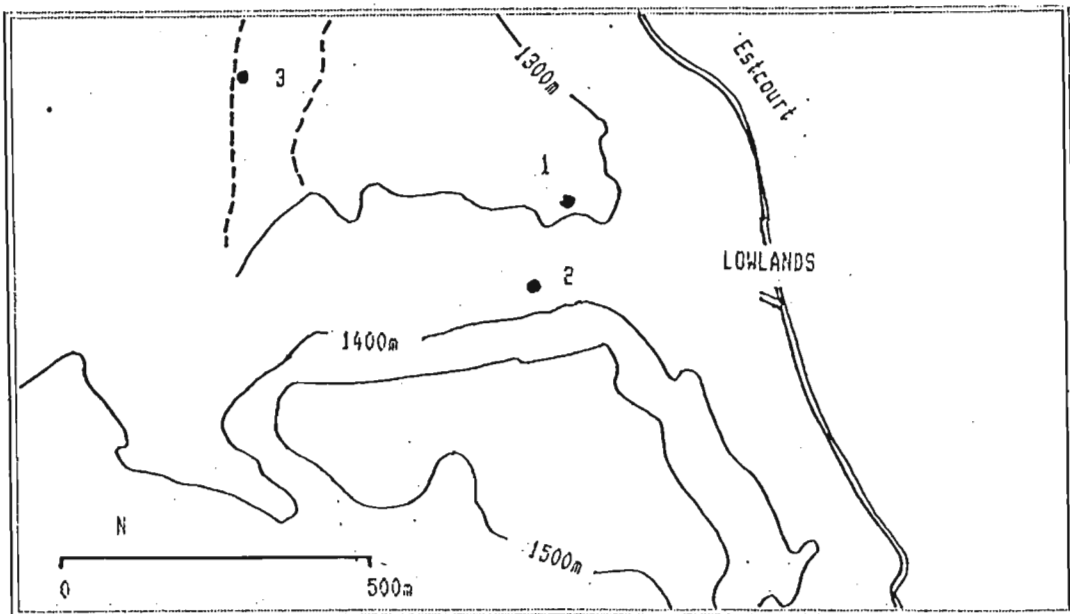


Figure 3.2 Simplified map showing location of fossils discovered at Lowlands. Location - marked (c) on Fig. 2.1 (From South Africa 1:50 000 2929BB Estcourt, 1978)

1. *Lystrosaurus* and *Dicynodon* skull occurring in same horizon. Topped by sediments containing *Dadoxylon*.
2. Rich bone bed containing numerous bones belonging to *Lystrosaurus*. Sediments of occurrence are the maroon shales defined as ancient levee deposits.
3. Area rich in *Dicynodon* remains, and location of carnivore teeth.

and was highly deformed. However all four skulls still occurred together with the lower jaw still in place. No accompanying skeletal remains were discovered. The length of the three undeformed skulls are 10cm, 19cm, and 15cm.

The Lowlands farm site includes three important areas (1, 2 and 3 in Fig. 3.2). At site 1 both *Lystrosaurus* and *Dicynodon* occurred in the same horizon. The importance of this will be discussed later.

The second site incorporates a wide area that contains various taphonomic classes of *Lystrosaurus* remains. These taphonomic classes are based on Smith's (1980) table of taphonomic classes of Lower Beaufort vertebrate fossil assemblages (Fig. 3.3). The fossils of this particular area fall under taphonomic classes B, C, G and H. This indicates that this fossil site contains bones of animals that were both preserved at the site of death, and preserved far from the site of death. The skulls also show carbonate perimineralisation, and are often found in calcareous concretions.

Two complete skeletons were discovered. The first was laid out flat with only slight spinal curvature, with some of the bones, and the skull covered in micrite (Fig. 3.4). The second skeleton was much smaller and totally encased in a concretion. The lone skulls found, were also covered in concretionary micrite. The bones belonging to taphonomic classes G and H, were often covered in micrite, whilst some occurred totally smooth.

The size of the skulls varied from small to large, the largest measuring 30cm in length. Three skulls, ventrally compressed measured 14cm, 12cm, 16cm in length. The entire stratum contains fossilised bones in various stages of disarticulation, and forms one of the richest collecting grounds for *Lystrosaurus* remains in the Estcourt area.

The third site explored in the area contains fossilised remains of the dicynodont *Dicynodon*. The taphonomic classes of these fossils include C, E and H. Six large skulls can be seen in the area, however most are extremely weathered and unidentifiable. Three are identifiable as belonging to *Dicynodon*. The largest measures 50cm in length, and has

Taphonomic class			Transportation	Duration of post-mortem/preburial
Preserved at site of death	A	Complete articulated skeleton in "curled up" attitude	No transportation	Very short
	B	Complete or near complete skeleton with straight or reflexed spinal curvature	Slightly rolled	Short
Preserved near site of death	C	Skull with articulating cervical vertebrae and lower jaw		Short
	D	Skull with displaced lower jaw	Lag-short distance transport	Long
	E	Skull without lower jaw		Long
	F	Lower jaw		Long
Preserved far from site of death	G	Accumulation of variety of small post-cranial elements into "bone bed"	Long distance transport reworked, winnowed and sorted	Very long
	H	Isolated and/or fragmented ribs, limb bones and vertebrae	Long distance transport	Very long

Figure 3.3 Taphonomic classes of the Lower Beaufort vertebrate fossil assemblages (From Smith, 1980)

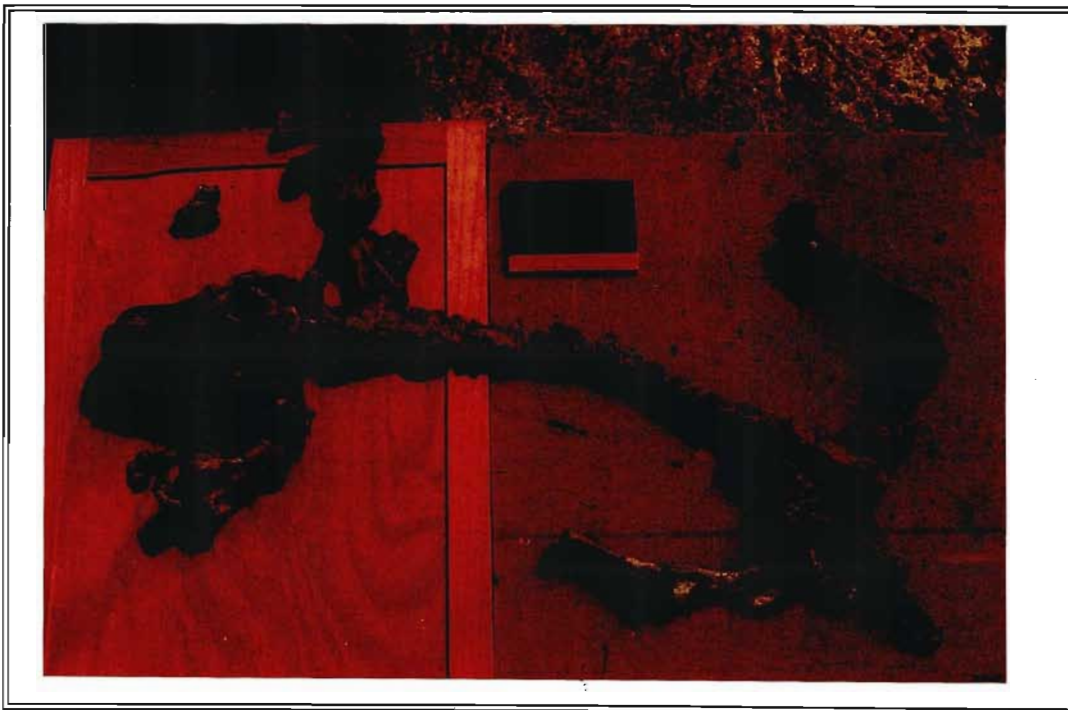


Figure 3.4 Almost complete *Lystrosaurus* skeleton excavated from levee siltstones in the Lowlands area, west of Estcourt. Scale - Notebook is 15cm long.

weathered out dorsal side up. A second *Dicynodon* skull occurs together with some vertebra and limb bones. Discovered in the same area is the only fossil find of a carnivorous therapsid, probably from *Theriognathus* (pers.com. R.Smith). The fossil is a single piece of an upper jaw containing four, serrated incisor teeth (Fig. 3.5 and Fig. 3.6). The fact that the teeth are still in the piece of jaw, indicates that the fossil is near the site of death.

Areas proximal to the above three sites yielded some fossils, however they were mostly isolated and of taphonomic class H. Any skulls that were discovered were too extensively weathered for identification purposes. A single skull was recorded as being identified as *Dicynodon*, measured 30cm in length and was laterally compressed.

Ennersdale Fossil Sites - The Ennersdale fossil sites are those areas occurring adjacent to the road that joins the Loskop road to the Wembezi road (Marked (d) on Fig. 2.1). Most of the fossils found in this area belong to taphonomic class E and H, and mostly occur in olive green mudstone. The disarticulated limb bones discovered were large indicating large animals. It is common to find single, broken tusks in the area, some reaching diameters of 4.5cm. Five skulls were found in the area, they were however extremely weathered and deformed. They did appear large in size, with lengths measuring greater than 30cm.

The maroon mudstones of the Ennersdale area, are relatively unfossiliferous. Found one small skull, 15cm long, once again very weathered and unidentifiable. Some calcareous nodules were also found to contain an array of small bones. Most of the remains found in this horizon were of taphonomic class H.

Loskop fossil site - This area (Marked on fig. 2.1) is dominated by a large exposure of maroon mudstone, and yet only small pieces of bone were discovered belonging to taphonomic class H.

De Hoek Fossil site - This site (Marked e on fig. 2.1) compares with the Lowland site as being one of the richest fossil collecting horizons surrounding Estcourt. Fossils have been

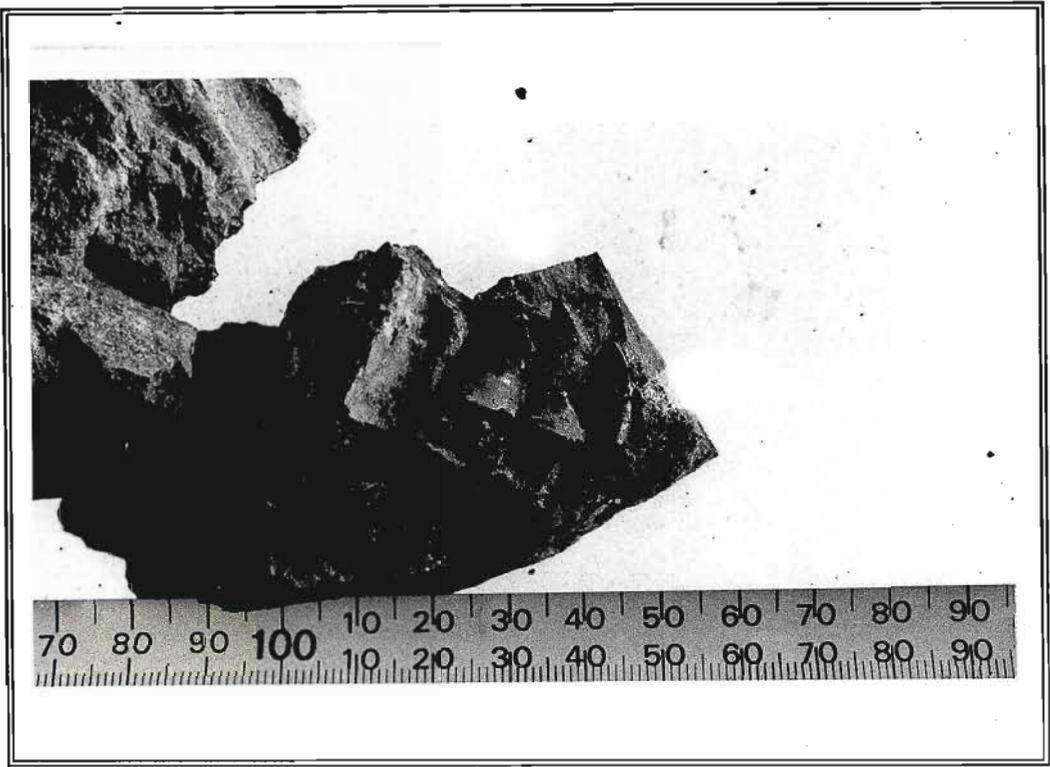


Figure 3.5 Photograph showing three of the incisor-like teeth found in the Lowlands area.

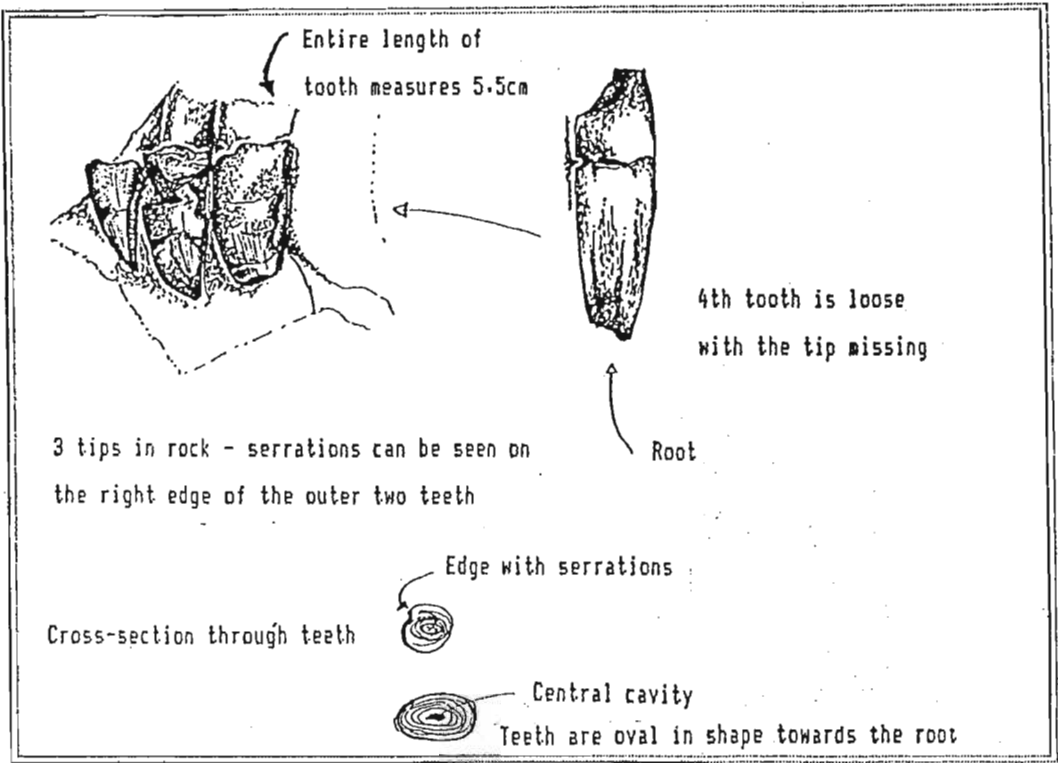


Figure 3.6 Diagrammatic, life size, representation of the fossilised carnivore teeth discovered near Lowlands.

collected from this site since 1992, with entire *Lystrosaurus* skeletons to the remains of the small amphibian *Lydekkerina* being discovered. Taphonomic classes range from A to H, and the size of the fossils from small to large.

The most common taphonomic class is D, with the sediments containing many skulls in various stages of weathering. The majority of the skulls were identified as belonging to *Lystrosaurus*. The skulls range in length from 10 to 17cm. Most of the fossil remains, from limb bones to skulls, are covered in nodular material.

This fossil rich horizon comprises the prominent maroon siltstone layer that can be followed along the western border of Estcourt. As in other areas, the siltstones of De Hoek show colour mottling plus and abundance of carbonaceous concretionary formation.

Moorleigh Fossil Site - The Moorleigh site (Marked f on fig. 2.1) is the second site to contain *Lystrosaurus* and *Dicynodon* fossils in the same horizon. Most of the fossils found at this site were fairly weathered and mostly comprised disarticulated limb bones, ie. taphonomic class H. The skulls found were mostly broken up, however the length of the skulls was greater than 35cm in most cases. However, at the top of the sequence, before the occurrence of maroon mudstone, a small part of a *Lystrosaurus* skull, and the back end of a *Dicynodon* skull were found in the same grey siltstone layer. Both of the skull fragments were undeformed.

3.3 Discussion

The fossil rich, maroon sediments of the Lowlands and De Hoek sites, are composed of siltstone, with lenticular bands of sandstone, and often show colour mottling. These sediments are interpreted as levee deposits, which Smith (1980) noted as being fossil rich sediments.

The fossils of these sediments, classified as taphonomic class B to F, all show perimineralisation of the bone surface with calcareous nodular material. This indicates that

the bones were only transported a short distance from place of death. Smith (1980), quotes Konizeski (1957), when considering the cause of the perimineralisation, who links the occurrence of calcareous nodules with the presence of "fresh" bones within the sediment.

The discussed sediments represent both Permian and Triassic deposits, and span the Permo-Triassic boundary which marks a large extinction event, where up to 96% of all species became extinct (Wignall, 1992). The extinction of terrestrial vertebrates during Permo-Triassic times can be divided into four major episodes, one each at the end of the Early Permian, Late Permian, Early Triassic, and Late Triassic (Maxwell, 1992). There are various reasons quoted for the cause of the Permo-Triassic event, with most research revolving around marine organisms. Pitrat (1973) goes as far as to say that this extinction was mainly a marine phenomenon for which marine causes should be found. Since then various hypothesis have been put forward; Wignall and Hallam (1993 and 1992) suggest that the extinction was a catastrophic event resulting from a rapid Griesbachian transgression resulting in habitat loss due to anoxia; Wang *et al* (1994) also suggest a catastrophic event; and Zhou and Kyte (1988) put forward a volcanic hypothesis. Erwin and Vogel (1992) say there is little evidence linking end-Permian volcanism to the extinction, and together with Maxwell (1992) feel that the extinction was due to a culmination of events leading to the gradual extinction of marine and non-marine organisms.

It is the Late Permian (Tatarian) extinction that is represented in the sediments that border the western areas of Estcourt, and marks the disappearance of the dicynodont *Dicynodon*, and its replacement by the dicynodont *Lystrosaurus*. This replacement is clearly indicated in the vertebrate fossil assemblage of Estcourt, where strata rich in *Dicynodon* bones are overlain by strata rich in *Lystrosaurus* bones. There is also clear indication of an overlap between the two biofacies. Evidence for this overlap was seen in both the Lowlands and Moorleigh regions of Estcourt. The fossil flora (discussed in a later section) will also show that this overlap occurred in the Late Permian, indicating that *Lystrosaurus* evolved during Late Permian, and not Early Triassic times as once thought (King, 1991; Kemp, 1982; Tucker and Benton, 1982; Hiller and Stavrakis, 1984).

4. PALAEOFLORA OF THE BEAUFORT SEDIMENTS AROUND THE ESTCOURT AREA.

4.1 Introduction

The fossil flora collected from the Estcourt area belongs to the *Daptocephalus* biozone, and are Permian in age. Lacey *et al* (1975) describes 35 flora taxa from this biozone, including sphenopsids, pteropsids, cycadopsids, glossopterids, coniferopsids and dispersed seeds and microsporangia.

4.2 Description of fossil flora

Most of the fossil plant impressions found belong to the glossopterid genus. Also found were some sphenopsids and a Permian filicophyte. The glossopterids (Fig. 4.1) were identified using Anderson and Anderson (1985), Lacey *et al.* (1975), and are described using Kovacs-Endrody's (1991) morphological terms.

Glossopteris indica - The leaf shape is lanceolate to ovate-lanceolate and has a cuneate base. The apex is usually acute, however the very tip may be blunt. The secondary veins are acute to the midrib, and pursue an oblique course to the margin at 45 to 90 degrees. The midrib is strong and persistent.

Glossopteris cf ampla - This leaf is characterised by large, broadly ovate leaves, and was the largest leaf found. The midrib is distinct and persistent and the secondary veins pursue a closely parallel course which, except close to the midrib, is nearly perpendicular to margin and midrib.

Glossopteris angustifolia - The leaf is small and oblong with an obtuse apex and cuneate base. The secondary veins arch from the midrib in a very steep curve. This form was common in the Mooi river collection.

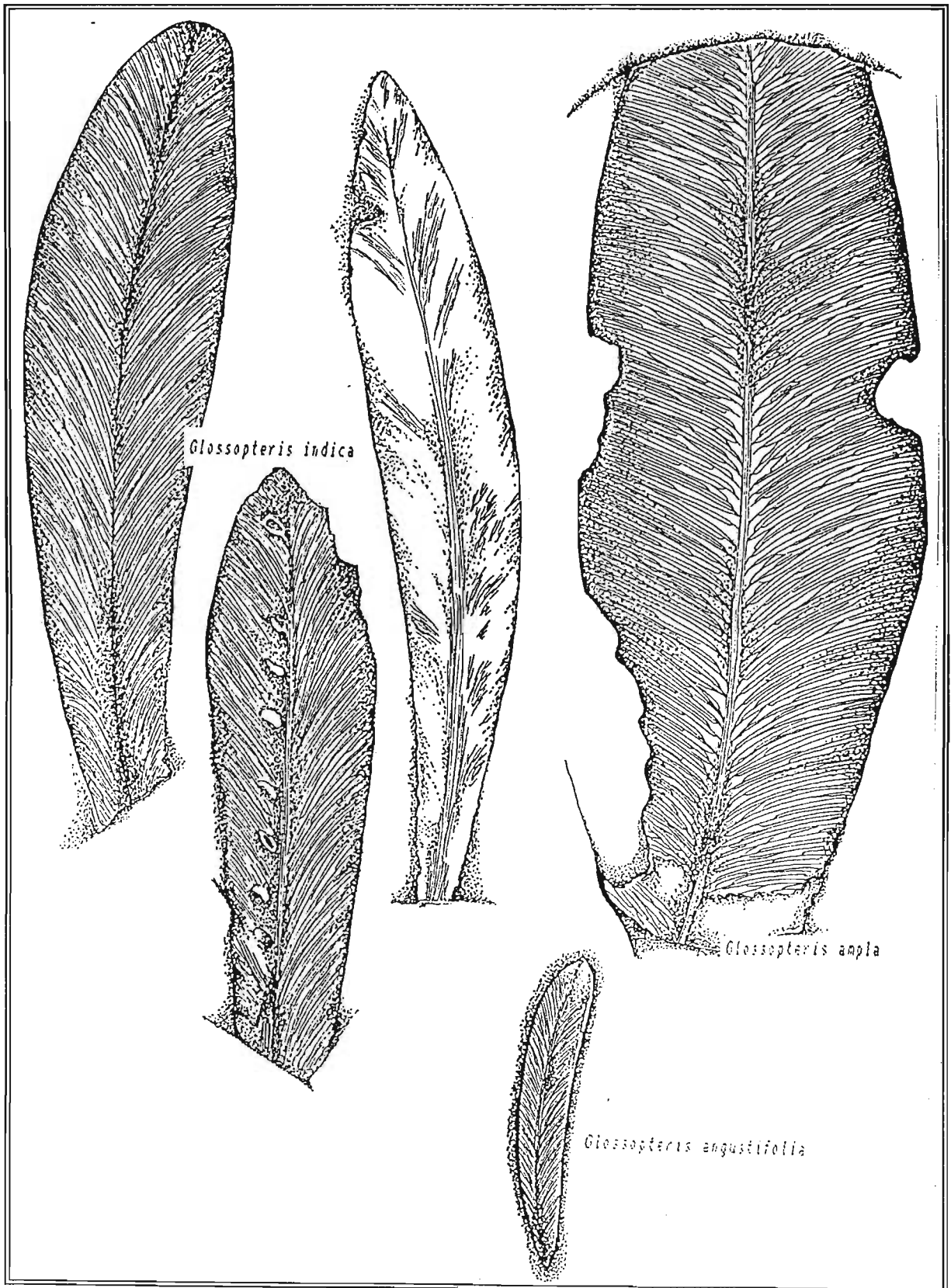


Figure 4.1 Some examples of *Glossopteris* leaves discovered in the Beaufort sediments of the Estcourt region. Scale - life size.

Glossopteris stenoneura - The leaf tapers gradually from a rounded apex into a cuneate base. The margins are rather straight and the secondary veins arch evenly and steeply towards the margin.

Specimens of glossopterid scale leaves of various sizes and shapes were also found. Although none could be properly identified, some are similar to the scale-leaves of Anderson and Anderson's (1985) *Lidgettonia inhluzanensis*, which are highly modified scale leaves which hold fruit (Fig. 4.2). The apex is bluntly cuspidate and the base truncate to broadly attenuate. It is the most diverse glossopterid genus and the dominant form in the Estcourt Formation. Its range is Upper Permian.

Sample 15 (Fig. 4.2) is attributed to Anderson and Anderson's scale-leaf gen.D. The leaves are small and lanceolate with a sharply acute apex and rounded base. Scale leaves like these occur in a few assemblages in the Estcourt Formation (Anderson and Anderson, 1985).

Sample 1 (Fig. 4.3) is the impression of the Permian sphenophyte, *Schizoneura gondwanensis*. This is better known as a horsetail and might have formed bamboo like stands fringing or actually in shallow waters and swamps (King, 1991). The leaflets are fused to form two opposite lobes at the axial nodes. The leaflets are broadly lanceolate with acute tips. The veins run parallel from apex to base. There are usually 5-14 fused leaflets. It is found in the Upper Permian.

Sample 19 (Fig. 4.3) is part of a large bipinate frond belonging to the Permian filicophyta *Sphenopteris lobifolia*. Each pinnule is strongly lobed with midrib and bifurcating veins to each lobe. This plant was found widespread throughout Gondwana Permian.

4.3 Discussion

The above described plants are all of Permian age. Of great importance is the distribution of the *Glossopteris* flora in the Estcourt region. *Glossopteris* disappeared before the end

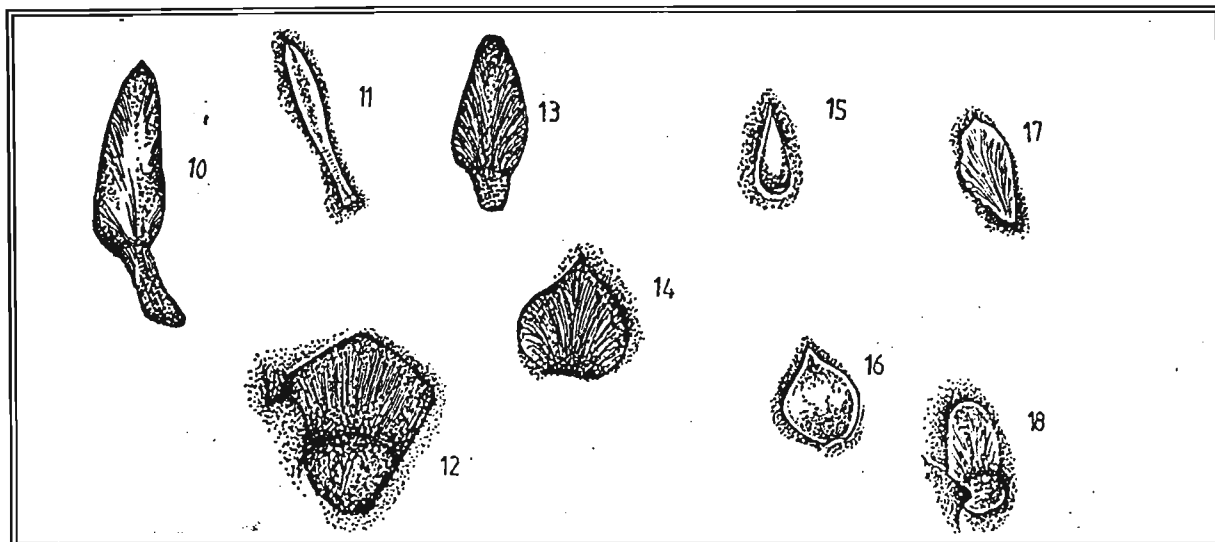


Figure 4.2 Life size diagrams showing glossopterid scale leaves.

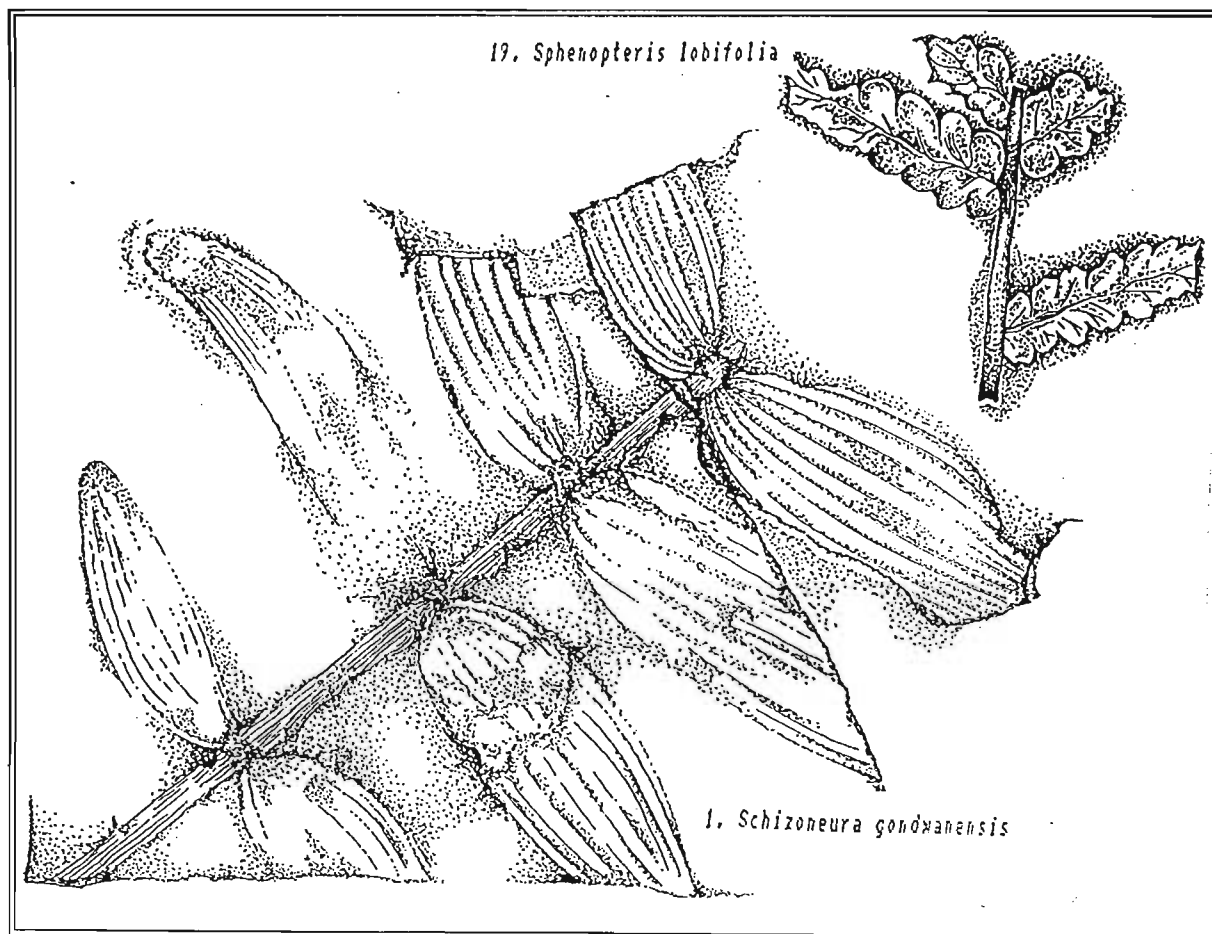


Figure 4.3 Life size diagrams showing the Permian sphenophyte *Schizoneura gondwanensis* and the Permian filicophyta *Sphenopteris lobifolia*.

of the Permian to be replaced by a transitional flora (Tucker and Benton, 1982; King, 1991; and Rayner 1992).

In the Lowland area, the horizon containing both *Lystrosaurus* and *Dicynodon* bones is overlain by sediments containing fossilised wood *Dadoxylon*, which is thought to most likely be the bearer of *Glossopteris* leaves (Rayner, 1992).

Based on the assumption that *Dadoxylon* and *Glossopteris* are of the same plant, it can be said that the sediments bearing the two dicynodon skulls are Late Permian in age, thereby indicating that *Lystrosaurus* evolved during Late Permian times.

5. FOSSILISED INSECT IMPRESSIONS.

Riek (1973) has found fossil insects from only four localities in the *Daptocephalus* biozone.

Two wing and one whole insect impressions were found in a dam excavation 10 km east of Estcourt. Using Riek's (1973) identification of fossil insects, it was found that the insects belong to the order *Hemiptera*. The entire insect impression (Fig. 5.1) is identified as *Ignotala mirifica*, meaning "strange, wonderful wing". The full length of the insect is 80mm (a length of 105mm is recorded by Riek), and at its widest point measures 55mm. The two wing impressions measuring 67mm and 40mm respectively, were identified as being *Megoniella multinerva* (Fig. 5.2).

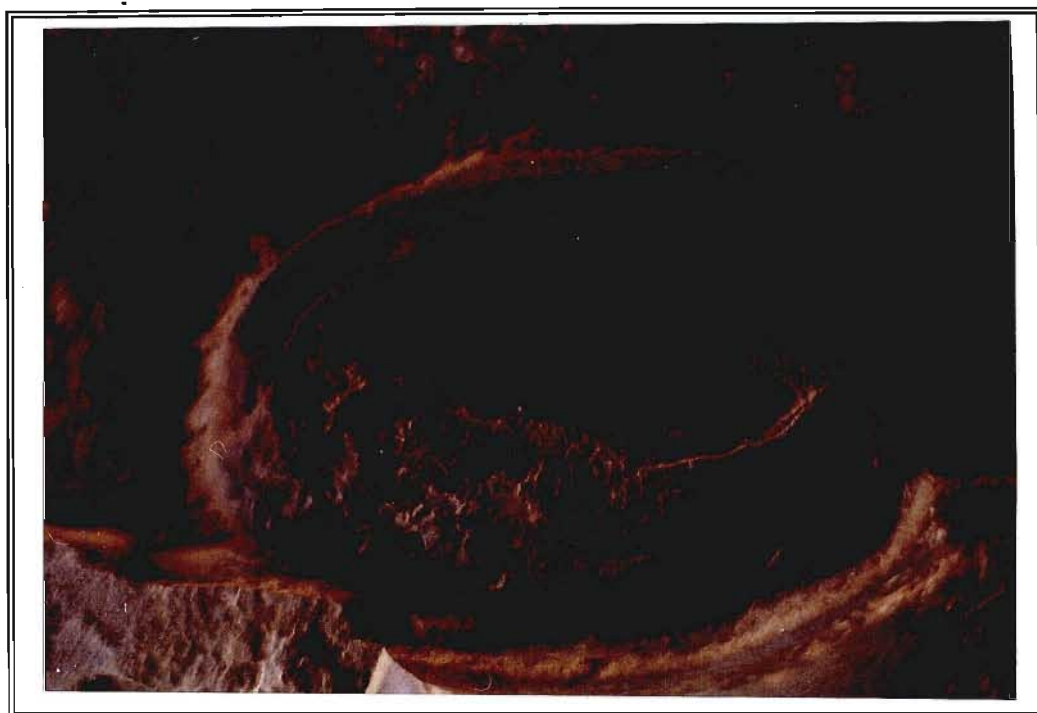


Figure 5.1 Entire insect impression identified as *Ignotala mirifica*. Line measures 80mm.

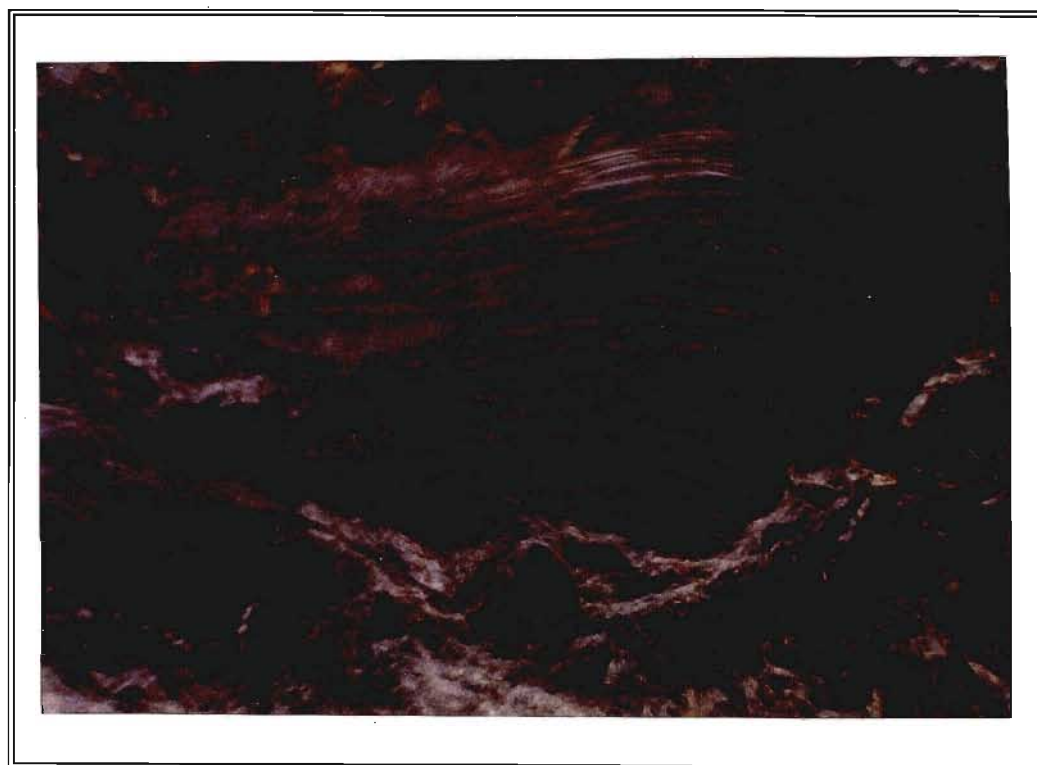


Figure 5.2 Fossilised wing impression identified as belonging to *Megoniella multinerva*. Line measures 67mm.

6. PALAEOICHOLOGY OF THE BEAUFORT SEDIMENTS

The study of fossil traces left by the activity of formerly living organisms is called Palaeoichnology (MacRae, 1990 and Sarjeant, 1975). The history of palaeoichnology officially began in 1828, with the description of tracks from red sandstones at Corncockle Muir in Scotland, later recognised as amphibian tracks (Sarjeant, 1975). However the first authenticated observation of fossil traces was made some 26 years earlier by a New England farmboy, who discovered dinosaur tracks impressed in the red sandstones of the Connecticut Valley, U.S.A (Sarjeant, 1975). The oldest tracks recorded are those of amphibians dating back as far as 380 million years (Lockley, 1991).

The Fossil dam log describes a series of shales that are traversed by numerous trace fossils, both invertebrate and vertebrate. The shoreline log also yields examples of both vertebrate and invertebrate trace fossils, and the Lowlands and Kudu stream logs also mention invertebrate traces along the surfaces of their sediments. These trace fossils are discussed in the following sections, and are divided into invertebrate and vertebrate sections.

6.1 Palaeoichnology of the Estcourt sediments (excluding tetrapod trackways)

The Permian fluvio-lacustrine strata of the Estcourt region are traversed by the numerous tracks and traces of various organisms, from soft-bodied worms to crustaceans and fish. Very little work has been done on fresh-water palaeoichnology, making comparisons and identification difficult. Smith (1993a) records biological colonisation of floodplain palaeosurfaces from the Beaufort Group, Late Permian, with very little information provided by other authors on Permian ichnofossils.

The invertebrate ichnofossils are classified on a morphological basis using Simpson's (1975) morphological classification.

6.1.1 Marginal lacustrine palaeoichnology

Planolites-like traces (Fig. 6.1) - These are tunnels and shafts of uniform diameter. Similar traces have been recorded by Smith (1993a) on proximal crevasse splay surfaces, and are thought to be made by soft-bodied worm-like organisms.

Thalassinoides-like traces (Fig. 6.2) - These are invertebrate tunnels and shafts of variable diameter which form an irregular network on the sediments surface.

Gordia-like traces (Fig. 6.3) - These are simple, trail-like traces left by invertebrates, that wind freely on surfaces showing no ornamentation.

Helminthoidea-like trace (Fig. 6.4) - These are trail-like traces that form complex patterns of winding trails that contact each other. The trail is simple with no ornament.

6.1.2 Basinal lacustrine palaeoichnology

Beaded-like trails (Fig. 6.5) - These invertebrate trails form scribble patterns or occur as overlapping circular loops, and consist of a series of linked pits. The same trace is noted by Smith (1993a) on crevasse splay palaeosurfaces, where they are compared to the trails of some modern nematode worms. Simpson's morphological classification quotes *Tasmanadia* as an example of this kind of track.

Undichmus sp. traces (Fig. 6.6 and Fig. 6.7) - These are the traces left by the caudal and pectoral fins of freshwater fish (Smith, 1993a).

Diplichnites type traces (Fig. 6.6) - These are the tracks left by freshwater arthropods. Similar traces are recorded from Permian floodplains by Smith (1993).



Figure 6.1 *Planolites* - like trace on surface of marginal lacustrine sandstone. Location - 13.5m mark on Shoreline profile. Scale is 5cm long.

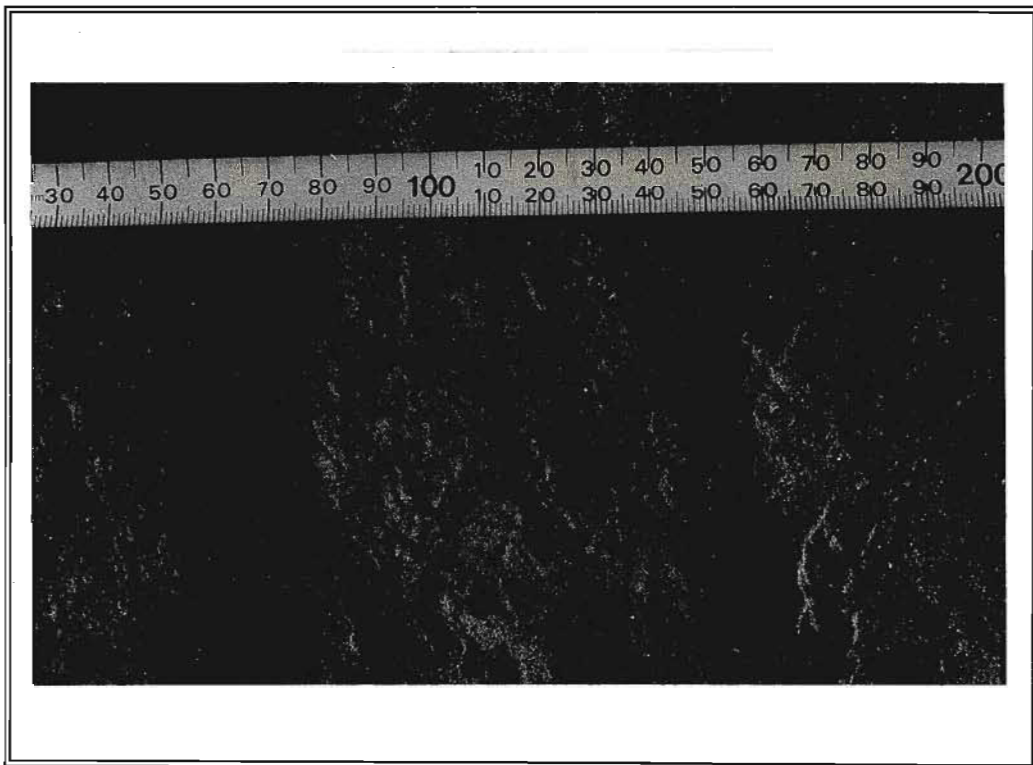


Figure 6.2 *Thalassinoides* - like trace on surface of marginal lacustrine sandstone forming part of silt/sand couplets. Location - 2.5m mark on Bedstead profile.



Figure 6.3 *Gordia* - like traces left on marginal lacustrine sandstone. Location - 13.5m mark on Shoreline profile. Scale is 5cm long.



Figure 6.4 *Helminthoidea* - like trace on marginal lacustrine sandstone. Location - 13.5m mark on Shoreline profile. Scale is 5cm long.

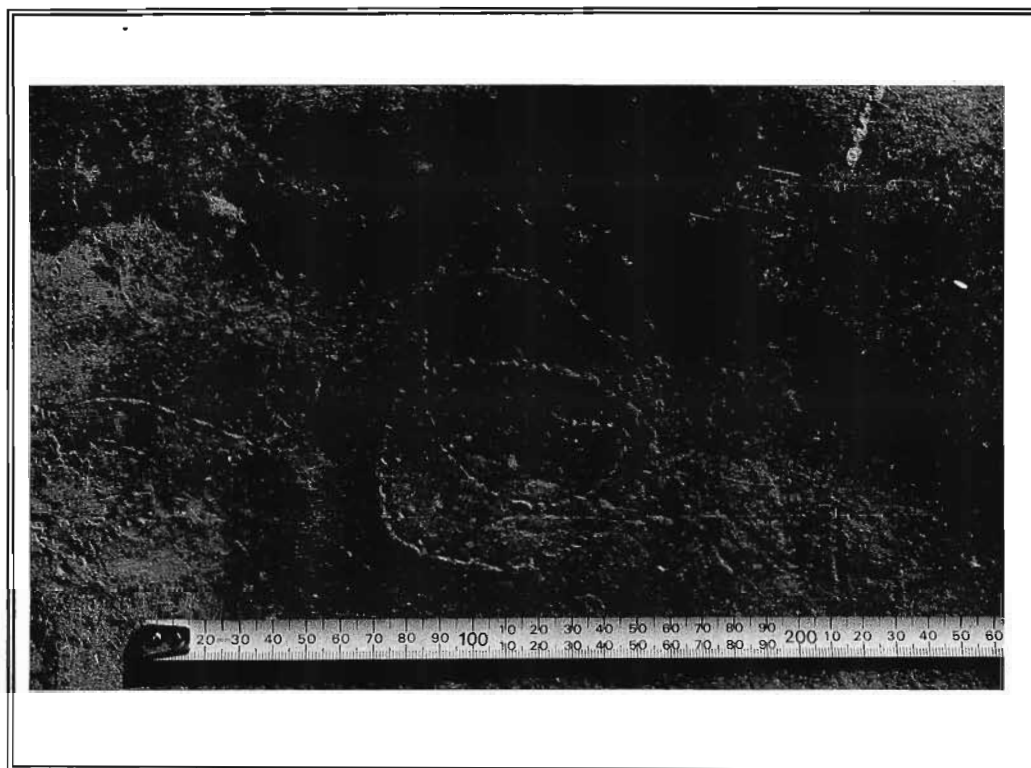


Figure 6.5 Beaded trail left on basinal lacustrine sediments.

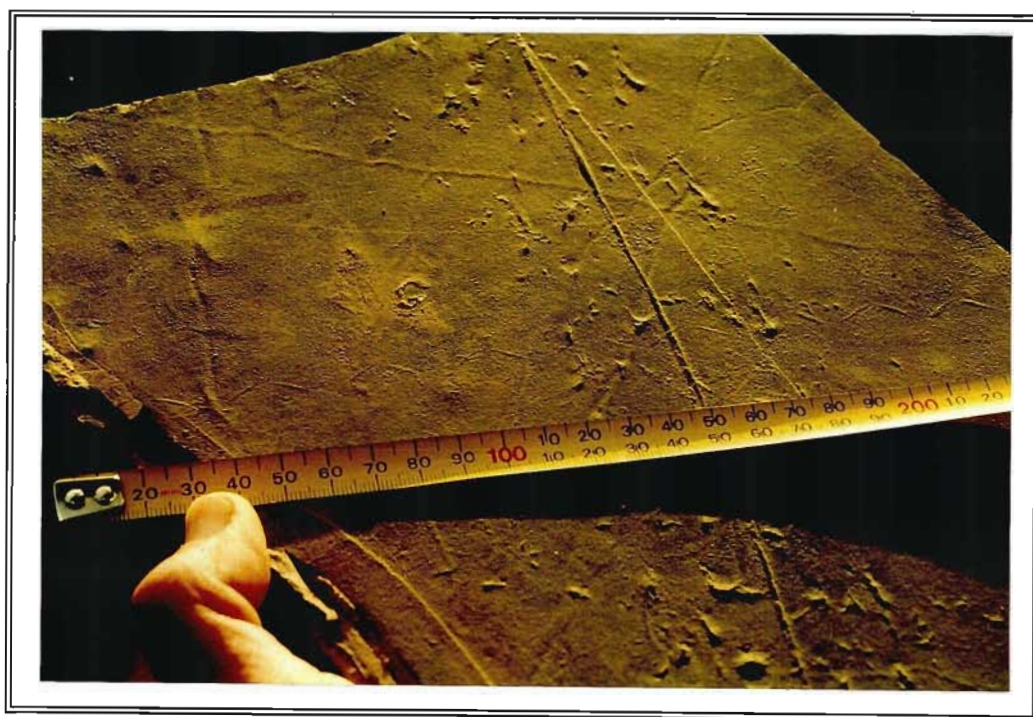


Figure 6.6 *Undichnus* trail made by a Late Permian fish on a basinal lacustrine mudstone (indicated by arrow).
Also note Diplichnites trackway traversing the slab north to south.



Figure 6.7 Fossilised basal lacustrine mudstone traversed by tetrapod footprints, *Undichnus* trails, and scribble-like, invertebrate beaded trails. Arrows mark location of *Undichnus*.



Figure 6.8 Palaeosol siltstone traversed by a burrow consisting of overlapping lobes of sediment.



Figure 6.9 *Repichnia* - like tracks on a basinal lacustrine mudrock. Arrows mark the position of the tiny footprints.



Figure 6.10 *Cubichnia* - like traces on a basinal lacustrine mudrock. Traces consist of paired lobes. *Rusophycus* trace of the arthropod *Triops*. (pers.com. T.R. Mason).

6.1.3 Floodplain Ichnofossils.

Figure 6.8 shows vertical and horizontal burrows made in a palaeosol siltstone. The burrow consists of overlapping lobes of siltstone indicating movement from right to left, and was most likely made by a deposit feeder.

6.1.4 Miscellaneous ichnofossils

Two sets of traces left on basinal lacustrine muds represent small animals. Both are classified using Simpson's (1975) behavioral classification. The first (Fig. 6.9) is a trackway consisting of tiny imprints consisting of splayed digit impressions. The causal organism is unknown, and is classified as *Repichnia*.

The second ichnofossil (Fig. 6.10) is a series of well-defined, paired lobes. They are thought to represent resting traces and are therefore classified as *Cubichnia*. They are similar in nature to *Rusophycus* traces found in East Greenland (Bromley and Asgaard, 1979), the only difference being the absence of striations in the Estcourt examples. These traces range from Lower Cambrian to Triassic in age and are found in both marine and freshwater deposits.

6.1.5 Discussion

Frey and Pemberton (1979) classify ichnofossils according to environmental conditions, and seven ichnofacies, six of which represent marine environments. Due to the lack of ichnological research, there is only one non-marine ichnofacies, the *Scoyenia* ichnofacies. All of the above ichnofossils fall into this ichnofacies and represent a common environmental denominator, namely the shore zone of ephemeral lakes and sluggish streams (Frey and Pemberton, 1979).

6.2 Vertebrate tetrapod trackways

6.2.1 Introduction

Of all the branches of palaeoichnology, the study of vertebrate footprints is the most viable as they indicate a more abundant and varied vertebrate fauna than can be deduced from skeletal remains (Sarjeant, 1975). Trackways are an important source of information as to the amount of animal activity in a certain area, especially if no bones are discovered.

A good example of this are the shales of the Fossil dam log. These shales occur in an area that is devoid of fossil bones, and yet they are traversed by many tetrapod trackways indicating a larger vertebrate population than can be deduced from the fossils. These trackways yield important information as very few Late Permian tracksites have to date been discovered despite the diverse Beaufort Group fauna (MacRae, 1990 and Smith, 1993a)

Information that can be obtained from the trackways includes the animals stride, pace, gleno-acetabular distance, in some cases speed of the animal (if the species of animal is known) (Alexander, 1976), and the stance of the animal deduced from the trackway width and pace angulation. These measurements can be made on both quadrupedal and bipedal trackways (appendix 5). Figure 6.11 shows how these measurements are taken from a quadrupedal trackway.

The vertebrate trackways of the Fossil dam log were uncovered and mapped during the winters of 1994 and 1995 during the excavation of a farm dam on the farm Rensburgspruit situated 10km east of Estcourt (Marked 4 on fig. 2.2). The more complete examples were mapped onto graph paper, from which the various measurements were taken (Appendix 6).

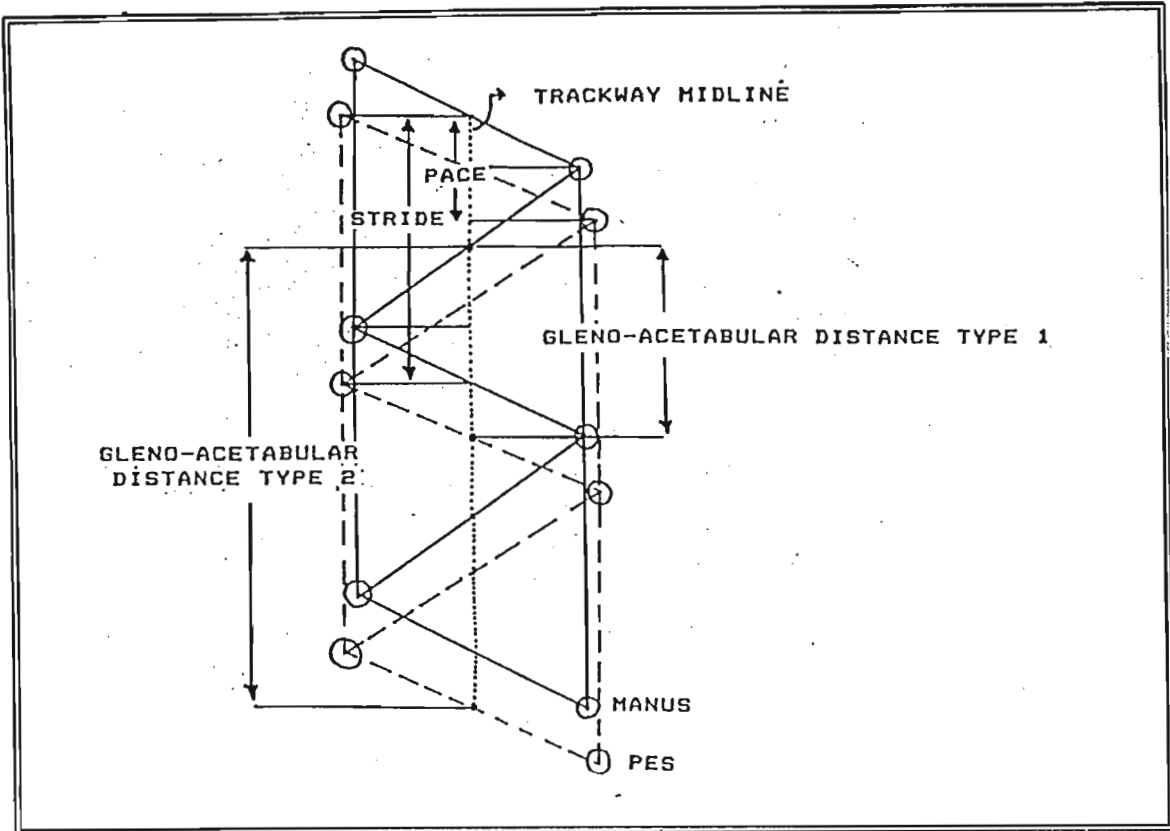


Figure 6.11 Diagram demonstrating how quadrupedal trackways are measured.

6.2.2 Detailed description of trackways.

A total of 15 trackways were mapped in detail. The trackways were uncovered in two excavations (Fig. 6.12, and 6.13), with 12 trackways measured from excavation 1, and two from excavation 2. Each trackway is discussed in detail with the aim of comparing the various trackways. The descriptions include a correctly scaled diagrammatic representation of the trackways, and a summary of the various measurements taken. The tables of all the individual measurements are contained in appendix 7, with the diagrammatic representation of how the measurements were obtained.

It must be remembered that all of the measurements are only approximate, especially if the causal animals are dicynodonts which move with a certain degree of lateral undulation of the vertebral column. In most of the trackways it is simple to distinguish the manus from the pes, as the prints occur in pairs, with the manus print in front of the pes print. In cases where this relationship is not so obvious, the manus prints are taken as those that are closer

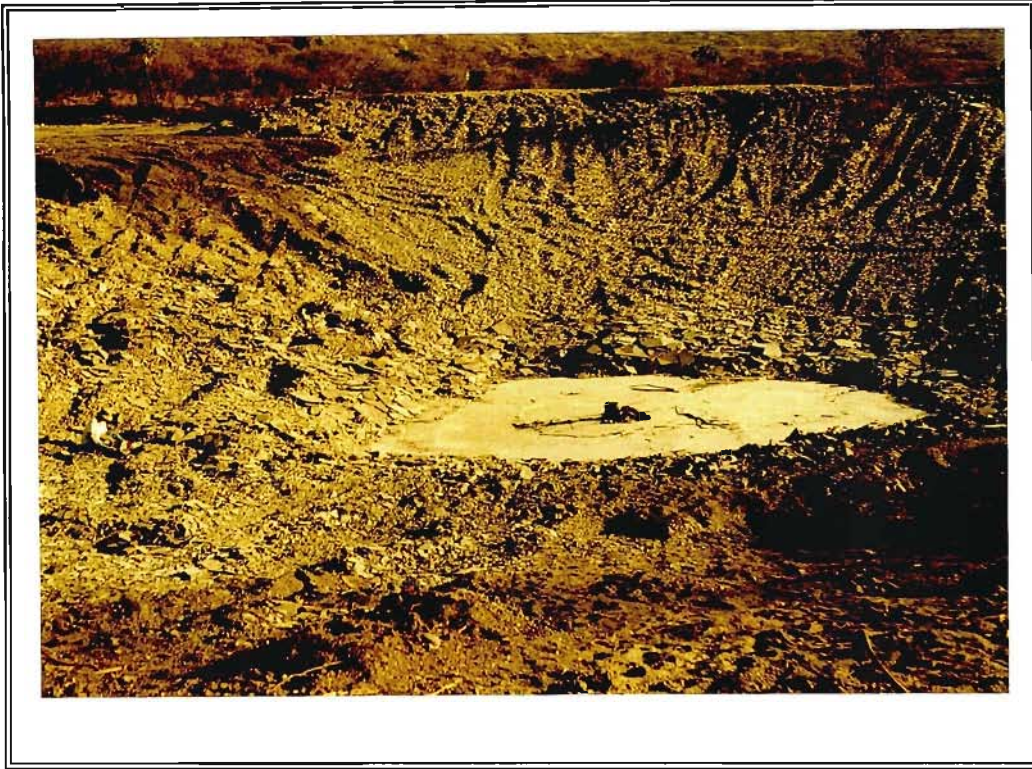


Figure 6.12 Dam excavation 1 on the farm Rensburgspruit. Attitude towards the northwest, person for scale.

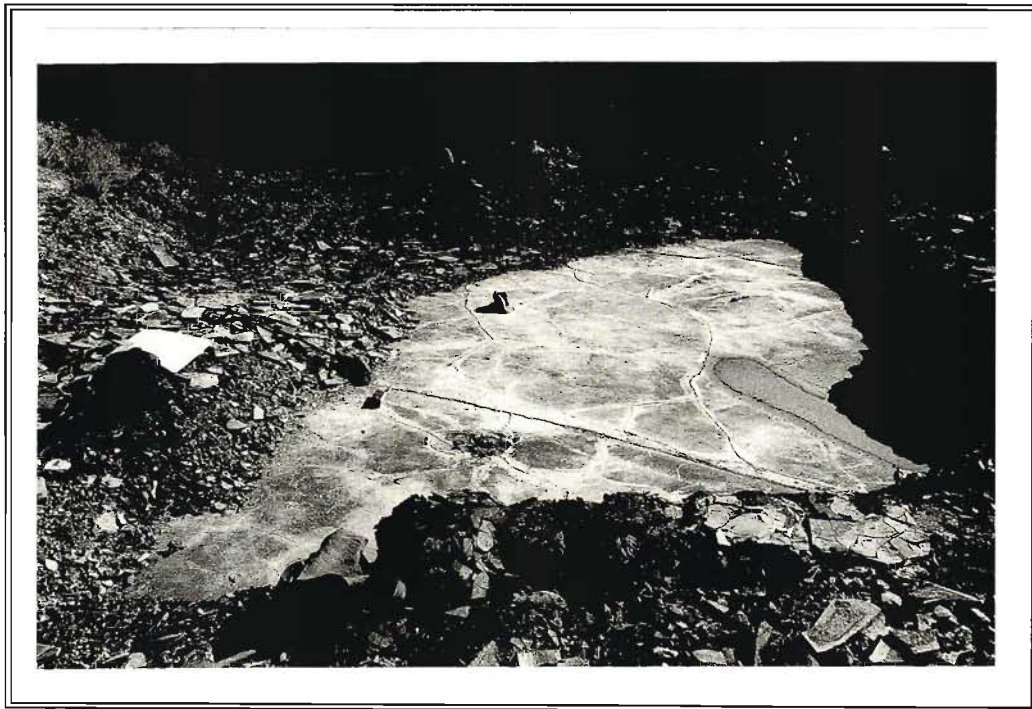


Figure 6.13 Dam excavation 2 over the northwest wall of excavation 1. Attitude towards the north, white cardboard square measures 50cm x 50cm.

to the midline, or show the most rotation towards the midline. It is not possible to define the type of GA with total certainty, as the type of causal animal is unknown. All of the trackways are composed of prints made up of digit impressions only, with only a few exceptions that show palm prints.

An important aspect of these measurements is to ascertain if there is a relationship between the pace angulation, the pace or stride, and the trackway width. In quadrupeds, a high pace angulation indicates an upright stance, and is accompanied by a decrease in the trackway width as the limbs are positioned further under the body. However if the causal animals were dicynodonts, the gait was accompanied by a certain degree of lateral undulation of the trunk. Therefore a narrower trackway may not necessarily represent a more upright stance, but rather a greater undulation of the body throwing the limbs further forward and nearer to the midline, thus resulting in a higher pace angulation. This greater undulation would therefore also be accompanied by a longer stride and pace.

Appendix 7 also contains tables listing the pace angulations in ascending order for the various trackways, to ascertain any relationship with the pace and trackway width measurements. However this proved unsuccessful, resulting in the trackways needing to be divided into left and right to see any relationships.

Excavation 1, Surface 1 - Trackway 1 (Fig. 6.14)

	AVERAGE	NO. OF READINGS	STD DEVIATION
STRIDE	75.2cm	9	5.4cm
PACE ANGULATION			
PES (degree's)	85.0	6	9.6
MANUS (degree's)	91.0	6	8.2
TRACKWAY WIDTH			
MANUS-PES (STANDARD)	38.5cm	11	2.3cm
MANUS-MANUS	35.4cm	8	1.7cm
PES-PES	40.3cm	8	2.8cm
PACE	36.9cm	10	5.3cm
GLENO-ACETABULAR DISTANCE			
TYPE 1	50.7cm	3	3.3cm
TYPE 2	123.5cm	2	7.5cm

This trackway trends towards the northeast, and is short consisting of only four manus and pes sets (includes left manus and pes pair and right matching manus pes pair). The majority the footprints consist of either three or four digit impressions, with one footprint made up of five digit impressions. The toe prints curve towards the midline, although the manus prints do so to a greater degree.

There is no significant difference between the distance of the manus and pes from the midline, although on the whole the pes trackway width is slightly wider. The pace angulation of the manus is higher than that of the pes, with a difference of 6 degrees. The average stride is 75.2cm, and remains fairly constant throughout the trackway.

The left side of the trackway shows a decrease in the pace angulation for both the pes and the manus when progressing up the trackway. The right side of the trackway shows the manus pace angulation decreasing, and a decrease in the last two pace angulations of the pes prints. This decrease in pace angulation is accompanied by an increase in the trackway width, and is most likely the result of a decrease in the lateral undulation

of the animals trunk, thus making the trackway wider. No comparisons were made with the stride length as there were too few readings for comparative analysis.

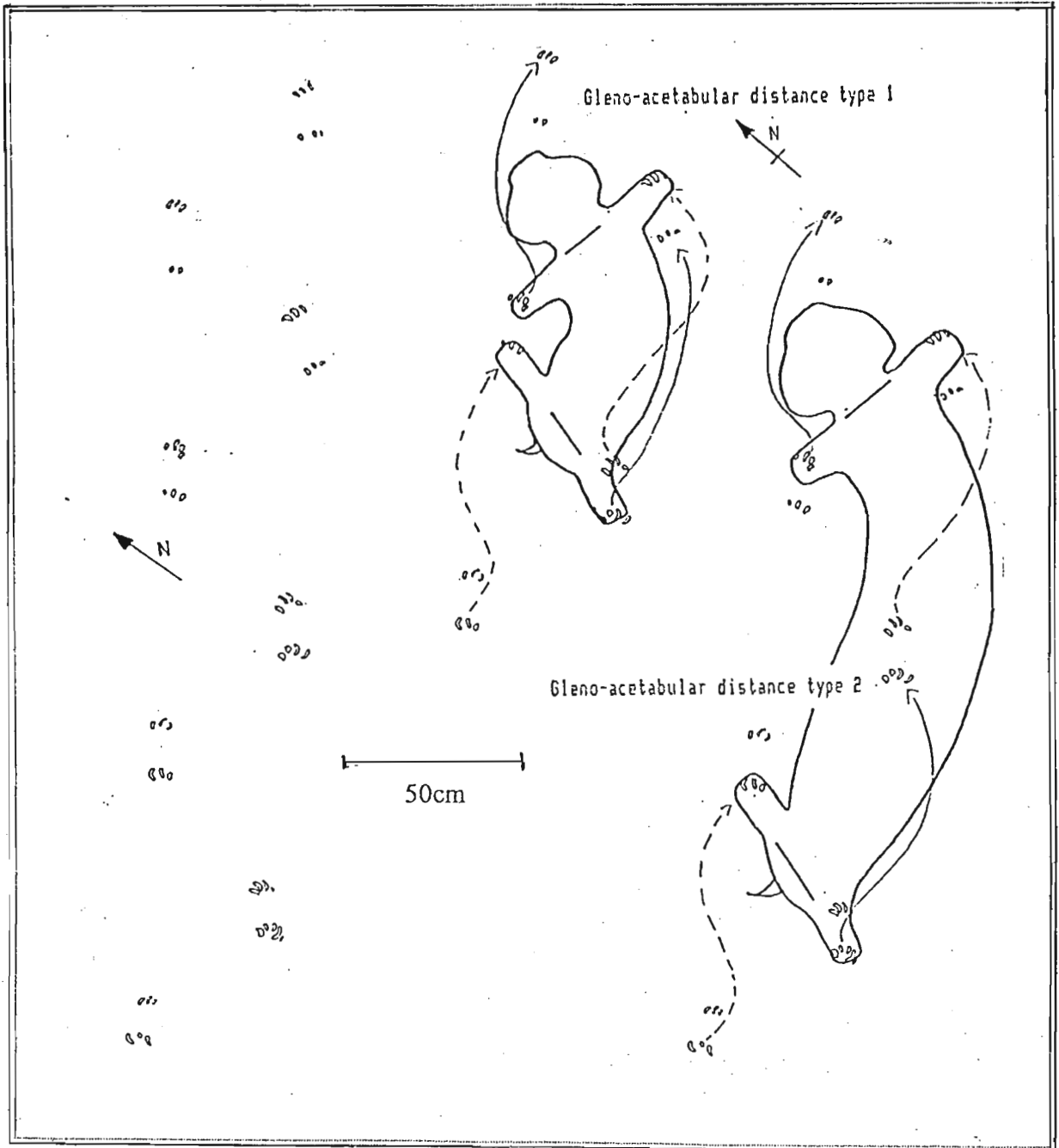


Figure 6.14 Excavation 1, Surface 1 - Trackway 1

Excavation 1, Surface 1 - Trackway 2 (Fig 6.15)

	AVERAGE	NO. OF READINGS	STD DEVIATION
STRIDE	51.7cm	10	2.4cm
PACE ANGULATION			
PES (degree's)	60.8	6	2.9
MANUS (degree's)	71.5	6	3.7
TRACKWAY WIDTH			
MANUS-PES (STANDARD)	40.3cm	13	2.9cm
MANUS-MANUS	36.2cm	6	1.5cm
PES-PES	43.8cm	5	1.7cm
PACE	26.1cm	12	4.2cm
GLENO-ACETABULAR DISTANCE			
TYPE 1	44.0cm	3	0.8cm
TYPE 2	95.0cm	2	0.0cm

This trackway moves in a west-northwest direction, and consists of four manus-pes sets, with individual footprints having only either two or three digits impressions. The individual digit impressions show little curvature, and are mostly just toe prods.

Both the pes and manus prints have relatively low, acute pace angulations, that differ by approximately 11 degrees. The pace angulation of the manus prints is higher than that of the pes prints. The stride averages at 51.7cm and is constant with a low standard deviation, indicating a fairly constant stride.

The left side of the trackway shows a greater distance of the pes prints from the midline than those of the right side of the trackway. It could also therefore be said that the right manus prints are further from the midline when compared to the left manus prints. This indicates a different degree of lateral undulation during one phase of the animals movement. It appears that the phase of movement where the left manus and right pes were brought forward, there was a greater degree of lateral undulation when compared to the next phase when the right manus and left pes were brought forward. This greater undulation would

place the left manus and right pes closer to the midline. This would result in the pattern seen. The above relationship can also be seen when comparing the pace angulations of the left prints with those of the right prints. As would be expected, the angles of the left manus prints are higher than those of the right manus prints, and the angles of the left pes prints are lower than those of the right pes prints. The only instance this changes is where the line joining the manus prints touches that of the pes prints, resulting in a decrease in the pace angulation indicating a decrease in the amount of lateral undulation.

This would indicate that there is a relationship between pace angulation and trackway width. By comparing the left side to the right side of the trackway, it can be seen that an increase in pace angulation is accompanied by a decrease in distance of that print from the midline.

It can also be seen that the pace angulation of the left pes prints and the pace angulation of the right manus prints are fairly constant, with small standard deviations. However, the pace angulation of the left manus prints decreases as the trackway progresses. This decreasing angulation is accompanied by an increasing pace angulation of the right pes. This created a stable stance, since, if both had increasing pace angulations, this would have to be accompanied by increasing angulations of the other two limbs, but since their angulations remain constant, the decreasing angulation of the left manus compensates for the increasing angulation of the right pes. This compensation results in no definite increasing or decreasing trackway width.

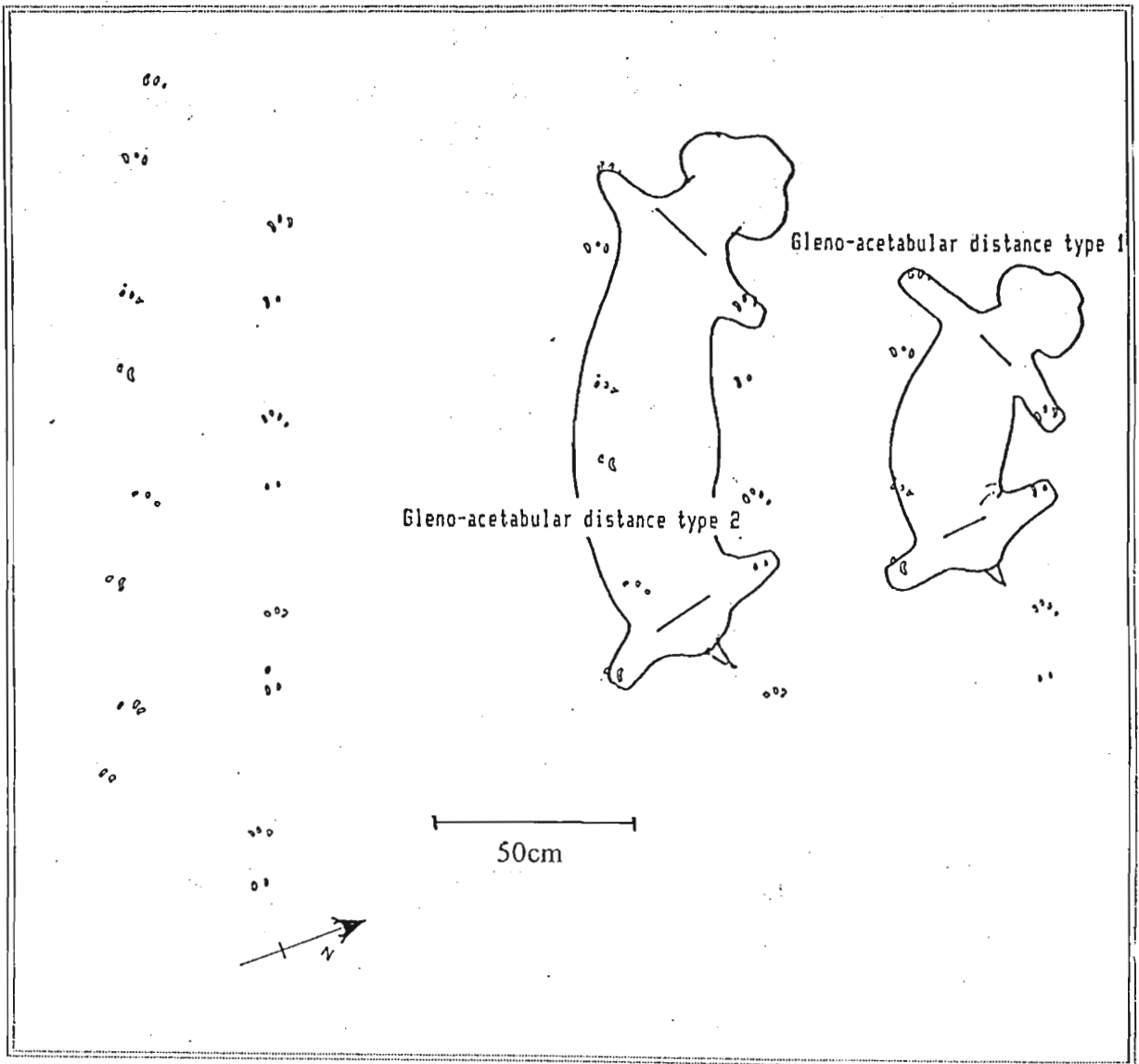


Figure 6.14 Excavation 1, Surface 1 - Trackway 2

Excavation 1, Surface 1 - Trackway 3 (Fig. 6.15)

	AVERAGE	NO. OF READINGS	STD DEVIATION
STRIDE	69.8cm	13	5.4cm
PACE ANGULATION			
PES (degree's)	81.6	8	5.9
MANUS (degree's)	99.6	8	5.2
TRACKWAY WIDTH			
MANUS-PES (STANDARD)	34.8cm	10	1.4cm
MANUS-MANUS	29.5cm	6	1.1cm
PES-PES	40.5cm	6	0.8cm
PACE	35.7cm	15	5.3cm
GLENO-ACETABULAR DISTANCE			
TYPE 1	52.3cm	4	4.1cm
TYPE 2	121.7cm	3	5.8cm

This trackway moves towards the north-northwest. The trackway consists of five manus-pes sets. Both the manus and pes prints are turned in towards the midline, however the manus prints do so to a greater degree. The width of the pes-pes and manus-manus trackways is fairly constant, with the pes prints being further from the midline than the manus prints. This indicates a regular sinusoidal movement throughout the length of this trackway. The standard deviations of the measurements is fairly minor representing a regular gait. The long stride and narrow trackway, plus the high pace angulations indicates an animal that was moving with a great deal of lateral undulation of the body.

The difference in the average pace angulation measurements of the pes and manus prints is high, measuring 18 degrees, indicating a higher rotation of the glenoid as opposed to the acetabular. There are no comparative relationships when dividing the trackway into left and right. This is most likely the result of the stable, regular gait of the causal animal.

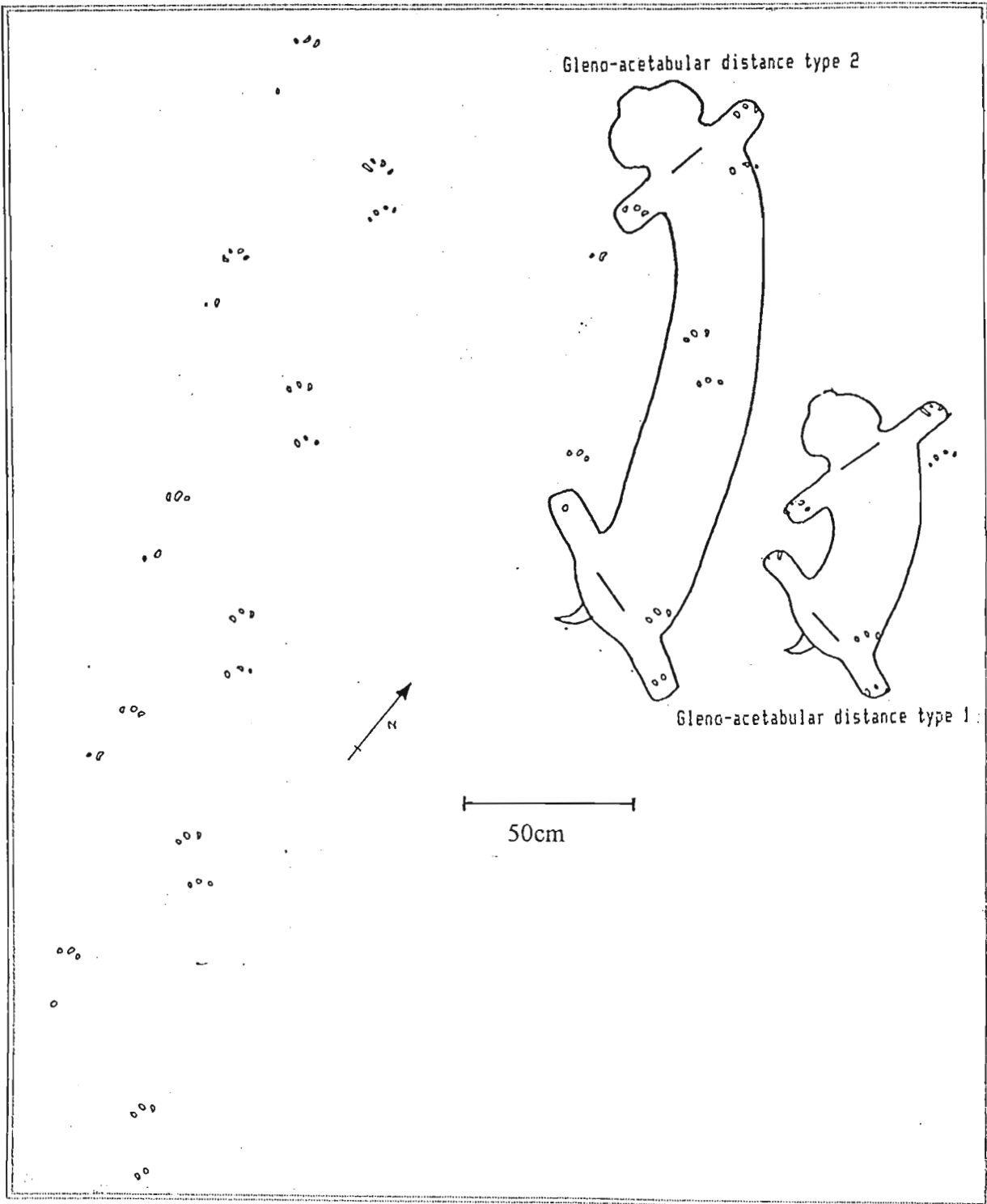


Figure 6.15 Excavation 1, Surface 1 - Trackway 3

Excavation 1, Surface 2 - Trackway 1 (Fig. 6.16)

	AVERAGE	NO. OF READINGS	STD DEVIATION
STRIDE	34.6cm	15	3.3cm
PACE ANGULATION			
PES (degree's)	77.3	7	5.3
MANUS (degree's)	95.6	7	7.9
TRACKWAY WIDTH			
MANUS-PES (STANDARD)	18.5cm	11	0.8cm
MANUS-MANUS	15.8cm	5	0.8cm
PES-PES	21.0cm	5	0.0cm
PACE	17.3cm	14	2.6cm
GLENO-ACETABULAR DISTANCE			
TYPE 1	27.8cm	4	1.6cm
TYPE 2	65.0cm	2	1.0cm

This south easterly moving trackway consists of five manus-pes sets composed of either two or three circular toe prods.

The first three sets of manus-pes prints show regular trackway widths, with the pes-pes trackway measuring wider than the manus-manus trackway. However with the last two sets of pairs, the trackway width alters, and again represents a phase in the stride of the animal where the lateral undulation of the trunk is different than in the following phase. However, unlike trackway 2 on surface 1, this change in the placement of the feet, is not accompanied by an increase in stride. Rather in this case the stride decreases, as does the pace angulation of both hind and fore limbs. There is also no great change in the trackway widths. The change in foot placement is likely due to a slowing of speed accompanied by a shorter stride, and lesser degree of lateral undulation of one phase of the step resulting in the trackway width pattern. This phase is where the left manus and right pes are brought forward.

The above relationship becomes apparent only when dividing the trackway into left and right. On both the left and right sides of the trackway, stride decreases in both manus and pes, as does the pace angulation for both manus and pes.

The average pace angulation of the manus prints is much higher than that of the pes prints, with an average difference of 18 degrees. Although there are only small standard deviations, this trackway shows that there is a relationship between the stride and pace angulation. As has already been seen, an overall decrease in stride is accompanied by an overall decrease in pace angulation. However there is no relationship to the trackway width which remains fairly constant.

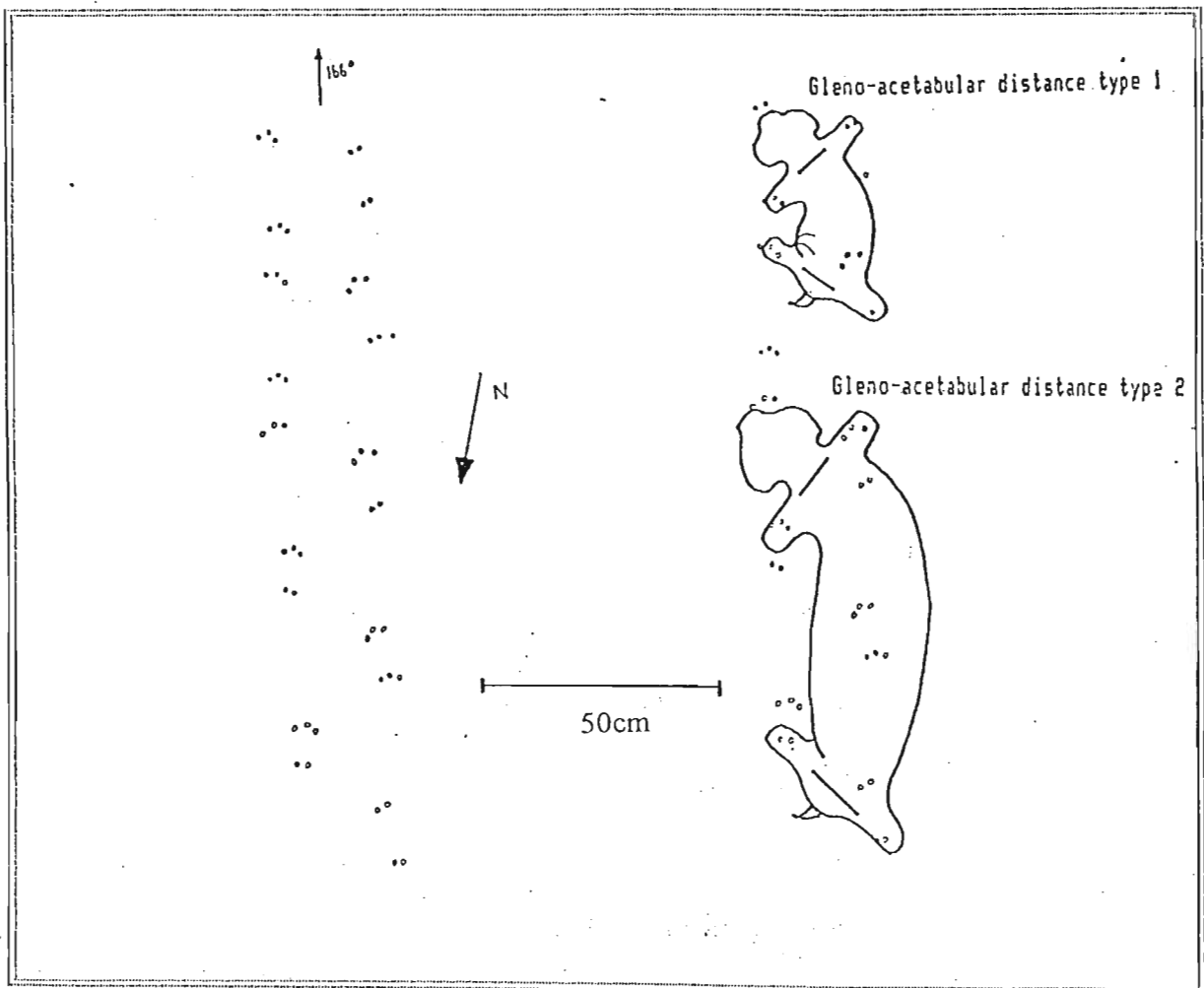


Figure 6.16 Excavation 1, Surface 2 - Trackway 1

Excavation 1, Surface 3 - Trackway 1 (Fig. 6.17)

	AVERAGE	NO. OF READINGS	STD DEVIATION
STRIDE	17.6cm	64	2.7cm
PACE ANGULATION			
PES (degree's)	67.5	32	8.5
MANUS (degree's)	73.3	34	9.4
TRACKWAY WIDTH			
MANUS-PES (STANDARD)	12.3cm	27	0.9cm
MANUS-MANUS	11.4cm	12	0.9cm
PES-PES	13.4cm	14	0.9cm
PACE	8.8cm	66	1.8cm
GLENO-ACETABULAR DISTANCE			
TYPE 1	15.4cm	16	1.2cm
TYPE 2	33.3cm	15	2.6cm

This trackway is the longest mapped consisting of 17 manus-pes pairs, and has a direction of movement towards the northwest. The individual prints consist of either three or four digits, and were extremely shallow. There is curvature of the digit impressions towards the midline, and on average, the manus prints are closer than the pes prints to the midline.

The standard deviations of the measurements are small, however when taking the size of the causal animal into consideration, small deviations are still indicative of large changes in the animals movement. Also, the standard deviations for the pace angulations are fairly high for any trackway. There is only a five degree difference between the pace angulation of the manus and pes, which is fairly acute reflecting an animal with a sprawled stance.

The trackway shows an irregular pattern of increasing and decreasing pace angulations. On both sides, the first four sets of pes and manus show an increasing pace angulation, and an approximate increase in the stride length. Following this is a complex array of increasing and decreasing patterns throughout the length of the trackway. These patterns

do match up across the midline, for example, if the angulation of the left manus increases, there is a corresponding increase in the angulation of the right manus. The length of the stride also corresponds across the midline. There is no apparent relationship between trackway width and the pace angulation and stride measurements.

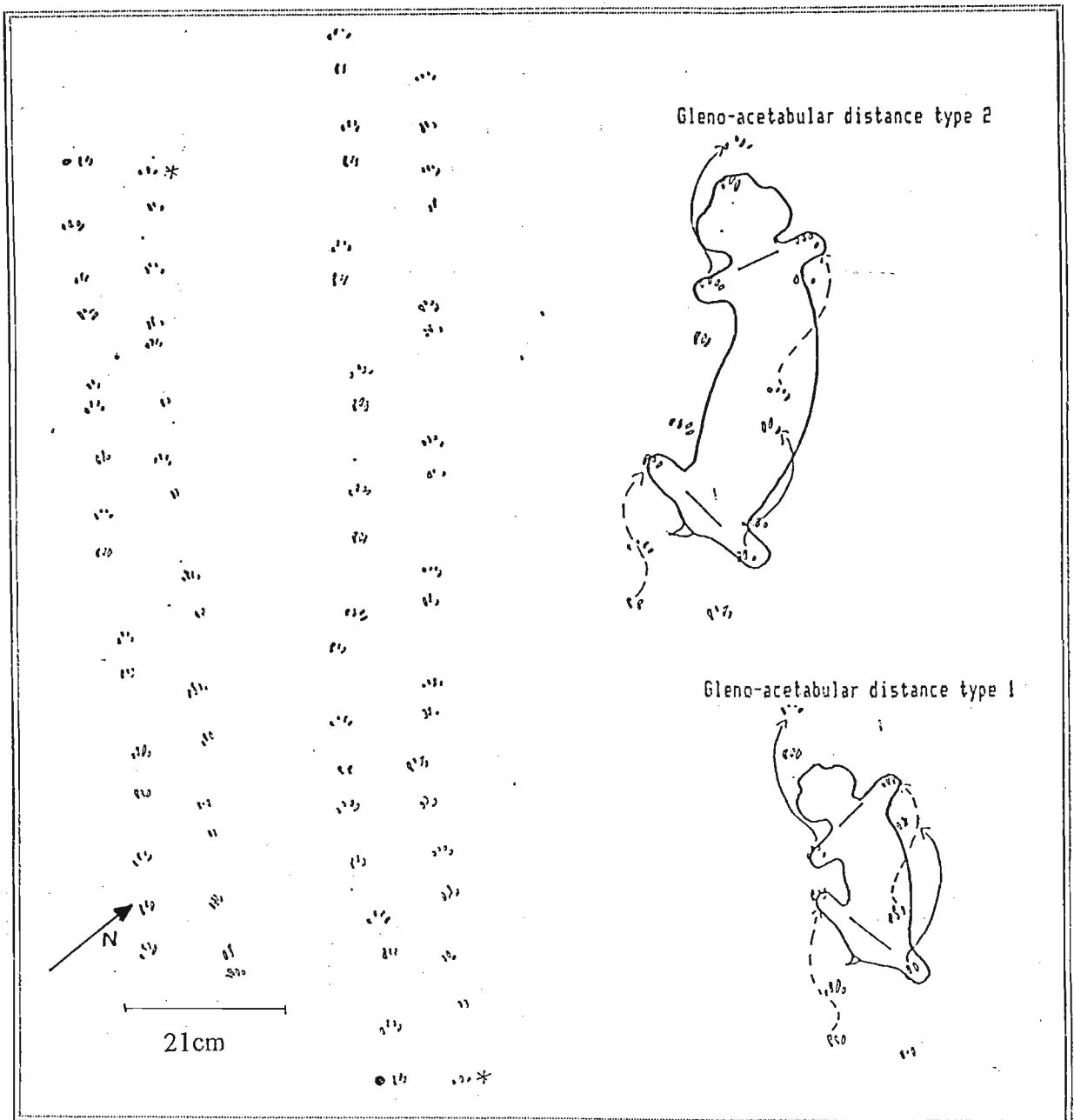


Figure 6.17 Excavation 1, Surface 3 - Trackway 1

Excavation 1, Surface 3 - Trackway 2 (Fig. 6.18)

	AVERAGE	NO. OF READINGS	STD DEVIATION
STRIDE	63.2cm	5	1.9cm
PACE ANGULATION			
PES (degree's)	96.0	4	7.8
MANUS (degree's)	109.3	4	7.3
TRACKWAY WIDTH			
MANUS-PES (STANDARD)	26.6cm	11	2.7cm
MANUS-MANUS	22.0cm	7	2.1cm
PES-PES	29.0cm	5	1.9cm
PACE	31.4cm	7	1.9cm
GLENO-ACETABULAR DISTANCE			
TYPE 1	43.5cm	2	0.5cm
TYPE 2	104.0cm	1	—

This short trackway consists of only three manus-pes sets and shows a direction of movement towards the southwest. The individual prints consist of either three or four digit impressions. The impressions are mostly just circular prods, with only slight curving towards the midline apparent in a few of the impressions. Again, the pes-pes trackway width is wider than that of the manus.

This trackway is narrow with a long stride, and the pace angulation is obtuse for both the hind and fore limbs. This pattern is most likely the result of a large degree of lateral undulation of the trunk throwing the limbs further forward and closer to the midline.

Comparisons of the two sides shows a trackway which narrows and a corresponding increase in pace angulation. The stride readings are too few for comparative analysis.

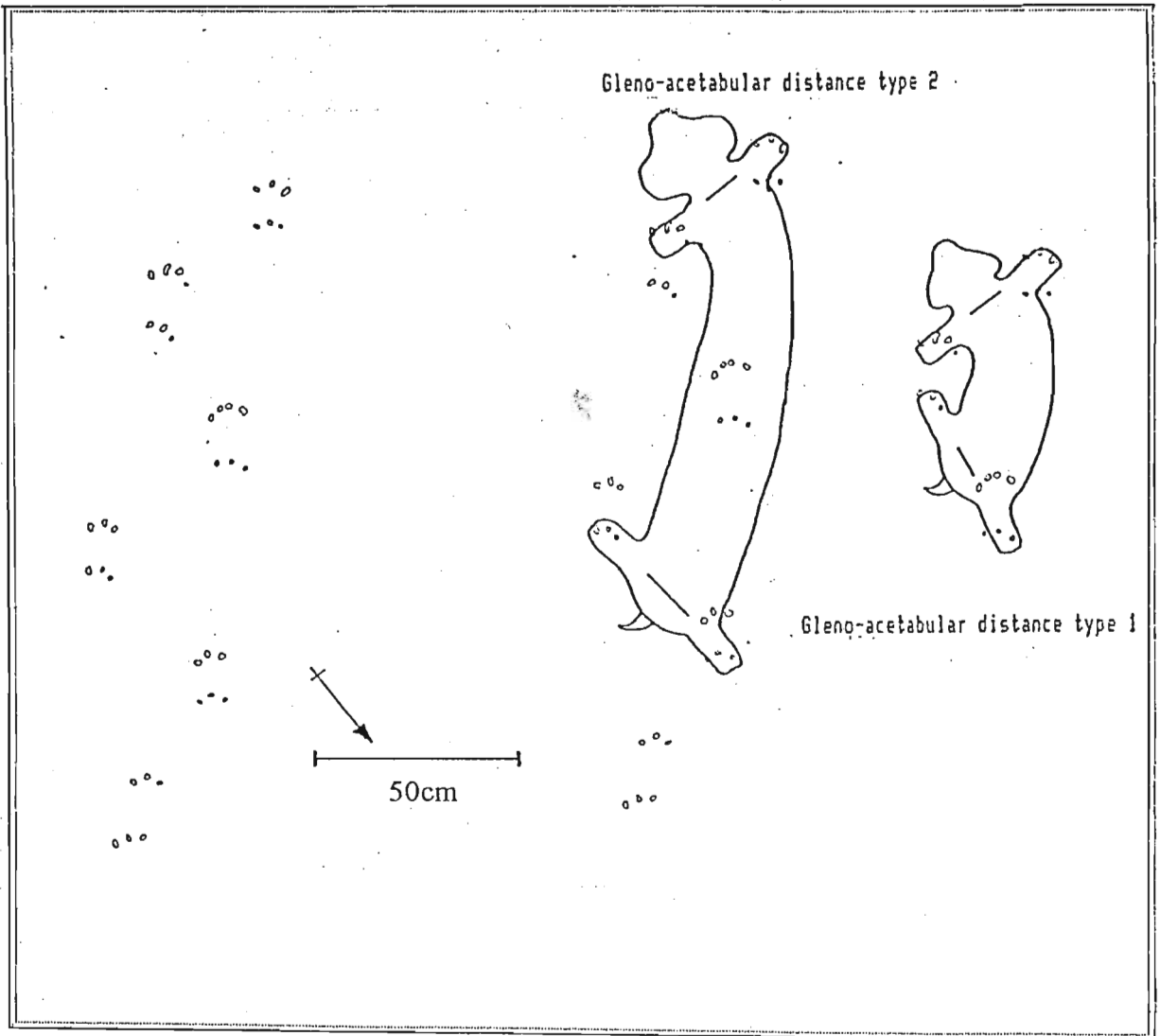


Figure 6.18 Excavation 1, Surface 3 - Trackway 2

Excavation 1, Surface 3 - Trackway 3 (Fig. 6.19)

	AVERAGE	NO. OF READINGS	STD DEVIATION
STRIDE	39.5cm	15	2.9cm
PACE ANGULATION			
PES (degree's)	75.1	7	5.9
MANUS (degree's)	83.8	8	5.8
TRACKWAY WIDTH			
MANUS-PES (STANDARD)	23.8cm	13	2.8cm
MANUS-MANUS	21.9cm	8	1.5cm
PES-PES	25.4cm	7	0.7cm
PACE	20.2cm	14	4.0cm
GLENO-ACETABULAR DISTANCE			
TYPE 1	35.3cm	3	0.9cm
TYPE 2	74.5cm	2	1.5cm

This southwesterly moving trackway consists of five manus-pes sets, with individual footprints showing two to four digits, some of which show curvature towards the midline, and in two cases digit drag impressions.

There is a difference between the two sides, in the positioning of the prints from the midline. The left side has the line of manus prints overlapping the line of the pes prints. The right side of the trackway follows form, with the manus prints closer to the midline than the pes prints.

The stride is short, and accompanied by low pace angulations that show high standard deviations. The stride is random with no particular increasing or decreasing pattern. The left manus, and right manus and pes pace angulations show a decreasing trend as the trackway progresses. This is accompanied by an overall decrease in the manus-manus trackway width, with the pes-pes width remaining fairly constant.

The stride averages at 39.5cm, and shows a repeatable pattern. For example, the first stride measures 38cm for the pes, and 43cm for the manus. The following stride then compensates by having a 43cm pes stride and a 37cm manus stride. This pattern occurs during the first stride of the left side and the last stride measured of the right side. Where this is not the case the stride lengths for the pes and manus are equal.

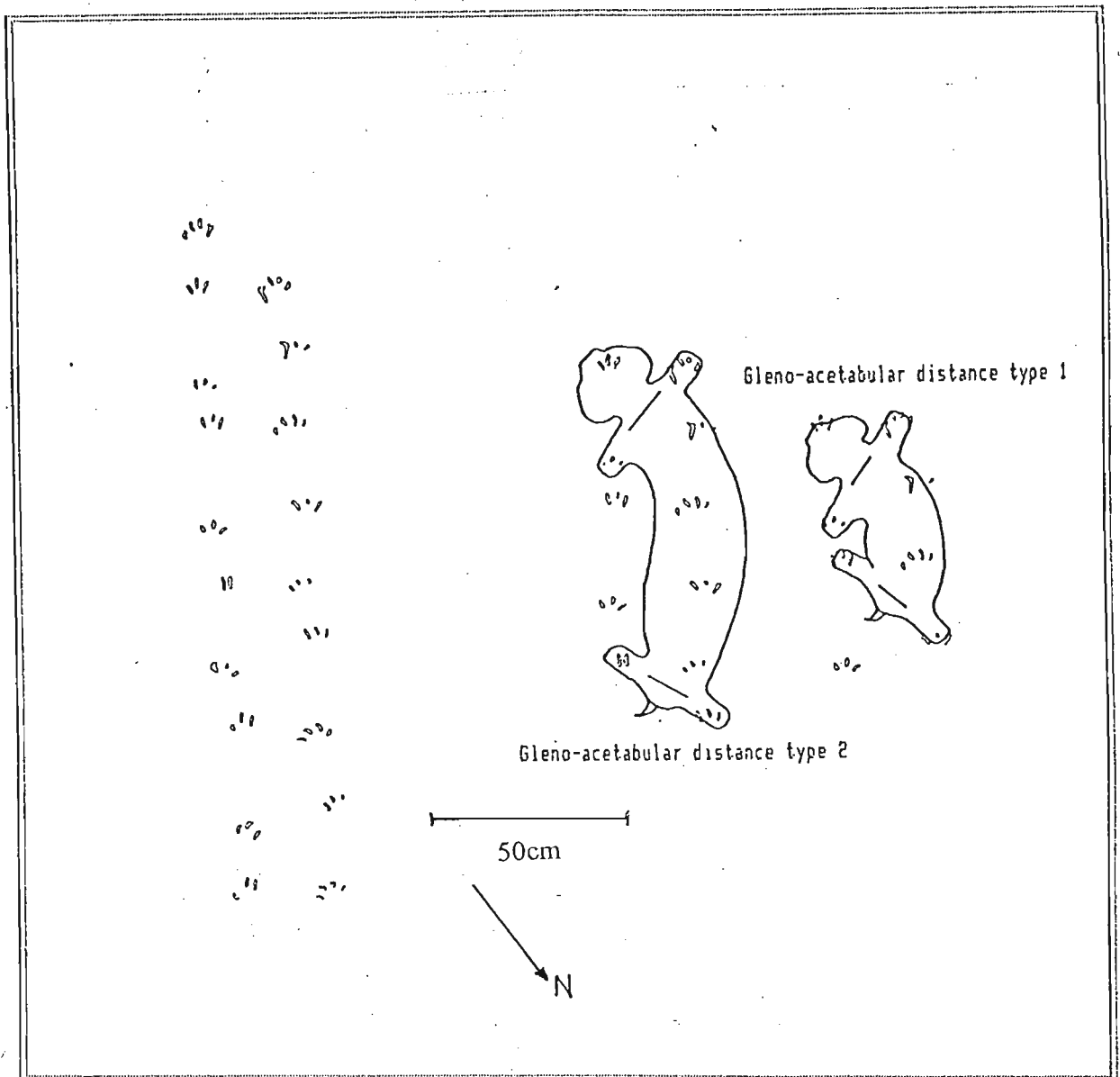


Figure 6.19 Excavation 1, Surface 3 - Trackway 3

Excavation 1, Surface 4 - Trackway 1 (Fig. 6.20)

	AVERAGE	NO. OF READINGS	STD DEVIATION
STRIDE	59.0cm	22	9.2cm
PACE ANGULATION			
PES (degree's)	76.2	11	12.4
MANUS (degree's)	84.1	11	7.5
TRACKWAY WIDTH			
MANUS-PES (STANDARD)	33.9cm	11	3.1cm
MANUS-MANUS	31.9cm	7	1.6cm
PES-PES	36.9cm	7	3.7cm
PACE	29.3cm	22	7.9cm
GLENO-ACETABULAR DISTANCE			
TYPE 1	48.7cm	6	3.9cm
TYPE 2	106.6cm	5	7.4cm

This trackway is composed of 6.5 sets of manus-pes pairs. The digit impressions are splayed and show curvature towards the midline. The number of digits in individual footprints ranges from two to four. The pace angulation averages are both acute, and show a difference of 8 degrees, with the manus prints having the higher pace angulation.

The left side of the trackway shows the usual pattern of the pes prints being further from the midline than the manus prints, with the right side of the trackway showing an overlap in the distances. The measurements show large standard deviations indicating changes in the manner of movement of the causal animal. This change is especially apparent on the left side of the trackway. The only patterns apparent are an approximate decrease in the stride of the left manus, and a decrease in the left pes stride except for the last measurement. The right manus and pes stride measurements show no trend, as do none of the pace angulation measurements, except for the right pes, which shows an approximate decrease.

The trackway width of the pes increases in the second half of the trackway, however there is no obvious change in the width of the manus-manus trackway. The increase in pes trackway width indicates an animal that has decreased its sinusoidal movement, and should be accompanied by a decrease in pace angulation, and decrease in stride. The strides of the left side of the trackway follows this assumption, as does the pace angulation readings of the right side of the trackway.

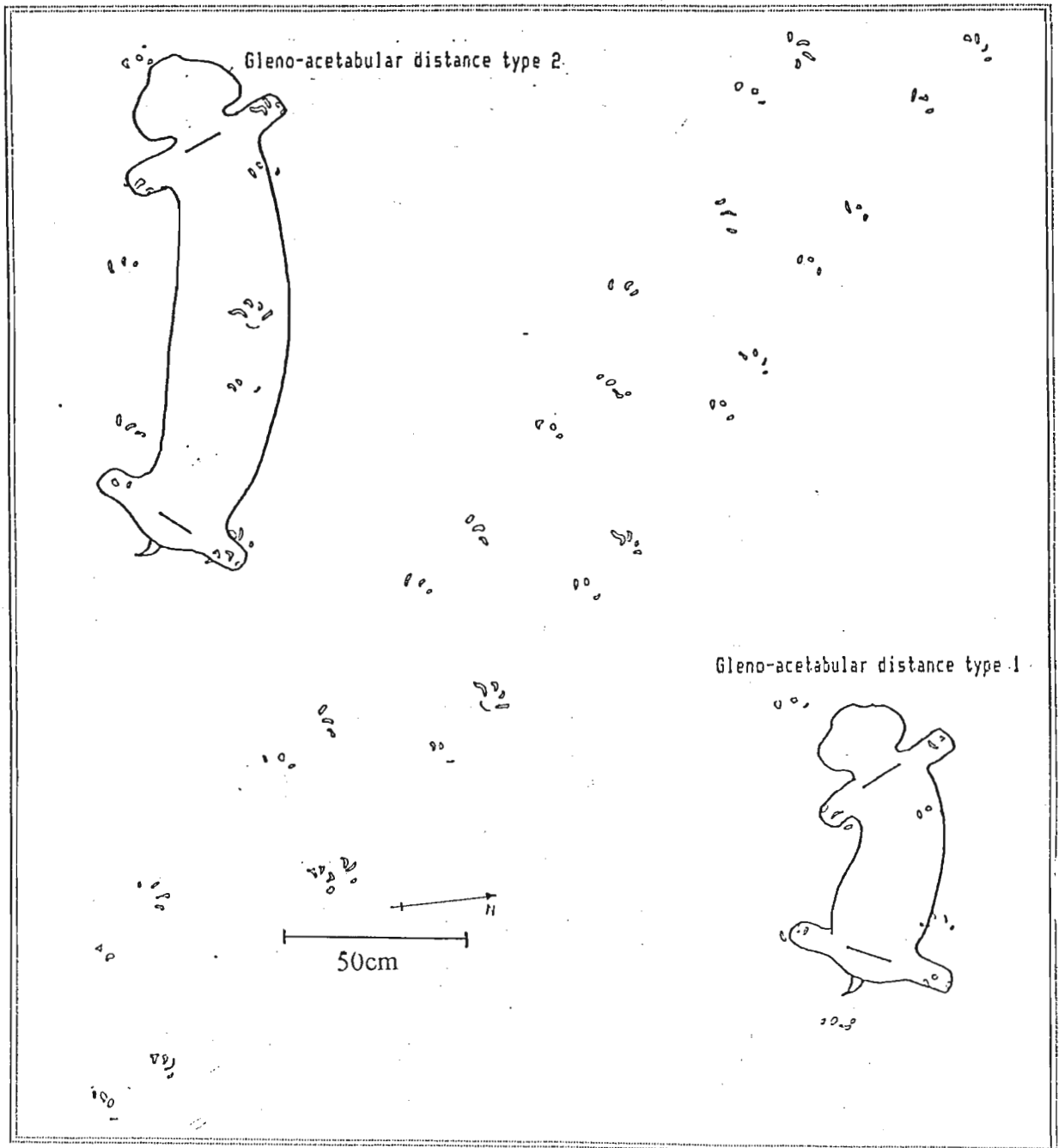


Figure 6.20 Excavation 1, Surface 4 - Trackway 1

Excavation 1, Surface 5 - Trackway 1 (Fig. 6.21)

	AVERAGE	NO. OF READINGS	STD DEVIATION
STRIDE	67.1cm	13	6.6cm
PACE ANGULATION			
PES (degree's)	66.5	8	3.4
MANUS (degree's)	79.0	7	5.3
TRACKWAY WIDTH			
MANUS-PES (STANDARD)	46.4cm	10	2.2cm
MANUS-MANUS	40.4cm	7	1.2cm
PES-PES	52.7cm	7	2.4cm
PACE	34.4cm	14	6.1cm
GLENO-ACETABULAR DISTANCE			
TYPE 1	70.3cm	3	0.5cm
TYPE 2	137.5cm	2	2.5cm

This trackway represents a large causal animal moving towards the west-southwest. The trackway consists of circular toe prods with minimal amount of curvature of the impressions. The number of digits making up the footprints ranges from two to four with the manus prints turned in towards the midline, and the pes prints facing forward or outwards. The pace angulations are fairly acute, with the pes prints averaging 12 degrees less than the manus prints.

The trackway width increases through the length of the trackway, as does the stride of both the left limbs, and the right pes. Also, there is an increase in the pace angulations of the right pes and manus, but a decrease in the angulation of the last three measurements of the left pes.

The above relationships are unusual when compared to the previous trackways. An increase in trackway width usually signals a decrease in the lateral undulation of the body, together with smaller strides and lower pace angulations. In this trackway, however, an increasing

stride accompanies an increasing trackway width, and increasing pace angulation on the

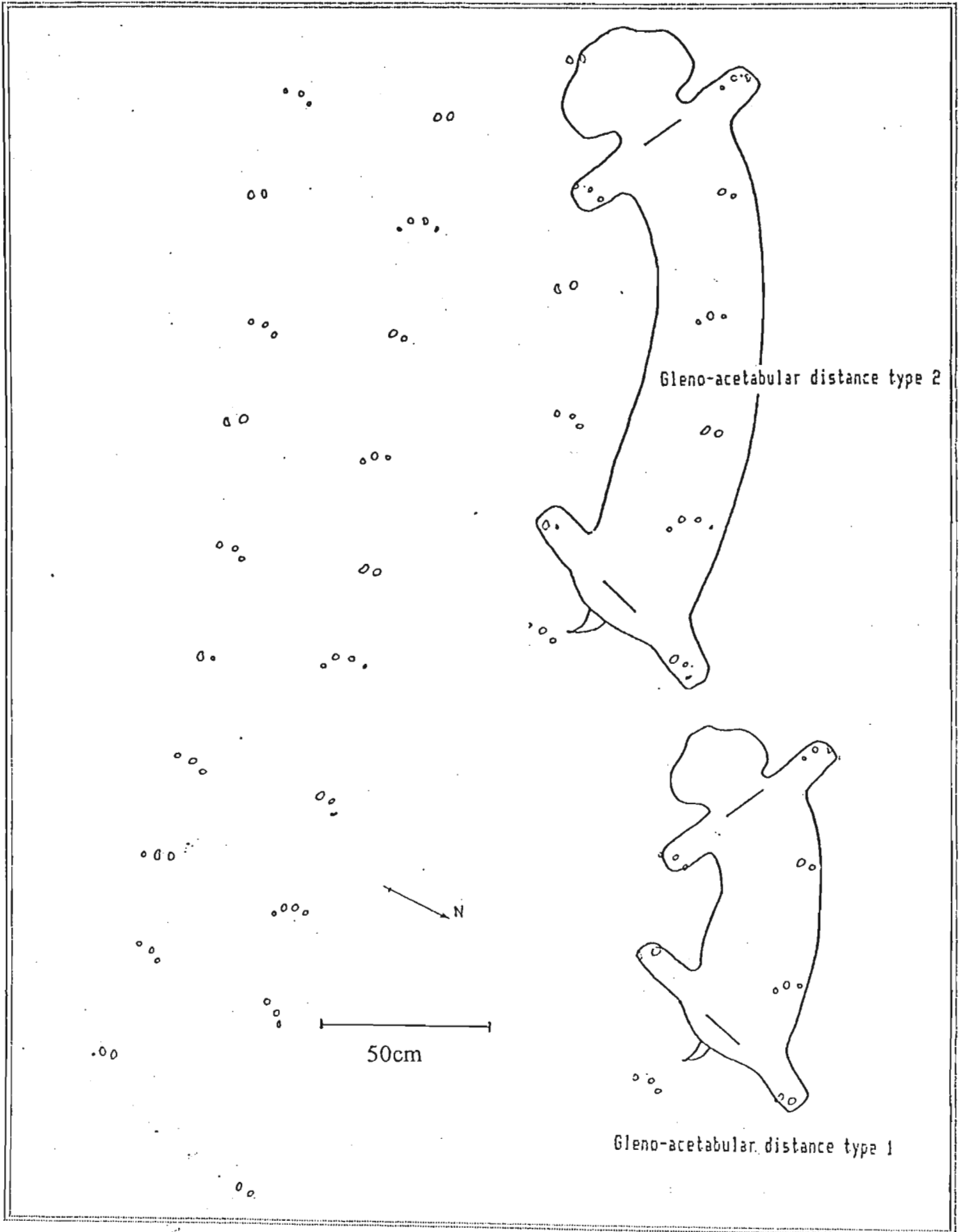


Figure 6.21 Excavation 1, Surface 5 - Trackway 1

Excavation 1, Surface 5 - Trackway 2 (Fig. 6.22)

	AVERAGE	NO. OF READINGS	STD DEVIATION
STRIDE	52.8cm	6	4.3cm
PACE ANGULATION			
PES (degree's)	73.2	5	7.5
MANUS (degree's)	82.0	5	5.5
TRACKWAY WIDTH			
MANUS-PES (STANDARD)	33.5cm	13	3.3cm
MANUS-MANUS	32.0cm	5	1.4cm
PES-PES	36.6cm	5	2.1cm
PACE	27.6cm	9	4.5cm
GLENO-ACETABULAR DISTANCE			
TYPE 1	48.5cm	2	0.5cm
TYPE 2	103.0cm	1	—

This trackway is composed of 3.5 sets of manus and pes pairs, with the number of digits composing each footprint ranging from two to four. The digit impressions of the pes prints show some degree of curvature towards the midline, with the digit impressions of the manus prints mostly represented by circular prods. The direction of movement is towards the north-northwest. The pes prints of the left side of the trackway are further from the midline, whilst the manus and pes prints on the right side tend to average the same distance. The pace angulations for both the limbs average high acute angles, with the average difference between the hind and fore limbs being 9 degrees.

The entire trackway narrows as the animal progressed, accompanied by a decrease in the stride lengths of both the fore and hind limbs. The pace angulation of the right manus and left manus decrease, with the angulation of the right pes remaining constant, and the left pes first decreasing, then increasing. As with the previous trackway, this presents an anomaly when compared to the other trackways. The decrease in trackway width should be accompanied by an increase in the stride, and an increase in the pace angulations.

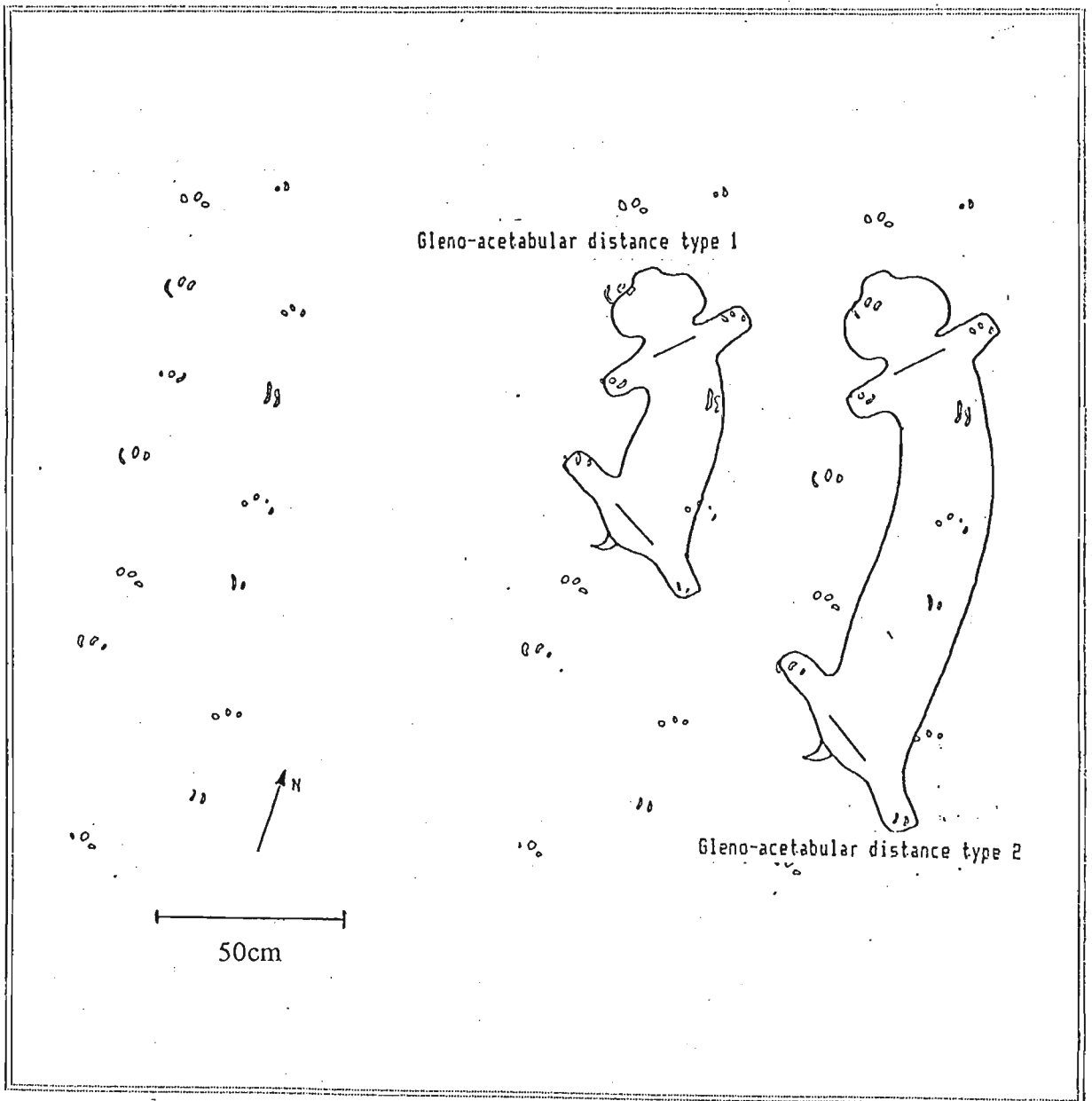


Figure 6.22 Excavation 1, Surface 5 - Trackway 2

Excavation 1, Surface 5 - Trackway 3 (Fig. 6.23)

	AVERAGE	NO. OF READINGS	STD DEVIATION
STRIDE	63.9cm	18	9.5cm
PACE ANGULATION			
PES (degree's)	80.7	9	6.2
MANUS (degree's)	87.3	9	2.8
TRACKWAY WIDTH			
MANUS-PES (STANDARD)	36.8cm	25	4.3cm
MANUS-MANUS	34.9cm	15	4.2cm
PES-PES	38.3cm	12	4.2cm
PACE	31.0cm	16	6.3cm
GLENO-ACETABULAR DISTANCE			
TYPE 1	55.1cm	8	5.1cm
TYPE 2	123.3cm	7	9.9cm

This incomplete trackway shows direction of movement towards north north-west and is composed of nine pairs of manus-pes sets. The majority of the individual prints are composed of four digit impressions which show a certain degree of drag indicating the foot's movement during its placement.

The stride of the causal animal was not constant, and the measurements show high standard deviations. Only measurements from the complete prints were taken, making comparisons difficult due to the gaps in the trackway. There is an overall increase in the stride length, however the pace angulations appear to remain fairly constant, with an average difference of 7 degrees between the pes and manus angulations. The trackway width trend is one where it narrows with decreasing stride, and widens with increasing stride.

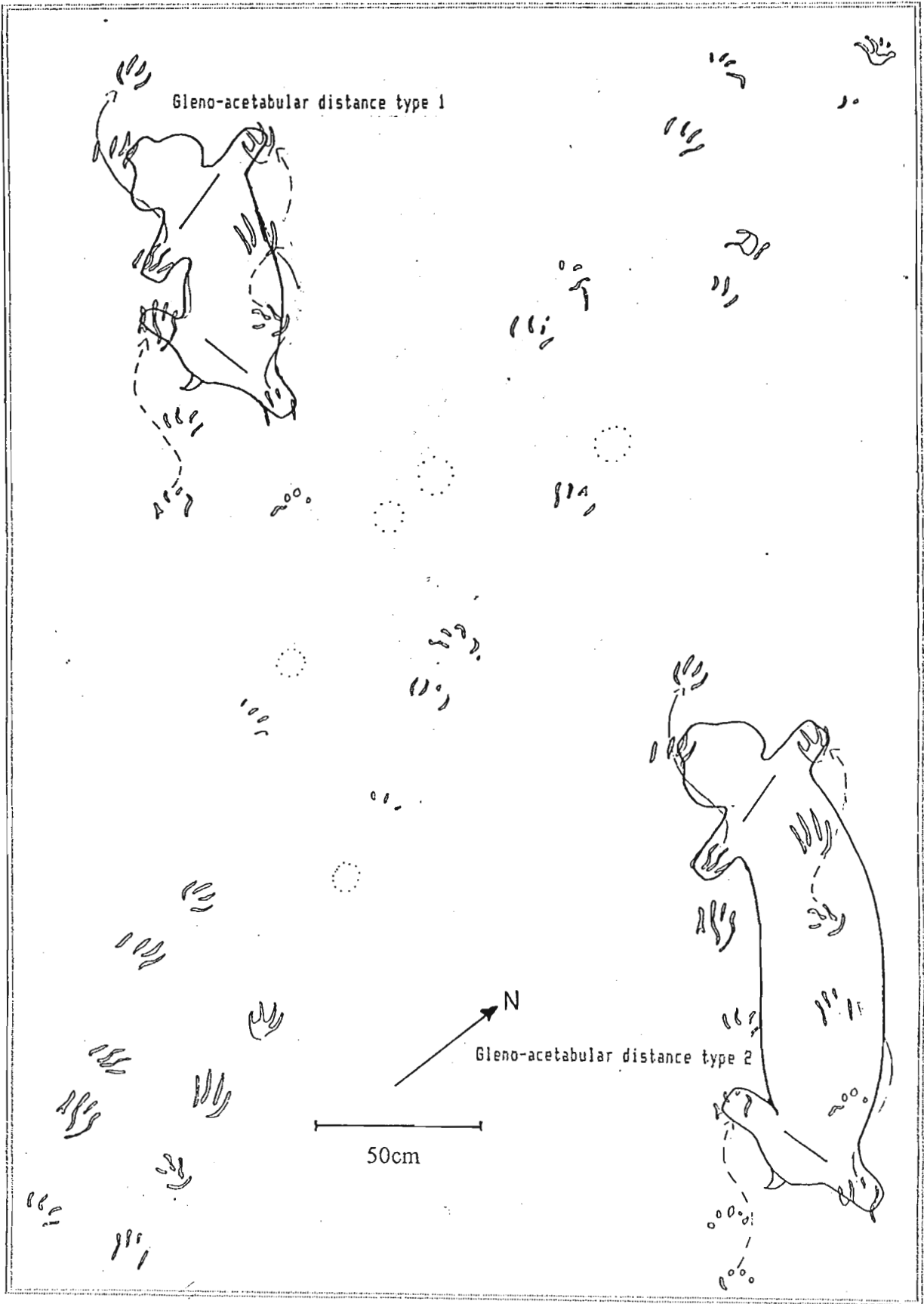


Figure 6.23 Excavation 1, Surface 5 - Trackway 3

Excavation 1, Surface 6 - Trackway 1 (Fig. 6.24)

	AVERAGE	NO. OF READINGS	STD DEVIATION
STRIDE	41.8cm	20	6.5cm
PACE ANGULATION			
PES (degree's)	48.7	10	8.2
MANUS (degree's)	46.8	10	5.8
TRACKWAY WIDTH			
MANUS-PES (STANDARD)	47.0cm	17	2.5cm
MANUS-MANUS	47.4cm	9	1.8cm
PES-PES	47.4cm	9	1.4cm
PACE	20.8cm	18	6.6cm
GLENO-ACETABULAR DISTANCE			
TYPE 1	37.6cm	5	3.6cm
TYPE 2	79.3cm	4	5.6cm

This north-northwesterly moving trackway is composed of 6 sets of manus and pes. The number of digits for each footprint ranges from two to five, with no palm print visible. The digit impressions are mostly prod-like, with occasional curvature of the prints. A noticeable facet of this trackway are the extremely low pace angulations, indicating an animal that is moving with very little glenoid or acetabular rotation, which would indicate a very slow moving animal. The difference in pace angulations for fore and hind limbs is only 2 degrees. However, this is the only trackway that shows a pes pace angulation higher than the manus pace angulation. This is accompanied by a higher average pes pace, indicating that the hind limbs of this animal were rotating to a greater extent than the fore limbs. This differs to the rest of the trackways which show greater rotation of the fore limbs.

There is a definite widening of the trackway as the stride decreases, and an accompanying decrease in the pace angulations.

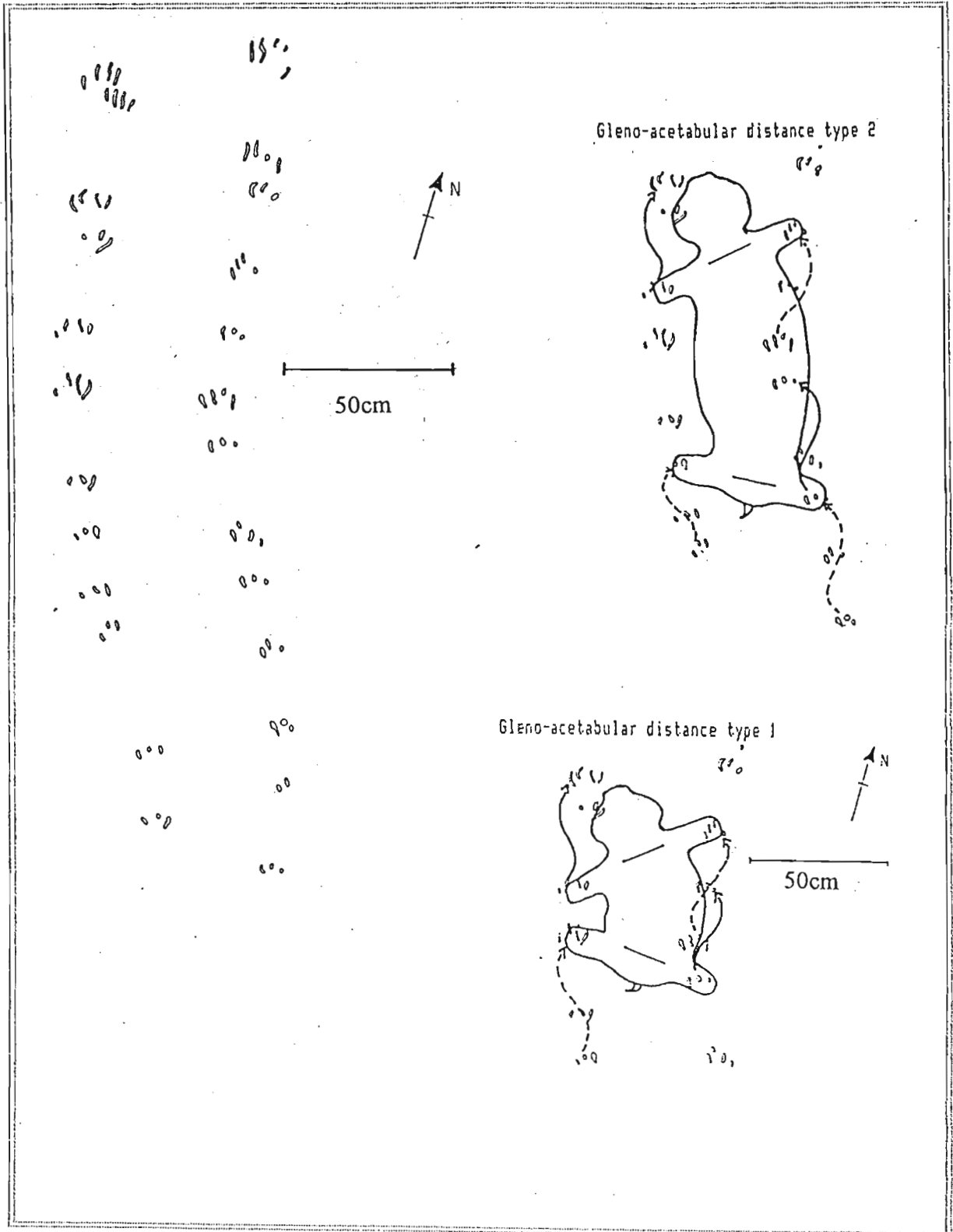


Figure 6.24 Excavation 1, Surface 6 - Trackway 1

Excavation 2, Surface 5 - Trackway 1 (Fig. 6.25)

	AVERAGE	NO. OF READINGS	STD DEVIATION
STRIDE	48.3cm	28	8.2cm
PACE ANGULATION			
PES (degree's)	77.2	17	10.5
MANUS (degree's)	84.9	18	13.9
TRACKWAY WIDTH			
MANUS-PES (STANDARD)	27.6cm	20	3.1cm
MANUS-MANUS	26.4cm	13	1.7cm
PES-PES	30.4cm	12	1.8cm
PACE	24.7cm	32	5.1cm
GLENO-ACETABULAR DISTANCE			
TYPE 1	48.0cm	16	1.7cm
TYPE 2	95.5cm	12	7.9cm

This trackway can be considered the most important of the trackways mapped as the drag marks left by the feet represent the way in which the animal moved its limbs. This trackway is composed of 11 sets of manus and pes, with most of the prints showing all five digits, and in some cases slight heel impressions. The stride of this trackway is erratic, measuring high standard deviations, accompanied by large changes in the pace, and pace angulations measured. The difference in pace angulations between the pes and manus averages at 7 degrees, with both averaging acute angles.

The trackway width widens with a decrease in the stride of the causal animal, and the pace angulations decrease dramatically.

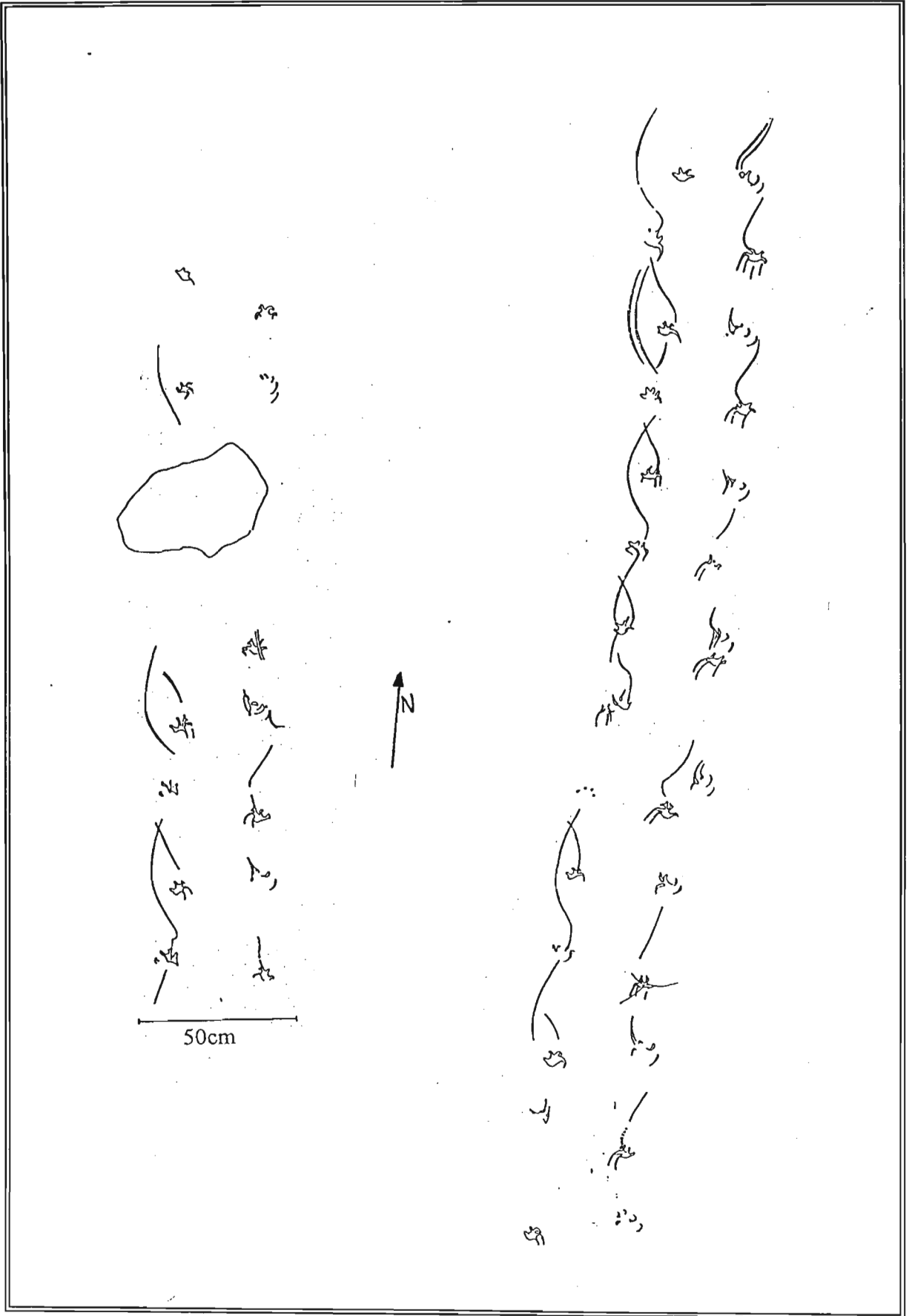


Figure 6.25 Excavation 2, Surface 5 - Trackway 1

Excavation 2, Surface 6 - Trackway 1 (Fig. 6.26)

	AVERAGE	NO. OF READINGS	STD DEVIATION
STRIDE	106.8cm	12	7.3cm
PACE ANGULATION			
PES (degree's)	82.8	7	6.7
MANUS (degree's)	96.6	7	9.2
TRACKWAY WIDTH			
MANUS-PES (STANDARD)	54.8cm	13	5.5cm
MANUS-MANUS	48.8cm	6	4.3cm
PES-PES	61.1cm	7	2.5cm
PACE	52.9cm	14	6.3cm
GLENO-ACETABULAR DISTANCE			
TYPE 1	90.3cm	6	2.5cm
TYPE 2	196.0cm	5	6.2cm

This is the largest trackway mapped and reflects a large causal animal. Its direction of movement is towards the south-southeast and it consists of 4.5 manus-pes sets. The digit imprints were the deepest found and were the only tracks to leave underprints on the surface below, in places giving a depth of 1cm. The number of digits comprising each footprint ranges from three to five, with the digit impressions showing curvature towards the midline. The average stride is over one metre, with the trackway width measuring 54.8cm. Once again the trackway width of the pes is wider than that of the manus, with the manus pace angulation being higher than that of the pes.

A relationship between pace angulation, stride and trackway width is seen in this trackway when dividing the trackway into left and right. Where the stride decreases, the trackway widens and the pace angulation decreases.

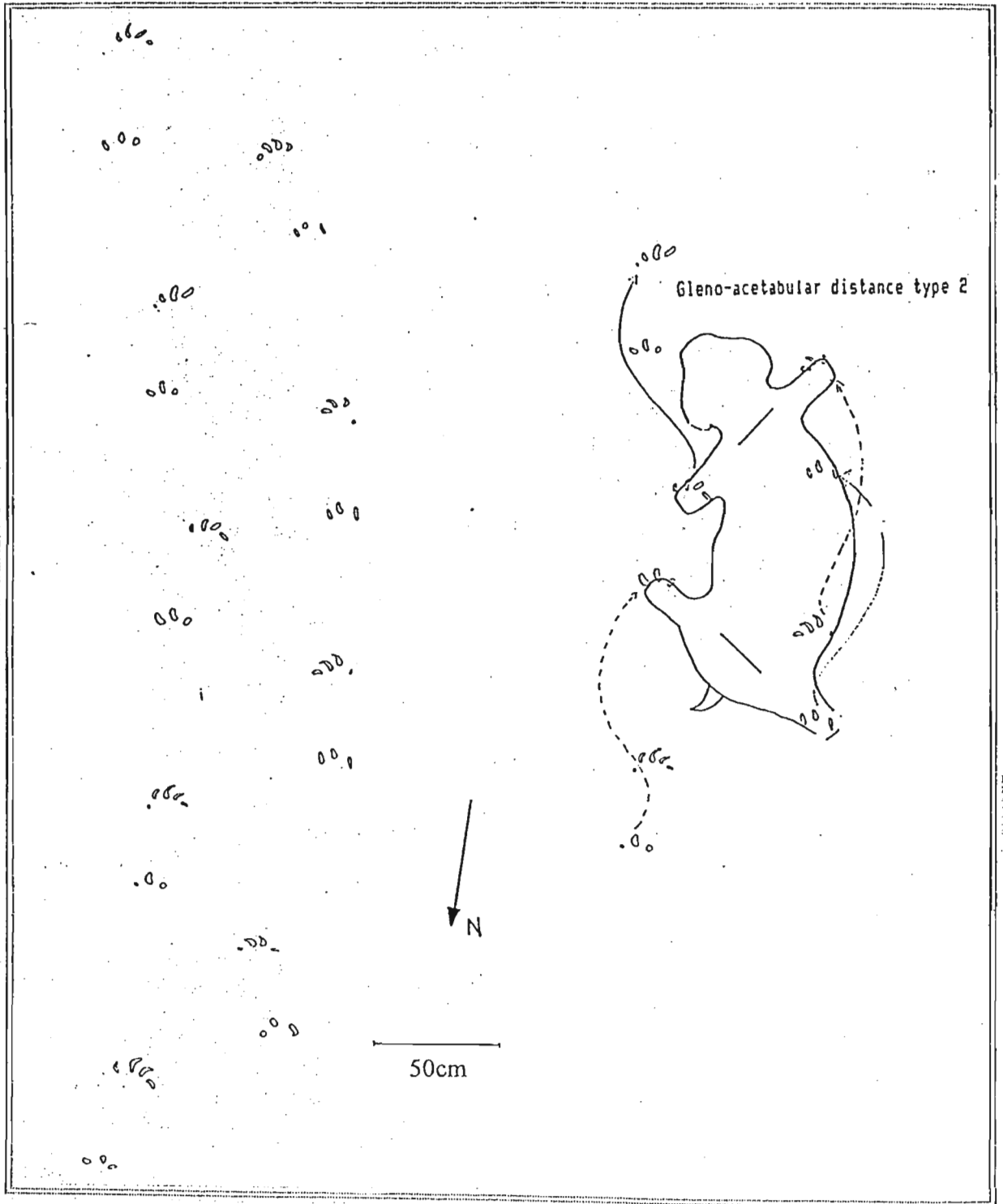


Figure 6.26 Excavation 2, Surface 6 - Trackway 1

6.2.3 Trackway comparison

Table 6.1 summarises the measurements taken from the fourteen trackways. From these measurements certain relationships between the trackways are seen -

- * There is an approximate linear relationship between the standard trackway widths and the size of the animal, or gleno-acetabular distance (Fig. 6.27). This indicates that overall, trackway width is a function of the animals size, and possibly shows that all the trackmakers were similar types of animals.
- * There is a linear relationship between the pace angulations of the pes and the pace angulations of the manus (Fig. 6.28). This indicates a set pace angulation relationship between the fore and hind limbs.

Assuming that all the trackmakers were of the same type, comparisons can be made between trackways with the same gleno-acetabular lengths.

Excavation 1, surface 4 - trackway 1 and surface 5 - trackway 2, are similar trackways both with gleno-acetabular distance type 1 measuring around the 48cm mark. All of the other measurements are also similar, indicating two similarly sized animals that have left trackways with the same characteristics.

Surface 1 - trackway 2 and surface 3 - trackway 2 in excavation 1 can also be compared. Here, although the gleno-acetabular lengths are similar, the animal that made the former trackway is moving at a slower rate than the latter trackway. This is seen by the shorter stride, the lower pace angulations, and the wider trackway. Assuming that the causal animals were dicynodonts, the latter trackway is moving with lateral undulation of the vertebral column creating a longer stride and narrower trackway, and thus also resulting in high pace angulations. As previously mentioned, an animal with a sprawling stance can still give high pace angulation readings if it is moving in a sinusoidal manner.

Trackway	Stride	PA _p	PA _m	TS	Pace	GA
E1S1T1	75.2cm	85°	91°	38.5cm	36.9cm	50.7cm
E1S1T2	51.7cm	60.8°	71.5°	40.3cm	26.1cm	44cm
E1S1T3	69.8cm	81.6°	99.6°	34.8cm	35.7cm	52.3cm
E1S2T1	34.6cm	77.3°	95.6°	18.5cm	17.3cm	27.8cm
E1S3T1	17.6cm	67.5°	73.3°	12.3cm	8.8cm	15.4cm
E1S3T2	63.2cm	96°	109.3°	26.6cm	31.4cm	43.5cm
E1S3T3	39.5cm	75.1°	83.8°	23.8cm	20.2cm	35.3cm
E1S4T1	59cm	76.2°	84.1°	33.9cm	29.3cm	48.7cm
E1S5T1	67.1cm	66.5°	79°	46.4cm	34.4cm	70.3cm
E1S5T2	52.8cm	73.2°	82°	33.5cm	27.6cm	48.5cm
E1S5T3	63.9cm	80.7°	87.3°	36.8cm	31cm	55.1cm
E1S6T1	41.8cm	48.7°	46.8°	47cm	20.8cm	37.6cm
E2S5T1	48.3cm	77.2°	84.9°	27.6cm	24.7cm	48cm
E2S6T1	106.8cm	82.8°	96.6°	54.8cm	52.9cm	90.3cm

Table 6.1 Summary of trackway measurements. Only gleno-acetabular distance type 1 is represented.

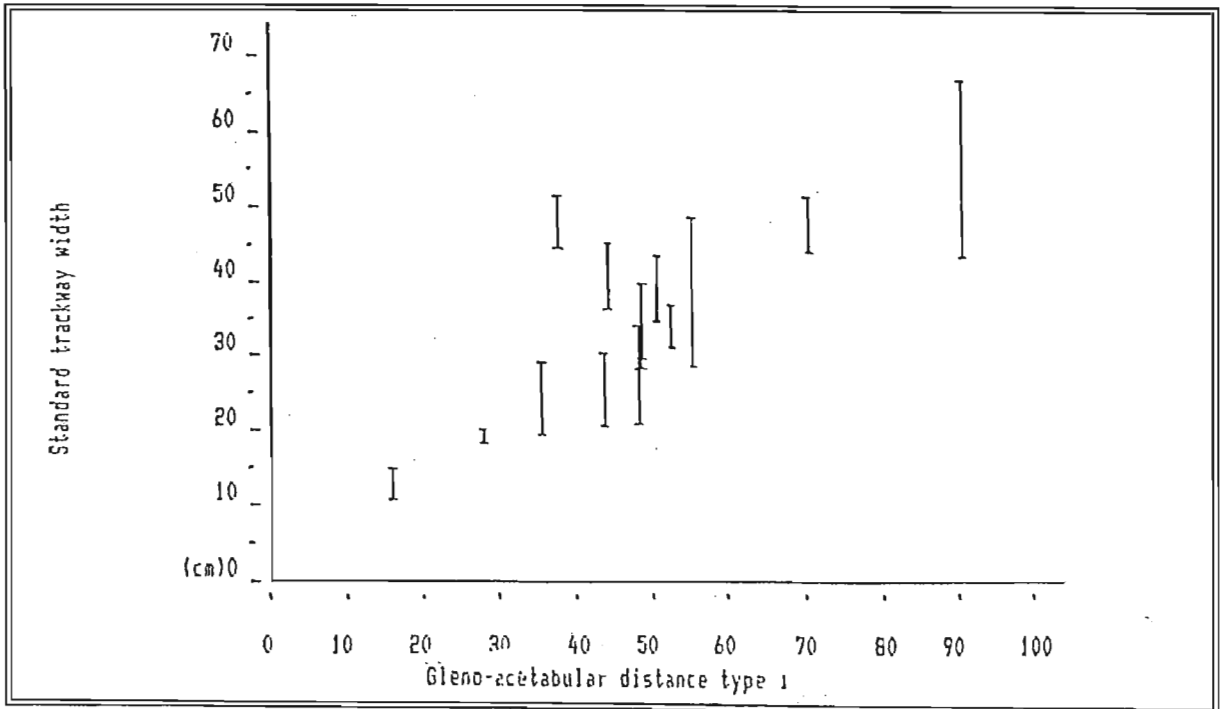


Figure 6.27 Gleno-acetabular distance type 1 versus highest to lowest range of standard trackway width.

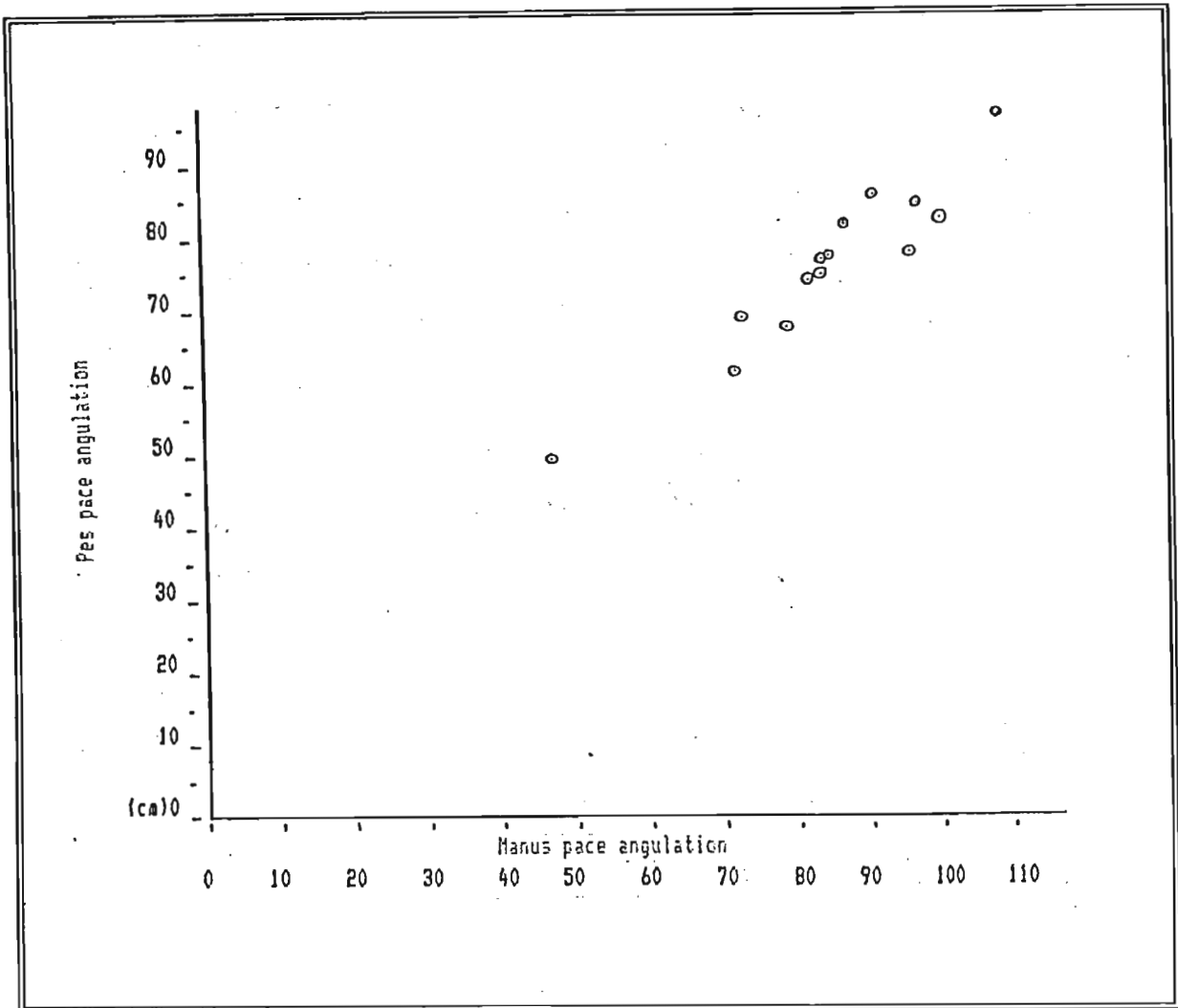


Figure 6.28 Pace angulation of pes versus pace angulation of manus.

Other characteristics seen in the trackways are -

- In seven of the trackways, the stride length of the manus is longer than that of the pes. In only two trackways, the pes stride is greater, and in three trackways the stride is equal.
- In 13 of the trackways the pace angulation of the manus is higher than that of the pes.
- In 13 of the trackways the manus-manus trackway width is narrower than the pes-pes trackway width.

The above three points indicates that the causal animals have forelimbs that are less sprawled than the hind limbs, and closer to the midline. The majority of the trackways also

show longer stride lengths for the forelimbs. However this may not necessarily be the case. It is possible that the forelimbs display such a pattern due to the glenoid showing more rotation than the acetabular, and that the forelimbs show greater protraction-retraction, throwing the foot further forward and creating a greater stride. If this is the case, then the forelimbs may actually have been just as sprawled as the hindlimbs.

When dividing the trackways into left and right, each trackway shows one of two trends -

1. The trackway narrows when the stride and pace angulations increase (E1S1T1, E1S1T2, E1S3T1, E1S4T1, E1S6T1, E2S5T1, E2S6T1), or,
2. the trackway narrows when the stride and pace angulations decrease (E1S3T3, E1S5T1, E1S5T2, E1S5T3).

The first trend is the expected trend. The higher the pace angulation, the more upright the animal and therefore the narrower the trackway as the limbs are further under the body. In dicynodonts, the lengthening of stride in this case could be due to two reasons - (a) a greater rotation of the glenoid and acetabular resulting in the limbs being pushed further forward and backward, or (b) an increase in the lateral undulation of the vertebral column also pushing the limbs further forward or backward.

The second trend shows a decreasing stride accompanied by decreasing pace angulations, as would be expected. However, this is also accompanied by a narrower trackway? Is this possibly explained by King (1991) who describes some mammal-like reptiles as being dual-gaited because the hind limb was capable of either sprawling or operating in a more upright position. Even though the limb was now more upright, it is possible that the pace angulations would still measure less than when the limb was more sprawling due to a marked decrease in the stride length due to a decrease in the lateral undulation of the body.

6.2.4 Discussion

It is known that these trackways were made by Late Permian tetrapods, due to the position

of the trackway bearing layers occurring stratigraphically under *Glossopteris* bearing sediments. It is therefore probable that the causal animals of the trackways were mammal-like reptiles. During Late Permian times the dominant mammal-like reptiles were the herbivorous dicynodonts. The fossil assemblage of the Estcourt region is also dominated by dicynodonts. Therefore it can be assumed that the most likely causal mammal-like reptile of the trackways were dicynodonts.

The following facts are known about the locomotion of dicynodonts -

- * They had relatively short limbs (King, 1991)
- * The front limb provides stability at the front of the body and the hind limb provides the main locomotory thrust to propel the body along (King, 1991).
- * Due to the shortness of the tibia and fibula compared to the femur, a permanent erect gait seems improbable (Kemp, 1982).
- * The hindlimb was in a semi-inturned position during part of the stride (King, 1991).
- * Dicynodonts have wide, flat feet that are plantigrade (King, 1991), *ie.* animals that walk flat footed with ankle bones on the floor (Lockley, 1991).
- * The short lower leg bones indicates a slow stride and a short stride which would have been supplemented to some extent by long axis rotation, extension of the lower leg, and glenoid rotation (King, 1991).
- * The short lower leg bones also result in a short protraction-retraction arc, producing a short stride (King, 1991).
- * Their skeletons were adapted for weight bearing rather than agility (King, 1991).
- * Sinusoidal movement of the vertebral column is reduced in dicynodonts both by osteological and muscular means, resulting in reduced stride length (King, 1991).
- * In late dicynodonts, the hind limb was turned in more towards the body, and the forelimbs were more sprawling (King, 1991).

In the discussed trackways it is also evident that the forelimbs were the main weight bearing limbs. Although very few heel prints are present, where they do occur they mostly form part of the manus prints. Also, the manus prints almost always show more digit

impressions than the pes prints. This would indicate that the manus prints were made with a greater force, or weight, than the pes prints.

Even though in the discussed trackways the forelimbs appear to be less sprawling than the hind limbs, it is possible that this is only due to a greater rotation of the glenoid. This is perhaps evidenced by the fact that the manus prints of the trackways are always turned in towards the midline to a greater degree than the pes prints, indicating greater rotation of the glenoid as compared to the acetabular.

There are two likely scenarios for the formation of the trackways -

1. The most probable scenario is that the prints represent underprints. Footprints have a low preservation potential, and if not buried within approximately 8 weeks will not be preserved (pers. com. R. Smith). If the trackways are the results of dicynodonts, their true prints would include the entire palm of the foot as they were plantigrade animals. However the trackways are mostly only composed of digit impressions. It is therefore thought that these trackways could be the underprints made through overlying layers that were subsequently removed by erosion. The impressions thus represent the phase of the step where the animal used the most force, *ie.* during the push-off phase.
2. The second scenario is that these trackways possibly represent an animal that is buoyed by water, thus only leaving toes impressions as the toes were used for pushing the animal along.

The Estcourt trackways can be divided into two types :

1. Those trackways composed only of circular prods.
2. Trackways composed of digit impressions with drag marks.

Examples of the first type include E1S1T2, E1S1T3, E1S2T1, E1S3T2, E1S5T1, E1S5T2. These impressions are underprints, and represent the moment when the most force was placed on the limb, creating enough pressure to leave prints on buried layers. These

circular underprints therefore probably represent the moment of push-off of the foot.

The remainder of the trackways give a more definite view as to how these animals moved. The majority of the trackways show curvature of the impressions. Since it is assumed that these tracks are underprints, and that they represent the phase of the step when the most force was exerted, then this outward rotation of the foot most probably represents the stage of the step where the weight was transferred to that foot.

Smith (1993a) analyses the curved toe impressions of quadruped tracks found on crevasse splay palaeosurfaces, and recognised three stages in the implantation of the footprints:

- (1) Positive rotation of the foot as it was carried forward in a lateral arc and lowered onto the substrate with toes I - IV being grounded in sequence;
- (2) Slight outward rotation, splaying and flattening of the planted digits as weight was transferred to them and the imprinting of the outermost digit V into the substrate;
- (3) overdeepening of the distal ends of digit impressions II - V as the foot was raised.

The above three phases can be recognised in the Estcourt trackways. The best trackway example for examining how these animals moved is trackway 1 on surface five in excavation 2 (Fig. 6.29). This is the only trackway where drag marks are visible showing the entire path the foot took to the next touchdown phase.

From this trackway the following stages of the step can be seen :

1. At lift-off the foot is moved straight and then swings outwards in a lateral arc. During this phase the foot is held in a position where the toes are at a 90 degree angle with the substrate. The drag marks are thus made by the "hanging" claws.
2. The foot then swings in towards the midline before touchdown. Just before touchdown, the toes lift off the ground in order to bring the palm down for placement on the substrate. During this phase the toes often leave drag marks (Fig.6.30).

3. The foot is then placed flat on the substrate.
4. The foot then rotates outwards as the bodies weight is transferred to that limb.
5. The palm is then lifted off the substrate and the foot moved forwards with the toes once again leaving drag marks.

Gleno-acetabular distance type 1 indicates an animal that was fairly agile, showing lateral undulation of the vertebral column, and a large stride relative to the body length.

Gleno-acetabular distance type 2 best represents dicynodonts, with long bodies, little degree of lateral undulation, and correspondingly short strides.

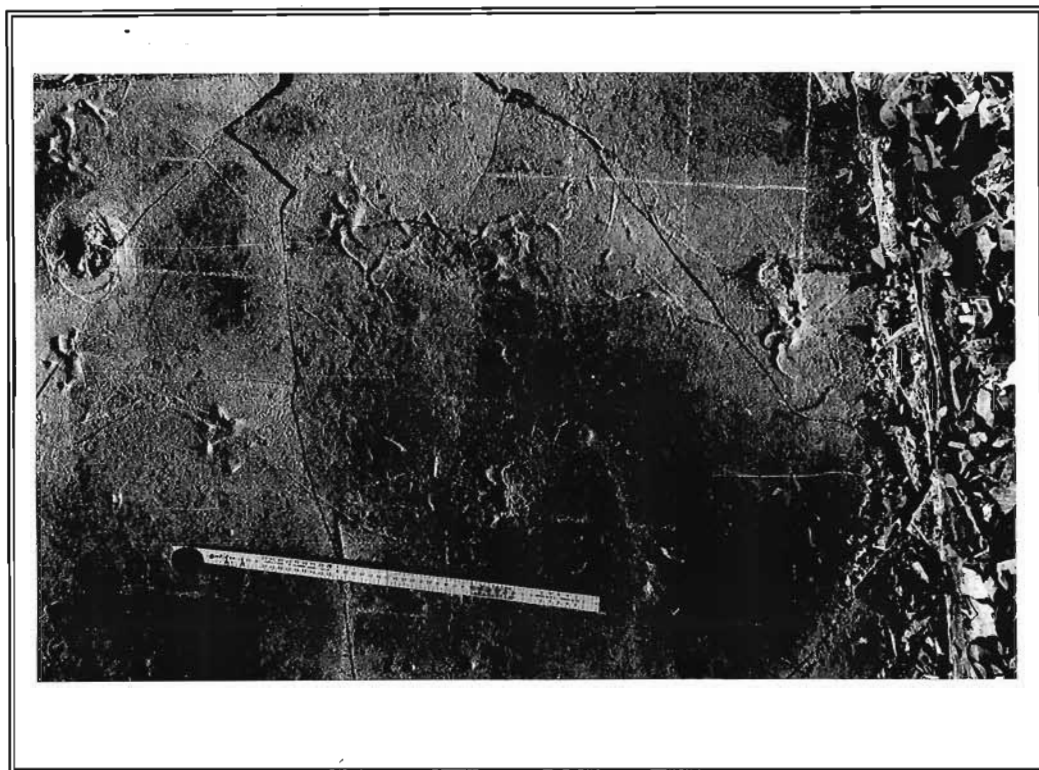


Figure 6.29 Birds eye view of first half of trackway E2S5T1. Chalk squares measure 10cm x 10cm.

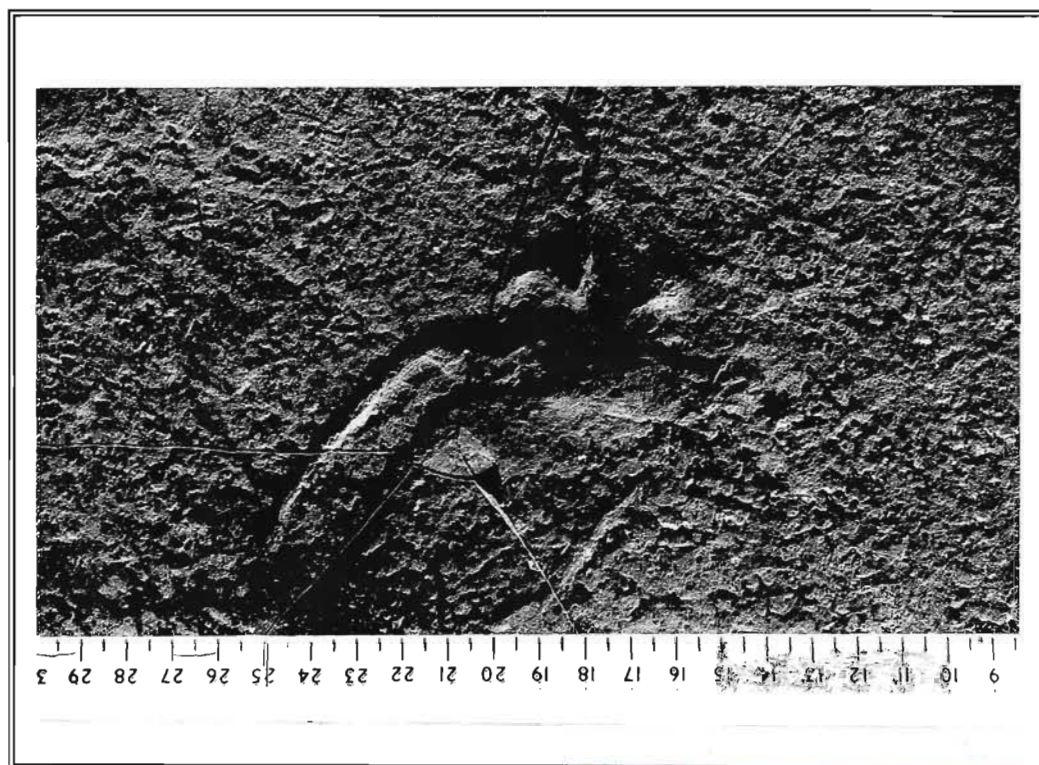


Figure 6.30 Right manus impression from trackway E2S5T1. The drag marks on the left side of the footprint are thought to represent incoming toe drags. Scale in centimetres.

7. THE MORPHOLOGY OF MAMMAL-LIKE REPTILE TUSKS

7.1 Introduction

The mammal-like reptiles found in the Estcourt area are the herbivorous Dicynodonts. These animals are characterised by the absence of teeth except for two upper jaw canines or "tusks", and a covering of horn on both the upper and lower jaws which functioned to crush, tear and generally break up the food (King, 1991). A preliminary investigation concerning the mammal-like reptile tusks was carried out in 1992. It involved sectioning tusks and then plotting the number of growth rings versus the diameter of the tusk. From this it became apparent that the tusks experience continual growth throughout the animals lifetime.

The mammal-like reptiles were so called as they were thought to show characteristics of both mammals and reptiles (King, 1991). The transition from the food trapping function to one of mastication can be traced in the evolution of the mammal-like reptiles, among which can be found all gradations from the reptilian to the mammalian grade (Halstead, 1974). The aim of this investigation is to determine any mammalian characteristics of the mammal-like reptile tusks. Hotton (1986) has already pointed out that the tusks of the Dicynodonts share many similarities with the tusks of mammals. For example - they show little evidence of replacement, they lack enamel when mature, and their pulp cavities are wide open at the base.

Tusks were collected from the Ennersdale region on the western border of Estcourt (Marked d on fig. 2.1). The analysis on the tusks was carried out in collaboration with Professor E.J. Raubenheimer, Head of the Department of Oral Pathology and Oral Biology, of the Medical University of Southern Africa (MEDUNSA). Professor Raubenheimers department carried out macroscopic, microscopic and chemical analysis on the tusks.

7.2 Analytical Results

Macroscopic examination was carried out on fossilised fragments of eight mammal-like reptile tusks measuring 0.8 to 12cm in length. The tips of the tusks are solid, with conical pulpal cavities measuring up to 1.5cm in diameter are present in the root area of the tusks. Cross sectioned surfaces of the solid parts of the tusks show black discolouration with variable numbers of concentric rings, resembling the incremental lines of von Ebner. Contour lines of Owen were also seen.

Microscopically, 50 micrometer polished tooth sections exhibit odontoblastic tubules which run from the pulp to the external surface. The tubules are approximately 5 microns apart, and each tubule has a diameter of less than 2 micrometers. The incremental lines of von Ebner are approximately 20 microns apart. Mineralised globules with interglobular dentine is evident. The outer dentinal surface is covered by cellular cementum.

Scanning electron microscopy revealed the openings of the odontoblastic tubules. The openings are approximately 8 microns apart and slightly more than 1 micron in diameter. A mantle of peritubular dentine is present around each tubule.

Inorganic and organic analysis was carried out, however due to leaching of elements and proteolysis, no conclusions can be drawn from the findings of the chemical analysis.

7.3 Development of teeth in mammals

Tooth development in mammals begins with the proliferation of the epidermal cells of the oral epithelium (Halstead, 1974). Early on in tooth development, known as the bell stage, the tooth germ consists of three components: the enamel organ, the dental papilla and the dental follicle (Osborne). The outer surface of the enamel organ is made up of cells termed the outer dental epithelium, whereas the cells enclosing the dental papilla form the internal dental epithelium (Halstead, 1974). It is the cells of the internal dental epithelium that are induced by the inner enamel epithelium to differentiate into the odontoblasts which are responsible for laying down dentine (Osborne). The odontoblasts

first lay down a dentine matrix against the basement membrane. Once dentine formation has been initiated, a component in the dentine matrix induces the cells of the inner enamel epithelium to differentiate into ameloblasts which secrete enamel onto the surface of the dentine (Osborne). The enamel will eventually wear off with time and use. In incisors and canines dentine is first laid down at the tip of the dental papilla and then extends laterally to cover the walls of the crown. After the shape of the crown has been established, the dental epithelium and papilla continue to grow downwards to form the root portion of the tooth (Osborne).

The odontoblastic cells continue to mature throughout the formation of the tooth. Each cell now possesses only one well developed odontoblast process, but may continue developing short lateral processes (Osborne). As more and more dentine is laid down, the cell bodies retreat in towards the pulp lengthening their processes. Matrix is deposited around these processes thereby producing a tubule (Osborne). The odontoblasts do not follow a straight course during their retreat in advance of the forming dentine. These deviations are probably caused by pressures between the cells set up as a result of the odontoblasts being increasingly more crowded together as the pulp becomes smaller (Osborne). It has also been suggested that the length of an odontoblast process formed in a given time may be greater than the distance travelled by the cell in the same time, this could result in a buckling of the process within the predentine to accommodate the excess, thus accounting for the secondary curves.

7.4 Discussion

Dicynodonts are herbivorous. Herbivory is a difficult strategy to be successful in (King, 1991), as large amounts of plant material need to be consumed in order to obtain sufficient protein. This problem is enlarged by the fact that mammals, unlike reptiles, have a limited amount of teeth throughout their lifetime. However this limitation is overcome to some extent by having open roots so that continuous growth of the teeth is possible. Therefore as wear proceeds, the tooth is able to keep pace (Halstead, 1974). The tusks of dicynodonts experience continuous wear and continuous growth, a decidedly mammalian feature.

Running from the pulpal cavity to the surface of the tusks are the odontoblastic tubules which once held the odontoblastic processes. In mammal-like reptiles the course of the tubules is linear, and give off several branches which communicate in all planes with the adjacent tubules. The course of the odontoblasts in modern mammals is usually irregular as explained previously (Osborne). This might be explained by the thicknesses of the incremental lines of von Ebner which are growth lines of the dentine. According to Osborne these incremental lines are usually 5 micrometers apart. In the mammal-like reptile tusks the incremental lines are 20 microns apart, most likely indicating a faster dentine deposition rate than eclipses that of modern mammals. Therefore the growth of the process remains proportional to the deposition of the dentine, therefore no buckling has to take place to accommodate an extra long process.

From the above it can be seen that the teeth of the mammal-like reptiles exhibit many morphological similarities with the teeth of modern mammals, with an almost identical fine structure. The presence of the odontoblastic tubules is proof of their dentine being vital tissue with a capacity to function as a sensory organ (Raubenheimer, 1993, unpub.data).

8. PALAEOENVIRONMENTAL RECONSTRUCTION.

The sedimentary rocks surrounding the Estcourt region range in age from Late Permian to Early Triassic, and form part of the Beaufort Group. It is the Late Permian sediments that form the main scope of this thesis, in an attempt to reconstruct the palaeoenvironment during these times.

The Estcourt Group Beaufort sediments are typical of the Beaufort sediments documented in other parts of the Karoo Basin. To date no real correlation has been made with other areas and an attempt to clarify this situation is done here.

The most obvious correlation is between the Katberg sandstone of the southern Karoo Basin and the Belmont sandstone of the northern Karoo basin. In the Estcourt region this sandstone wedge is approximately 50m to 70m thick and runs along the western border of Estcourt. It is unfossiliferous, and represents stacked channel sandstones of a braided river environment.

Underlying this sandstone wedge is a thick interval of maroon shales that can be traced from Rosetta to Loskop. These shales are extremely rich in *Lystrosaurus* fossils, and show characteristics typical of a meandering river - floodplain environment. These maroon shales in the Estcourt region are thought to correspond to the Palingkloof Member. Smith (1995) describes the Palingkloof Member as characterised by red and maroon mudrocks which gradually coarsens into the Katberg. This is in contrast to the underlying dark grey and greenish-grey mudrocks of the underlying strata.

There are also similarities in the fossil assemblage zones. Smith (1995) found that the last occurrence of *Dicynodon* in the Bethulie section is about 25m above the base of the *Lystrosaurus* Assemblage zone, coinciding with the first rubified rocks of the Palingkloof Member. The same can be seen in the Estcourt region in the Lowlands area, where the dual occurrence of a *Dicynodon* skull and a *Lystrosaurus* skull occurs in sediments just below the first occurrence of maroon shales.

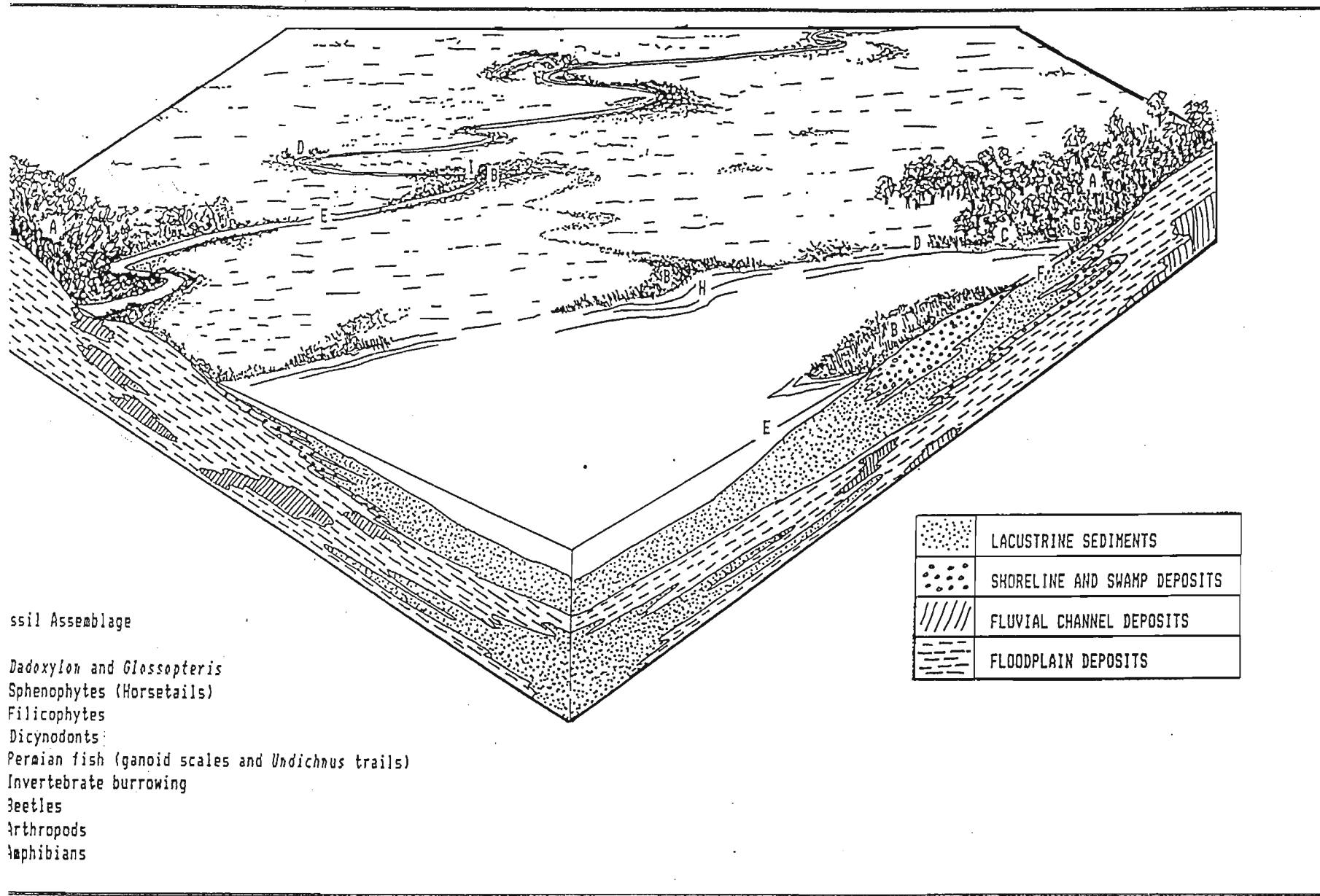
No *Dicynodon* bones have been found in the Palingkloof Member in the Estcourt region. It is the sediments underlying the maroon shales that form the core of this thesis. These sediments were divided into 11 facies defining two sub-environments in a common terrestrial fluvial environment.

The first palaeoenvironment is characterised by meandering rivers crossing large open floodplains. The lithofacies defined for this environment are typical channel, proximal and distal floodplain deposits. The banks of these rivers hosted a variety of flora and fauna, including the mammal-like reptiles, amphibians, and insects. The presence of fossilised wood indicates areas of forest, and the remains of horsetails indicates that the rivers were fringed with this reed-like plant.

Adjacent to these meandering rivers were ephemeral lakes. These form the second sub-environment and are characterised by marginal and basinal lacustrine deposits. Indications are, that these lakes were forever undergoing transgressive and regressive phases, often drying up completely. The lakes were mostly shallow and well oxygenated, and contain a rich biodiversity. Palaeoichnology and fossil remains indicate that these lakes hosted fish, arthropods, and a rich insect life. The presence of tetrapod trackways also indicate that these lakes formed part of the mammal-like reptiles daily routine. Perhaps the rich plant life surrounding the lakes formed feeding grounds for these animals, or perhaps they formed common drinking grounds.

The lakes were surrounded by monospecific forests (indicated by the dominance of *Glossopteris* and *Dadoxylon* in the fossil plant record), and commonly fringed with swampy and marshy areas (indicated by the coal formation in the rock record).

These two sub-environments were closely linked and alternate in the rock record, with lacustrine conditions often giving way to fluvial-floodplain conditions, and visa-versa. Both palaeoenvironments are dominated by the mammal-like reptiles, especially *Dicynodon* and *Lystrosaurus*. A palaeoenvironmental reconstruction can be seen in fig. 8.1.



g. 8.1 Late Permian palaeoenvironmental reconstruction based on the assemblage and sedimentary rock record of the Estcourt region.

9. CONCLUSIONS

The Karoo Supergroup sediments of Estcourt are Permo-Triassic in age and show the typical fluvio-lacustrine characteristics documented in other areas of the Karoo Basin (Smith 1990a). It is possible to correlate these sediments with the Beaufort Group in the southern and central Karoo Basin. The Estcourt Formation corresponds to the Balfour Formation (le Roux, 1992), and the Belmont Formation corresponds to the Katberg Formation (Smith, 1990a). The Palingkloof Member at the top of the Balfour Formation can also be traced to the top of the Estcourt Formation. This correlation indicates that the Estcourt formation is Late Permian in age.

The Estcourt Formation consists of two lithofacies associations:

(A) Fluvial-floodplain facies association - Composed of lithofacies A to F representing typical fluvial, upward fining sequences composed of channel-fill sandstones, distal floodplain silts and muds and proximal floodplain sediments. Also represented in the sequences are crevasse splay deposits, and palaeosol formation.

(B) Lacustrine facies association - Composed of lithofacies G to K. These sediments include marginal lacustrine sandstones and basinal lacustrine muds. Also included in this association are deltaic sandstones and sediments associated with swamp formation.

These terrestrial sediments contain a fossil assemblage dominated by the mammal-like reptiles *Dicynodon* and *Lystrosaurus*. The *Lystrosaurus* remains can be correlated with *Glossopteris* remains indicating that *Lystrosaurus* evolved during the Late Permian (King and Jenkins, 1997), and places the *Lystrosaurus* assemblage zone beneath the Permo-Triassic boundary.

There is an overlap between the *Lystrosaurus* assemblage zone and the *Dicynodon* assemblage zone, which in the Estcourt region occurs just beneath a series of maroon shales thought to represent the Palingkloof Member. This overlap is also noted by Smith (1995).

The Permo-Triassic boundary is thought to coincide with the base of the Palingkloof Member where the mammal-like reptile *Dicynodon* disappears in the fossil record (Fig. 9.1).

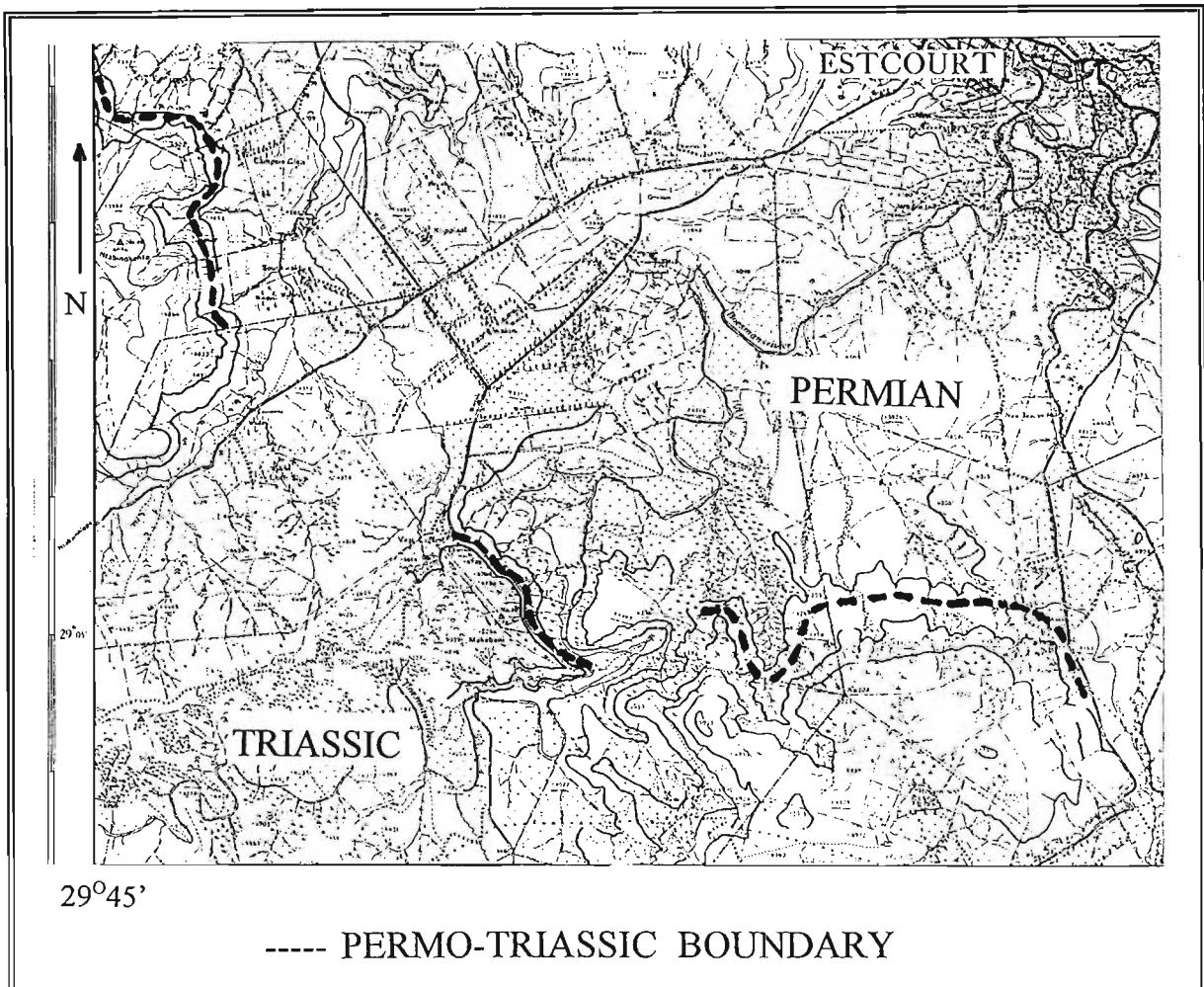


Figure 9.1 Topographical map of southwestern Estcourt showing the approximate position of the Permo-Triassic boundary, and marking the base of the Palingkloof Member. Scale 1:100 000
(From South Africa 1:50 000 2929BB)

The body fossil evidence indicates a high herbivore to carnivore ratio with only one fossil attributed to a carnivorous mammal-like reptile, most likely *Therapsid*. The Late Permian mammal-like reptiles show an intermediateness between mammals and reptiles, having a mammalian dentition, and a reptilian locomotion.

Appendices


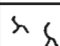
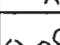
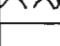
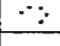


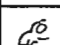
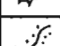
Key to Appendices 1 - 4

Letters A to K represent facies associations as defined in table 2.1.

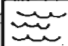
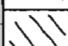
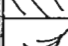




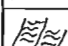
COLOUR KEY :

GG	GREENISH/GREY
LG	LIGHT GREY
DG	DARK GREY
LD	DARK AND LIGHT GREY BANDING RESULTING FROM SILT/SAND COUPLETS
GB	GREYISH BROWN
B	LIGHT BROWN
OG	OLIVE GREEN
BG	BLUEISH/GREY
G&G	GREEN AND GREY BANDING
G&B	GREEN AND BROWN BANDING
G	DIRTY GREY
O	ORANGE


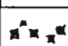
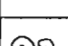
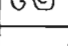

FOSSIL KEY :

	INVERTEBRATE BURROWING
	FOSSILISED ROOT IMPRESSIONS
	PLANT FRAGMENTS
	TETRAPOD TRACKWAYS
	FISH SCALES
	BONE FRAGMENTS
	VERTEBRATE SKULL
	ARTHROPOD TRACKWAYS
	FISH TRAILS

SEDIMENTARY STRUCTURE KEY :

	RIPPLE CROSS-LAMINATION
	PLANAR CROSS-BEDDING
	TROUGH CROSS-BEDDING
	HORIZONTAL LAMINATION
	WAVY LAMINATION
	MASSIVE BEDDING
	CLIMBING-RIPPLE CROSS-LAMINATION
C	SILT/SAND COUPLETS
	HUMMOCK CROSS-BEDDING
	MICRO-TROUGH CROSS-BEDDING

GEOLOGICAL FEATURE KEY :

	PEBBLES
	RIP-UP CLASTS
	SOFT-SEDIMENT DEFORMATION
	CALCRETE BOULDERS
	COAL FORMATION

Appendix 1

Description of Bedstead Log.

This profile is mapped up a stream which passes through the farm camp known as Bedstead, and will therefore be known as the Bedstead log.

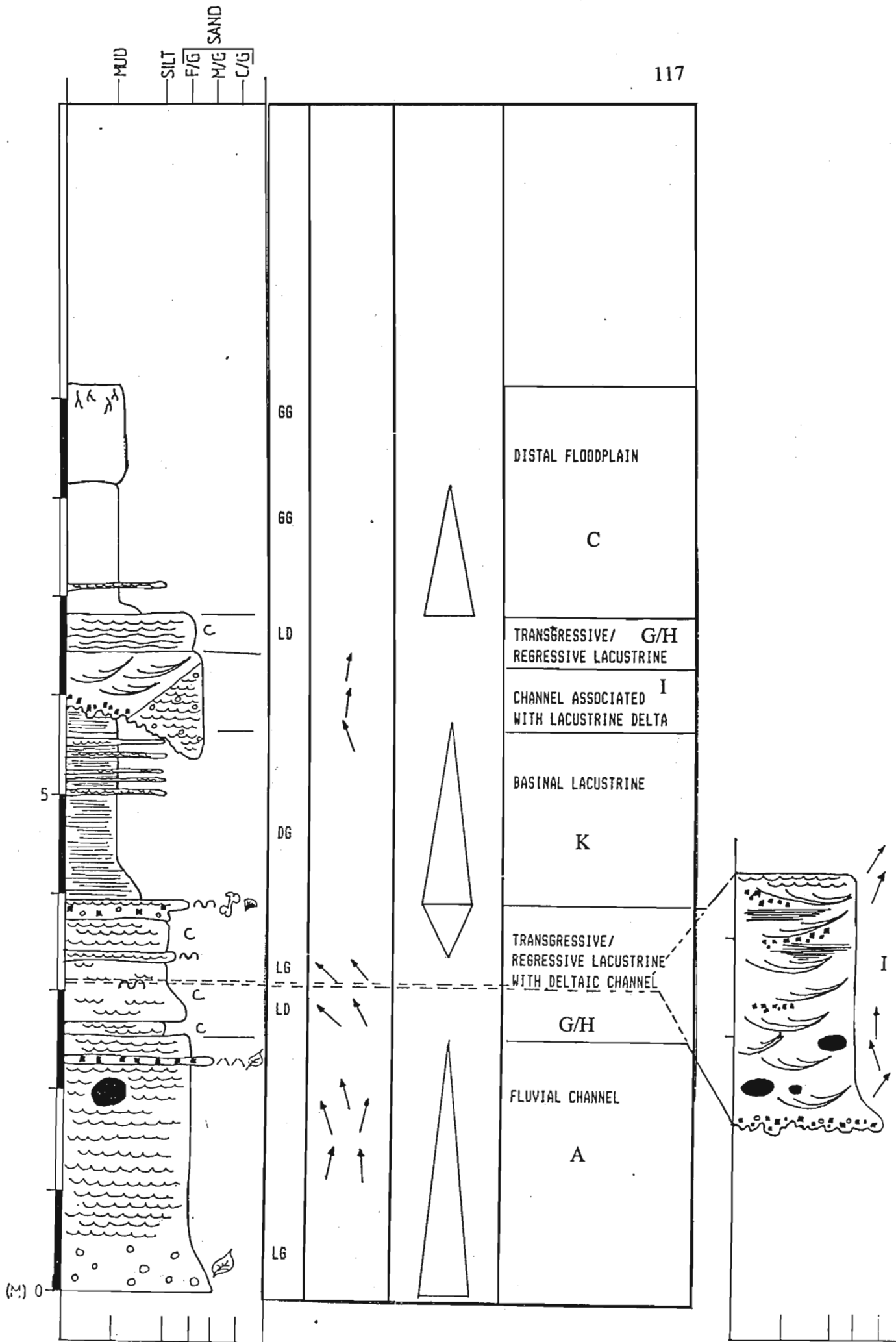
0 to 4m

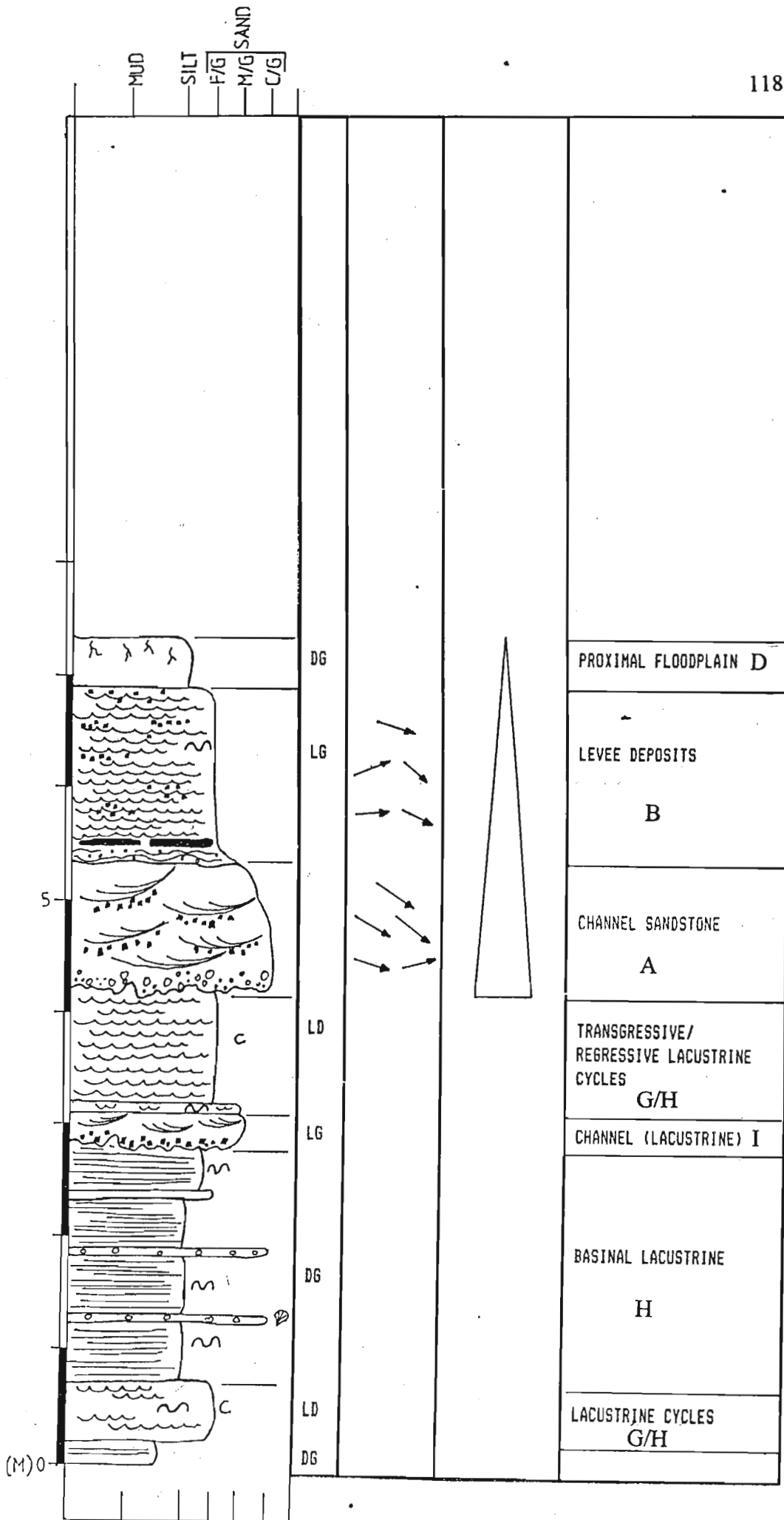
The log begins below the road cutting where Kemps road passes through Bedstead stream. The first unit logged is a 2.5m thick, fine grained sandstone unit, the base of which is composed of medium grained sandstone, appears massive and contains sandstone pebbles ranging in size from 2cm to 6cm, and an abundance of *Glossopteris* leaf impressions. Where the sandstone unit fines, is a change in structure to ripple cross-lamination. The sandstone is micaceous, light grey in colour, and contains numerous thin, dark grey siltstone incursions.

1.5m into the above unit is a layer of large calcretised boulders ranging from 40cm to 3m in diameter. They have weathered brown, and the sedimentary structures of the enclosing sediments pass uninterrupted through them. Towards the top of the unit is a 10cm thick layer of medium grained sandstone containing rip-up clasts, and fossilised stem and leaf impressions. Palaeocurrent directions from rib-and-furrow include 011°, 356°, 342°, 013°, and 345°.

Overlying the above is a 10cm thick layer composed of silt/sand couplets. The unit is micaceous, bioturbated and ripple cross-laminated. It is topped by a fining-upwards unit of fine grained sandstone becoming siltstone. The sandstone factor of the couplets decreases towards the top of the unit with the loss of apparent structure towards the top of the unit. Palaeocurrent directions from rib-and-furrow include 311°, 332°, 314°, and 321°.

There is lateral variation in the above unit, as within a short distance upstream, the couplets are interrupted by a 2.5m thick trough cross-bedded sandstone that is based by a coarse grained lag containing large mud clasts and quartz grains. Clast size reaches 15cm in diameter. The sandstone then fines into a fine grained, trough cross-bedded sandstone. The troughs are shallow and small scale reaching 0.5m in length, and towards the top of the unit





are filled with horizontally laminated siltstone, and in one occasion by alternating siltstone and fine grained sandstone, reaching only 15cm in thickness. The individual foresets are only millimetres thick, and the troughs are based by dark grey silt rip-up clasts. Scattered throughout the bottom half of the unit are calcretised boulders ranging in size from 0.5m to 1.5m across. The top of the unit is ripple cross-laminated. Palaeocurrent readings from the troughs include 034°, 341°, and 359°, and from rib-and-furrow of the top rippled sandstone include 021° and 031°.

Continuing the section before the lateral interruption, is a 10cm band of fine grained, light grey sandstone that shows invertebrate burrowing. It is topped by a 30cm layer composed of silt/sand couplets, however the siltstone component is dominant and therefore the unit appears dark grey and silty in composition. There follows a very prominent layer which can be followed for a great distance upstream. This layer reaches a maximum thickness of 20cm and appears to be composed of silt/sand couplets, however it is extremely bioturbated and has lost most of its structure. Its surface shows prominent ripples, giving a wavelength of 9cm, and an amplitude of 1cm. The ripples are symmetrical, with a palaeocurrent orientation of west-northwest to east-southeast. The layer also contains bone chips, fish scales, rip-up clasts and small pebbles.

4m to end

The above layer is overlain by a fining upwards mudstone layer which shows lateral variation in thickness. At its thinnest the unit is only 50cm thick and composed of dark grey, micaceous, silty mudstone, that is laminated on a millimetre scale. Further upstream the unit thickens to include a further 1.5m of finely laminated mudstone. The last 80cm of the mudstone contains five bands of ripple cross-laminated sandstone, varying in thickness from 2cm to 5cm.

The mudstone is eroded by a medium grained sandstone unit that is based by a lag conglomerate. Again, there is lateral variation, with the unit changing from a 50cm thick trough cross-bedded sandstone, to a 1m thick ripple cross-laminated finer sandstone. Directions taken from rib-and-furrow include 340°, 006°, and 008°. The rippled sandstone

also contains sandstone pebbles, which average 5cm to 6cm in diameter.

Conformably overlying the sandstone is a 40cm thick unit of fine grained silt/sand couplets. The base of the unit is wavy laminated becoming rippled towards the top. It is overlain by a sequence of fines, which begins with 14cm of grey silty mudstone, grading into greenish/grey mudstone. Approximately 20cm into the mudstone is a 10cm thick layer of rippled greenish/grey siltstone. The unit continues with 10cm of massive mudstone which, 100m upstream, thickens to 1m. The mudstone is topped by 1m of greenish/grey silty mudstone, and contains vertical fossilised rootlets at the top of the unit.

0m to end

The sequence is then interrupted by a dolerite dyke and fault. Since no reliable continuation could be found, the sequence is restarted at 0m with a 20cm thick layer of extremely carbonaceous, horizontally laminated siltstone that is pyritic. It is topped by 50cm of silt/sand couplets. However the silt factor is minimal, thereby imparting an overall light grey colour to the unit. The unit is bioturbated to an extent that often destroys the structure.

The above unit is overlain by four separate units of horizontally laminated siltstone separated by thin layers of conglomeratic sandstones, which tend to pinch-and-swell. All of the siltstone layers show invertebrate burrowing, and the fourth unit is slightly coarser in nature than the other three as it has a few incursions of centimetre thick layers of fine grained sandstone. The first conglomeratic sandstone is 5cm thick and contains 0.5cm to 1cm diameter quartz and feldspar pebbles, and fish scales. The second sandstone layer is similar in nature. The quartz and feldspar grains are sub-rounded. The third layer is not conglomeratic and is composed of fine grained sandstone.

This is eroded by a 30cm thick layer of trough cross-bedded, medium grained sandstone unit based by a lag conglomerate containing rip-up clasts. The sandstone is light grey and the troughs small scale, and is topped by a 10cm layer of extremely bioturbated, rippled sandstone.

The sequence continues with a 1m thick unit of silt/sand couplets, showing lamination on a centimetre scale. It has been eroded by a 1.1m upward fining trough cross-bedded unit, the base of which is extremely coarse grained with quartz and feldspar grains ranging from 1mm to 10mm across. Five separate troughs with basal rip-up clasts were measured from the unit -

1. width = 0.5m, length = 1.5m, direction 107°,
2. width = 1m, length = 2m exposed, direction 076°,
3. width = 1m, length = 2m exposed, direction 120°,
4. width = 1m, length = poor exposure, direction 128°,
5. width = 6m, length = poor exposure, direction 124°.

Conformably overlying the troughs is a 1.5m thick sequence of wavy laminated sandstone becoming ripple cross-laminated. At this structural transition is a continuous layer of large, flat calcretised boulders reaching 10m in length. Throughout this bottom horizon are millimetre to centimetre sized quartz and feldspar grains. Palaeocurrent directions from rib-and-furrow include 085°, 115°, 067°, 131°, and 108°.

Above the calcretised zone the sandstone is bioturbated and contains small rip-up clasts reaching 2 to 3cm in length. Again there are thin siltstone incursions. The log ends with a 40cm thick, dark grey, massive siltstone that contains fossilised roots in its upper reaches.

Appendix 2

Detailed description of Kudu stream profile.

The Kudu stream profile begins where Kemps road cuts a small stream which passes the homestead known as Kudu Cottage. For the sake of this thesis the stream will be called Kudu stream.

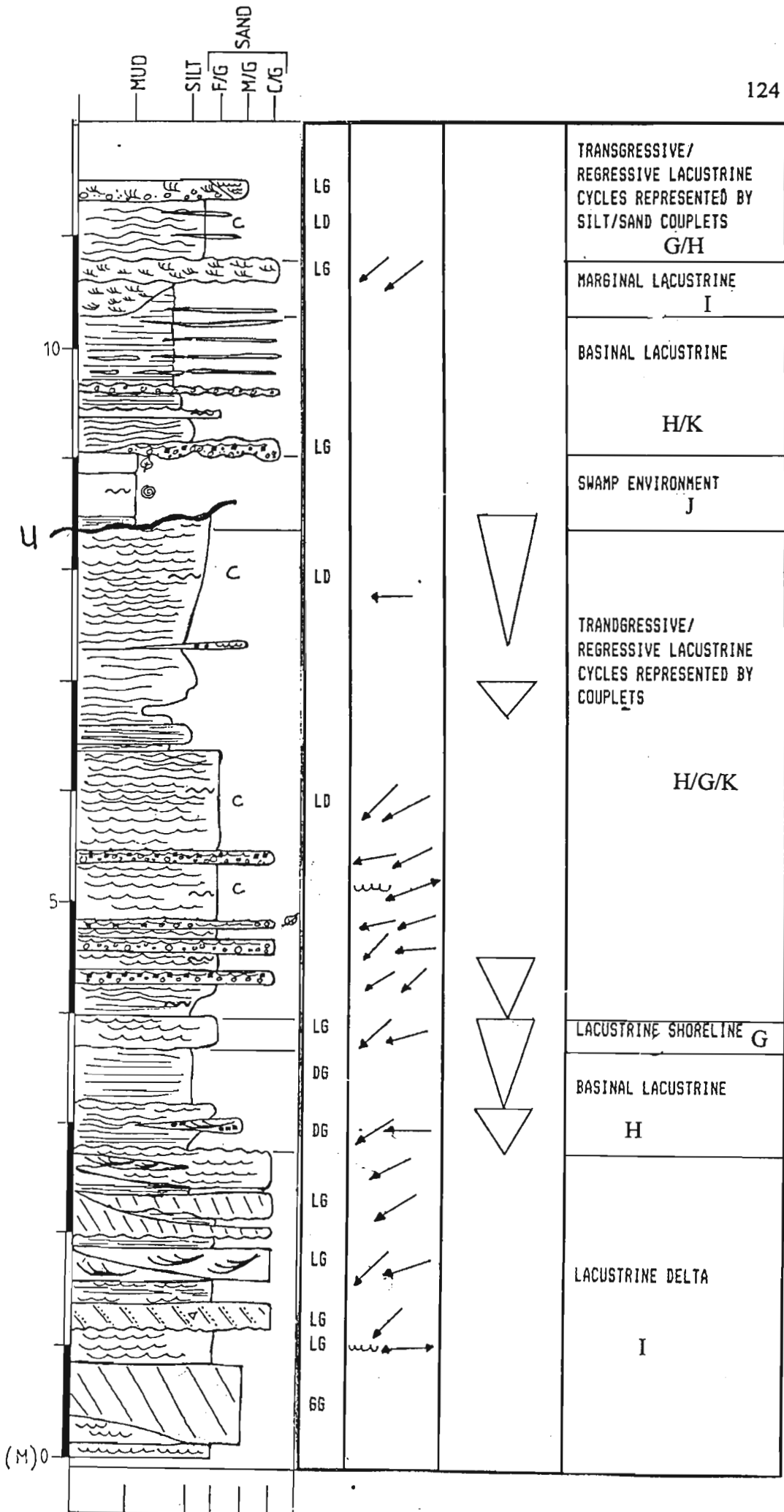
0 to 4m

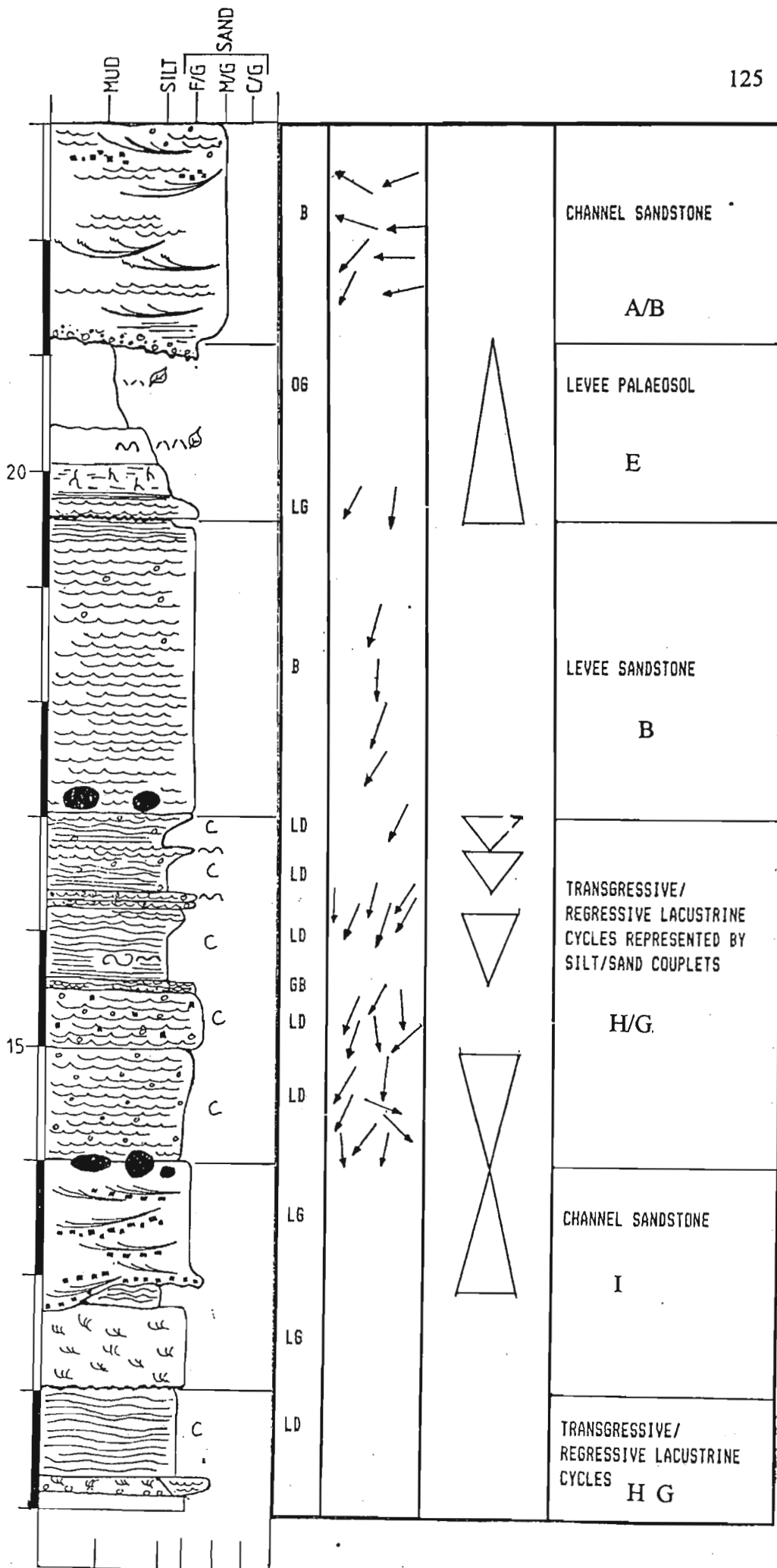
The section begins at the road cutting with approximately 30cm of ripple cross-laminated, fine grained sandstone which has been eroded by a large single planar unit. This planar unit ranges in thickness from 50cm to 70cm, and is composed of medium grained, greenish-grey, micaceous sandstone.

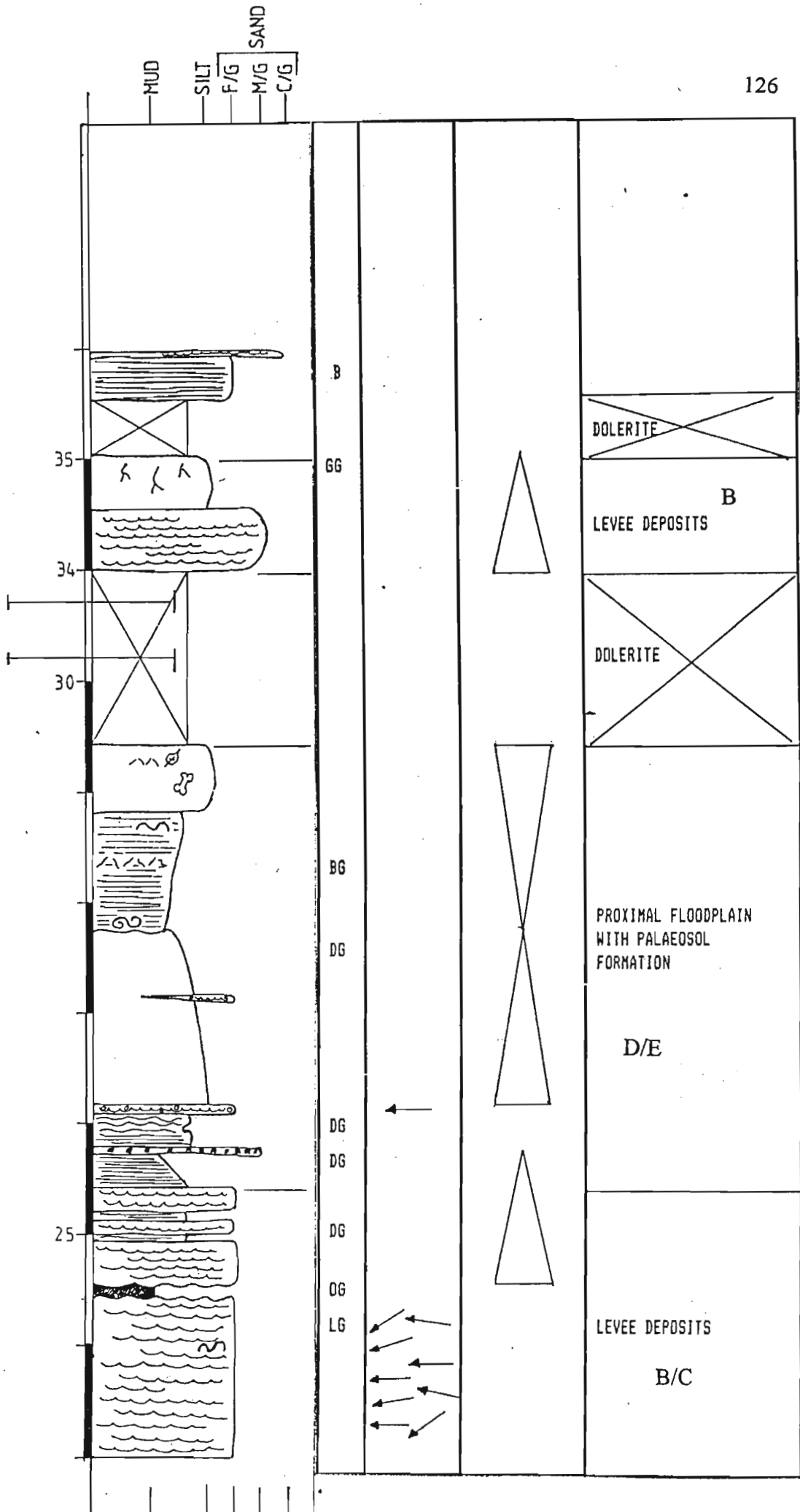
Overlying the above unit is another section of ripple cross-laminated, fine grained sandstone, light grey in colour and micaceous. A single ripple surface is exposed, traversed by parallel, symmetrical ripples, and gives a wavelength of 3cm and an amplitude of 0.5cm. The palaeocurrent trend is $267^{\circ}-087^{\circ}$ (all compass readings are corrected for magnetic declination). The overall palaeocurrent direction from rib-and-furrow is west south-westerly.

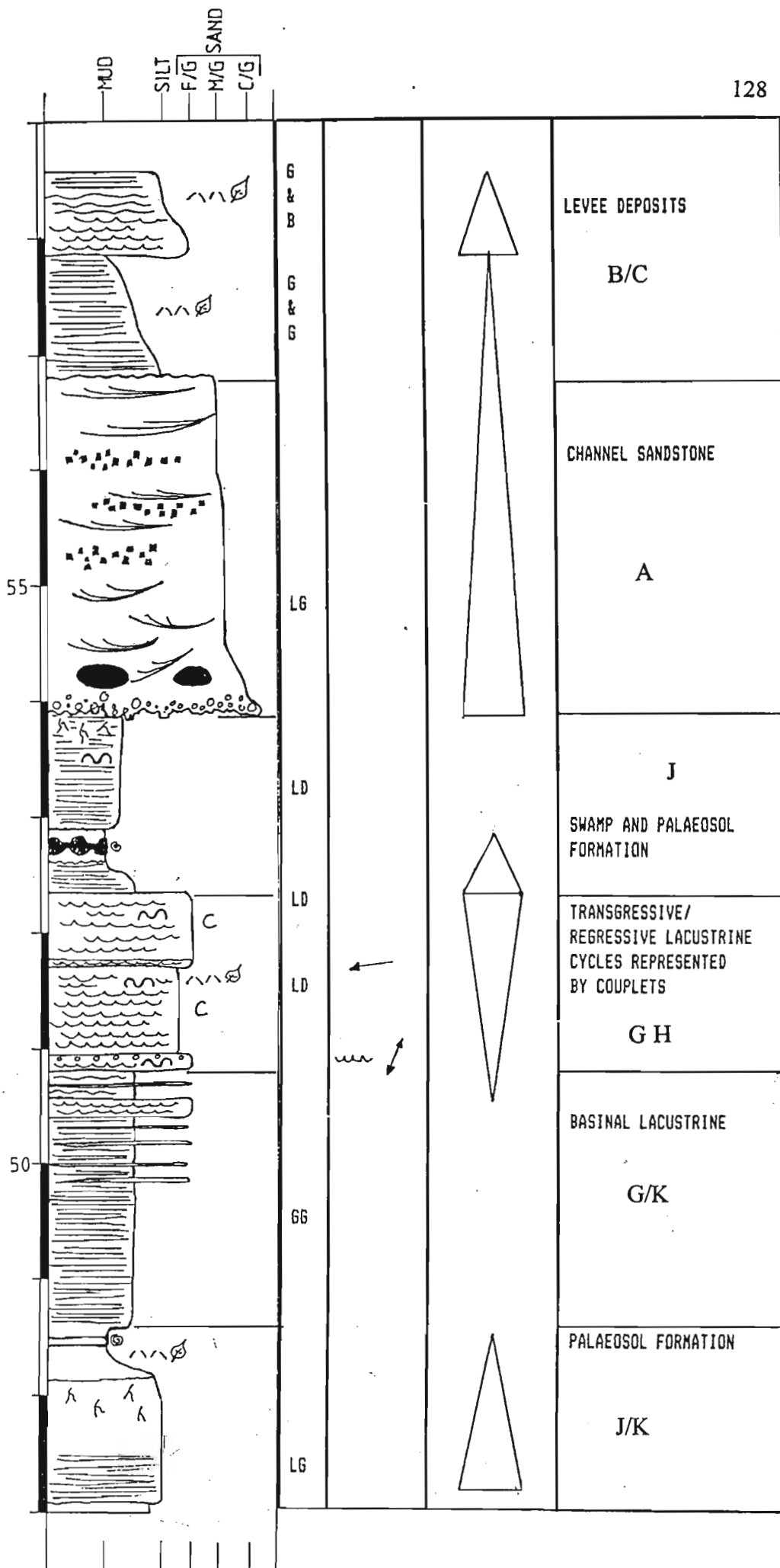
The rippled section is eroded by a second, light grey planar cross-bedded unit, which is coarser than the first, with individual cross beds tending to fine upwards from an extremely coarse base composed of millimetre sized grains (2mm quartz grains seen), to a medium grained sandstone. The palaeocurrent direction is southwest (226° compass reading).

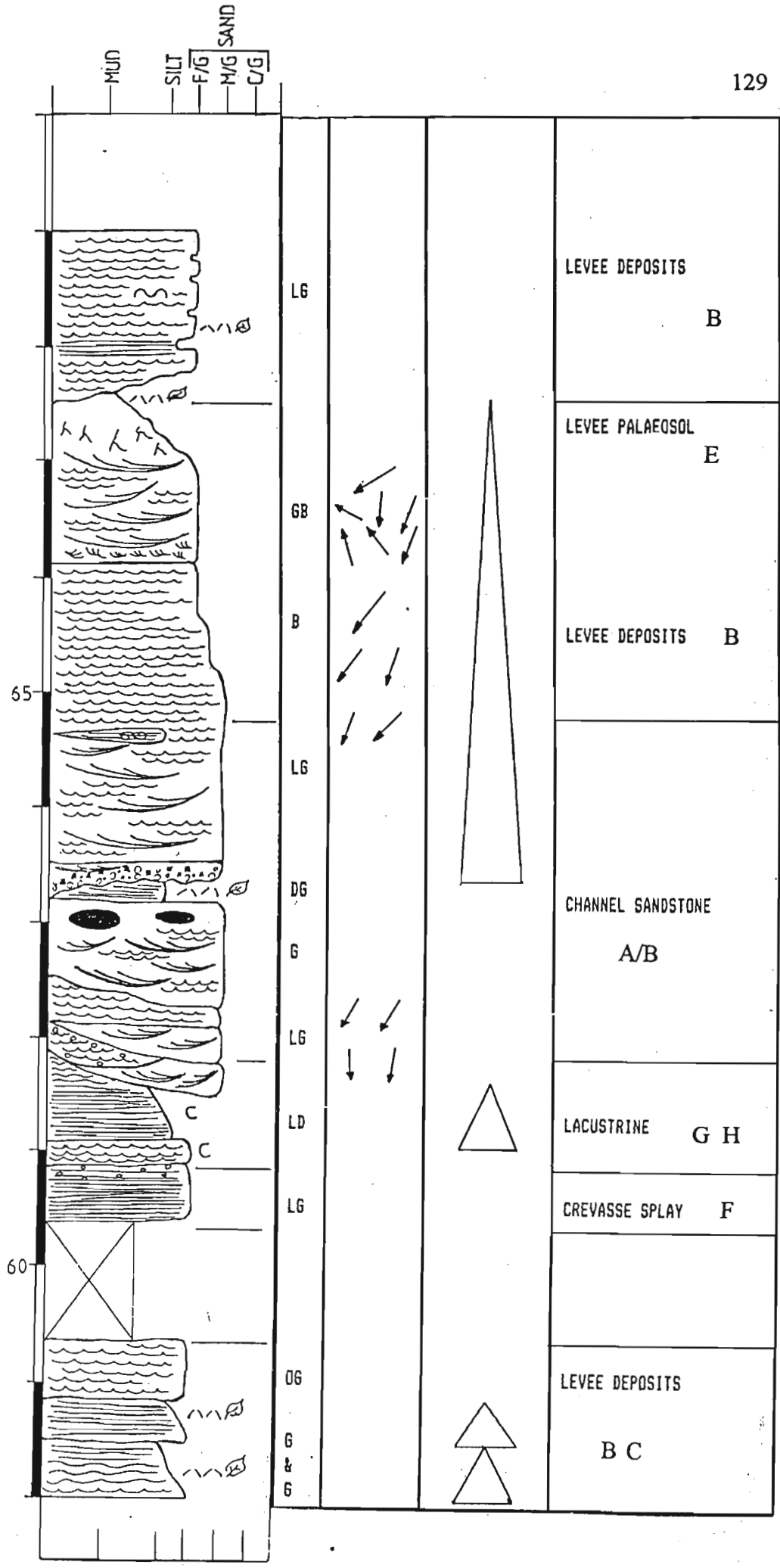
Following this is a 15cm thick sequence which begins with 6cm light grey, ripple cross-laminated sandstone, followed by 5cm dark grey, horizontally laminated sandstone, topped by another 4cm rippled sandstone. The top rippled sandstone is eroded by a 30cm thick sequence of troughs composed of extremely coarse grained, light grey sandstone containing both quartz and feldspar. The lower troughs are smaller in scale than the upper troughs, the former having widths of 50cm to 100cm, and the latter reaching 200cm across. Palaeocurrent directions include 252° , 232° , 226° , and 229° , giving a general direction towards the south-west.

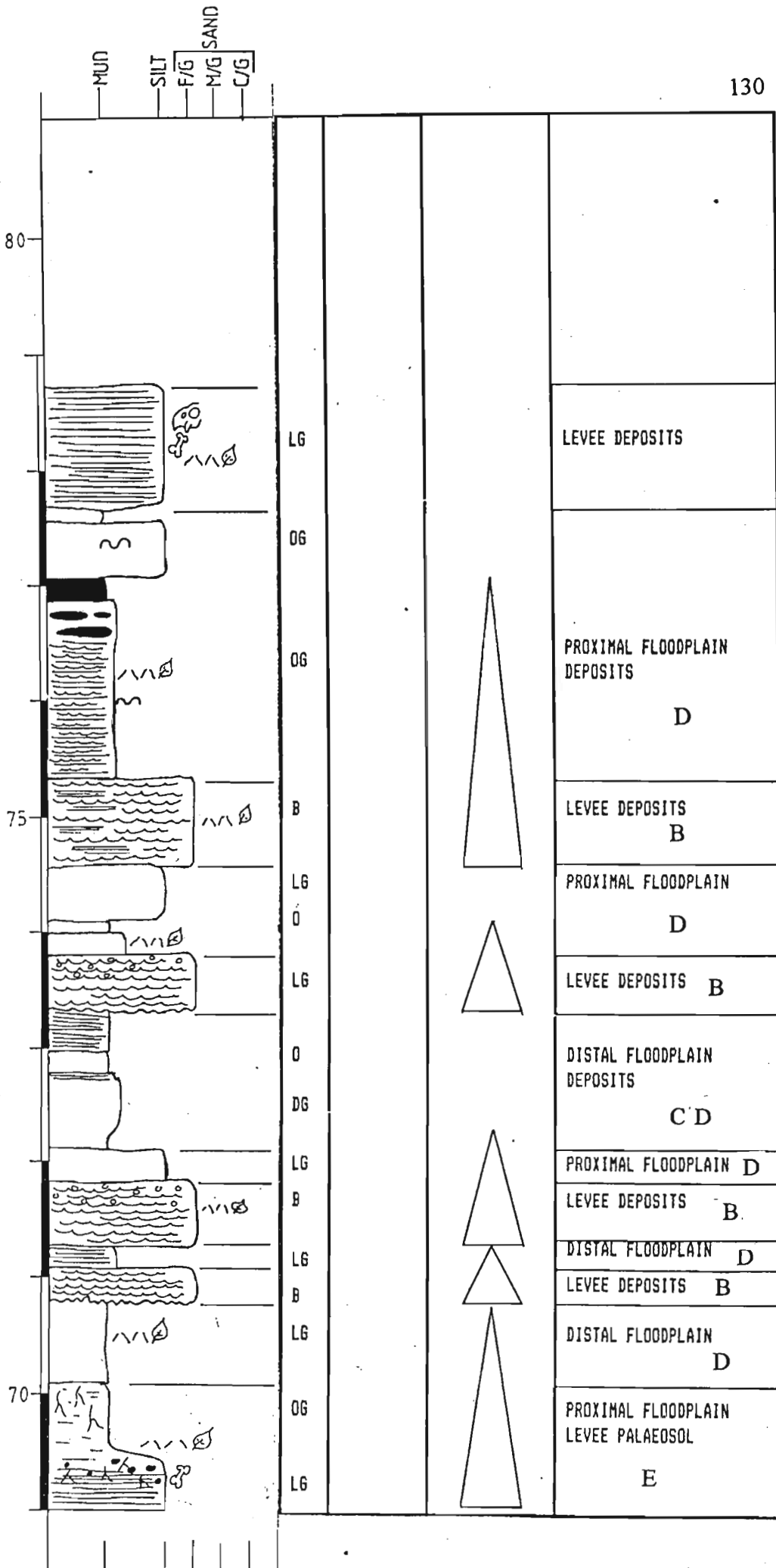












The following 0.5m is composed of two planar units which are both bounded and separated by thin layers of fissile, dark grey, fine grained, carbonaceous sandstone. The planar units are composed of coarse grained, light grey sandstone and have cross beds which reach 1-2cm in thickness. The second planar bedded unit has a coarse grained layer along its erosive base. The palaeocurrent direction recorded is 238°.

Overlying the planar units is a coarse grained, ripple-cross laminated sandstone which shows lateral variation with small scour troughs. Quartz grains reach 2 to 3mm in diameter. Palaeocurrent directions from rib-and-furrow include 243°, 243°, 259°, and 238°, giving a general current direction towards the south-west.

The following 40cm consists of a coarsening upwards, dark grey, micaceous unit which spans the 3m mark of the log. It grades from a horizontally laminated siltstone to a ripple cross-laminated, fine grained sandstone and is interrupted by scour troughs. Palaeocurrent directions from rib-and-furrow include 270°, 245°, 237°, and 253°. The scour troughs are composed of medium grained, light grey sandstone. A single trough measured 1m wide and contains rip-up clasts from the enclosing siltstone. Trough palaeocurrent readings include 246° and 229°.

The sequence continues with a 0.5m thick, dark grey, micaceous siltstone horizontally laminated on a millimetre scale. It has been eroded by a 30cm thick, fine grained, light grey, ripple cross-laminated sandstone. Palaeocurrent readings from rib-and-furrow include 251°, 237°, 232°, 239°, 240°, 227°, 244°, and 254°, an overall direction towards the southwest.

4m to 8.3m

The next 2.5m grades from a horizontally laminated siltstone to a fine grained sandstone. The sandstone is composed of silt/sand couplets, each composed of a massive layer of dark grey siltstone grading into a layer of light grey, massive sandstone with a sharply defined top which is rippled. The couplets range in thickness from a few millimetres to an occasional few centimetres. The surface of the sandstone component of the couplet often

shows invertebrate burrowing in the horizontal and vertical planes (Plate 1). Only a single complete ripple surface is exposed giving a wavelength of 8cm and an amplitude of 0.5cm. The ripples are symmetrical and give an azimuth trending southwest-northeast (compass reading of 250°-070°). Palaeocurrent readings taken from rib-and-furrow include 242° and 224°.

The above sandstone unit contains four layers of conglomeratic sandstone ranging in thickness from 5cm to 10cm, which occasionally pinch-and-swell. Their internal structure consists of massive sandstone containing pebbles and rip-up clasts, topped by a thin rippled surface showing large wavelengths ranging from 10cm to 12cm. The sandstone pebbles are well rounded and range in length from 3cm to 7cm; some containing pyrite. The massive sandstone is extremely coarse grained and composed of both quartz and feldspar grains that are sub-rounded and reach diameters of 2cm. The third conglomeratic layer was found to contain fossilised stem imprints. Palaeocurrent readings from these four layers include 239°, 226°, 222°, 258°, 266°, 258°, 253°, 253°, 260°, 241°, 244°, 228°, and 236°, indicating a southwesterly direction.

The above sandstone unit becomes wavy laminated towards its top, and is overlain by a thin layer of dark grey, fine siltstone which is wavy laminated on a millimetre scale. This siltstone is covered by a coarser siltstone which is horizontally laminated and contains a 1cm thick layer of light grey, ripple-cross laminated sandstone at its centre.

The siltstones are topped by a 2m thick sequence of sediments which alternate between mudstone and siltstone and coarsens to a unit of silt-sand couplets. The internal structures of the sediments ranges from horizontally laminated, in the case of the mudstone, wavy lamination for the silts, and ripple cross-lamination for the sandstones.

The sandstone component of the unit is composed of the silt/sand couplets previously described, with a large degree of invertebrate burrowing. The top of the unit is shown to coarsen as the sandstone component of the couplets thickens resulting in an overall coarser appearance. Approximately 70cm into the sequence is a thin conglomeratic sandstone

similar to those found further down in the sequence. It contains pebbles and rip-up clasts, is light grey and tends to pinch-and-swell. A palaeocurrent reading taken from the surface ripples measures 268° . At the same level, a calcretised boulder was seen measuring 0.5m in diameter.

8.3m to 12m

The above unit abruptly ends due to the presence of an unconformity which dips at 020° towards the southeast. Moving in a northwest direction, the above sandstone unit thickens to 5m. The depression formed by the unconformity is filled with a 70cm thick layer of organic rich sediments, including a seam of low grade coal. In the vicinity where the log is recorded, the unconformity is topped by a thin layer of finely laminated siltstone, followed by 50cm of low grade coal containing silt layers and showing bioturbation, becoming an organic rich mudstone containing plant mats of *Calamities* and *Glossopteris* remains. Approximately 50m to the northwest the coal seam decreases to a thickness of only 15cm, and is not topped by organic rich mudstone. It has been eroded by an extremely coarse channel lag containing 1 to 2cm diameter quartz and feldspar grains and large mudchips. The siltstone under the coal seam also thickens towards the southeast.

Continuing with the logged section, the organic rich mudstone is eroded by a pinch-and-swell layer of light grey, coarse grained sandstone containing 70% quartz. It is rippled and contains rip-up clasts. The wavelength of the ripples averages 40cm with a 5cm amplitude, with crest orientation measuring 201° . Conformably overlying this rippled layer is a 30cm thick, wavy laminated, grey siltstone which contains millimetre thick layers of fine grained sandstone. It is topped by a 10cm layer of the same fine grained sandstone which is light grey with a large degree of invertebrate burrowing.

The sequence continues with a dark grey, 12cm thick, horizontally laminated, silty mudstone which is micaceous and laminated on a millimetre scale. It has been eroded by a thin, extremely coarse grained, pinkish sandstone containing large subrounded pebbles and feldspar grains which reach 2cm in length.

The above is conformably overlain by a 90cm thick section of silty mudstone. The mudstone is horizontally laminated and contains small lenticular sandstone layers which gain a maximum thickness of 10cm. Each sandstone layer consists of a coarse base with a ripple cross-laminated surface, and contains rip-up clasts of the surrounding silty mudstone.

The above mudstone unit has been eroded by two separate units. The first erosional unit is a 30cm section of light grey, fine grained sandstone which shows an internal structure of micro-trough cross-bedding. The second erosional unit erodes into both the silty mudstone and the fine grained sandstone, and is more of a continuous layer than the first unit. It is composed of a coarser sandstone and shows a larger scale of micro-trough cross-bedding. Two palaeocurrent readings taken include 229° , and 232° , giving a direction towards the southwest.

Conformably overlying the above is a 1.3m thick sequence composed of silt/sand couplets forming wavy lamination. This sequence of couplets contains two thin, and one thick, lenticular, coarse grained sandstone layers. The thicker unit is 15cm thick, and contains rounded pebbles at its base. It shows micro-trough cross-bedding, which laterally becomes ripple cross-lamination where it pinches out.

12m -15m

Eroding the above is a 70cm thick light grey, micro-trough cross-bedded, fine grained sandstone. It is followed by a wavy laminated unit of silt/sand couplets resulting in light and dark grey colour lamination on a millimetre scale.

Both of the above units are eroded by a 30cm thick, fine grained sandstone which has a coarse base composed of rip-up clasts, millimetre sized grains, and coalified plant material. Its associated sandstone unit reaches a thickness of 1.3m and is composed of a light grey sandstone which shows very shallow trough cross-bedding. The base of the troughs contain rip-up clasts, which are small and average 5mm in length. The internal layering of the troughs is on a millimetre scale.

At the contact between the above sandstone and its overlying sediments is a layer of calcretised boulders ranging in size from 0.5 to 3m in diameter.

Conformably overlying the above sandstone are two separate units composed of silt/sand couplets. The first unit is 1m thick and shows a slight overall upward coarsening as the sandstone component of the couplets tends to thicken. The couplets contain sandstone pebbles ranging from 3 to 6cm in diameter. Palaeocurrent readings from rib-and-furrow include 175°, 191°, 202°, 135°, 113°, 209°, 186°, 208°, and 216°.

15 to 21m

The second couplet unit is slightly coarser than the first reaching a thickness of 0.5m, containing both pebbles and rip-up clasts throughout its thickness. Palaeocurrent readings from rib and furrow include 197°, 228°, 172°, 202°, 207°, and 176°.

There follows an erosive contact with a 10cm thick band of 'dirty' grey-brown sandstone which is ripple cross-laminated, and has a 1cm band of wavy laminated, dark grey siltstone at its centre.

Overlying this is a 1.5m section composed of three upward coarsening couplet units of varying thicknesses. Each unit appears to coarsen up from a horizontally laminated siltstone to a rippled sandstone as the sand component of the couplets slowly increases.

The first upward coarsening unit is 60cm thick and shows soft sediment deformation as well as invertebrate burrowing. Sediment deformation occurs at the base of the unit where it is composed predominantly of siltstone. Palaeocurrent readings from rib-and-furrow include 202°, 197°, 203°, 197°, 209°, and 196°. It is topped by two thin, lenticular layers of fine grained sandstone which is rippled and contains sandstone pebbles ranging in size from 2cm to 5cm. Palaeocurrent readings from the two layers include 184°, 191°, 213°, 208°, 194°, 199°, and 204°.

The second upward coarsening unit is 40cm thick and contains sandstone pebbles averaging

6 to 7cm in diameter. It also shows invertebrate burrowing. The third unit is only 30cm thick with no bioturbation. A single palaeocurrent reading of 207° was taken.

The following 2.5m consists of 'dirty' brown, fine grained ripple cross-laminated sandstone based by a layer of calcretised boulders reaching 2m in diameter. The top 20cm of this unit is composed of a horizontally laminated siltstone, dark grey in colour. Palaeocurrent readings from rib-and-furrow include 211°, 199°, 183°, and 196°, giving a south-southwest direction.

There is an erosional contact with the overlying rippled sandstone. This sandstone is light grey and forms the base of the first palaeosol recorded in the sequence. Rib-and-furrow from the sandstone give palaeocurrent readings of 208°, and 187°. The sandstone grades into a 10cm thick horizontally laminated, grey siltstone, which in turn grades into a 30cm thick, root horizon, which together with the invertebrate burrowing, has destroyed the sedimentary structure of the sediment. The profile of the palaeosol continues with 20cm of silty mudstone which has weathered orange. Where it is not weathered, the sediment appears to be olive green in colour. It has also lost all sedimentary structure, shows vertical and horizontal invertebrate burrowing, and contains hashed organic matter. The profile ends with approximately 1m olive green mudstone containing hashed organic material.

21m to 25.5m

The mudstone topping the palaeosol profile is eroded by a 2m thick sequence of micaceous, light brown sandstone dominated by trough cross-bedding. Its base consists of a thin layer of horizontally laminated fine grained sandstone with a coarse grained base. The sandstone coarsens to medium grained throughout the rest of the unit. There are layers of ripple cross-lamination, and often the base of the individual foresets are rippled. Towards the top of the unit are areas containing large rip up clasts, which reach diameters of 10cm, plus the uppermost rippled areas contain pebbles ranging in diameter from 2-3cm. The individual troughs are ovoid in shape; measurements from two troughs include - 1. width = 50cm, length = 1m, and 2. width = 1m, length 3m. Compass readings taken from the rib-and-furrow structures of the rippled sandstone include 212°, 205°, 236°, 258°, 256°, 288°, 251°,

and 268°. Palaeocurrent directions taken from the troughs include 221°, 271°, 301°, 250°, and 263°. The ripples give current directions ranging from west-northwest to south-southwest, and the trough readings range from southwest to northwest.

The next 2.5m is dominated by a light grey, ripple cross-laminated, fine grained sandstone with minor incursions of silts and muds. The sandstone is laminated on a millimetre scale and is micaceous with a small amount of invertebrate burrowing. Palaeocurrent readings from the rib-and-furrow structures include 270°, 234°, 260°, 282°, 267°, 269°, 269°, 252°, 278°, 237°, and 258°.

The first fine grained layer is olive green and chert-like in appearance reaching a maximum thickness of 15cm. There are two more fine layers (2-3cm and 5-10cm thick respectively) both consisting of fissile, dark grey siltstone.

25.5m to 30m

The sandstone is topped by 30cm of upward fining siltstone to mudstone, which is horizontally laminated and dark grey in colour. This in turn is eroded by a 10cm layer of medium grained, brownish-grey, massive sandstone containing rip-up clasts from the underlying silt and mudstone. Next in the sequence is a 30cm thick unit of extremely finely laminated, dark grey, micaceous, silty mudstone.

Again, a thin sandstone layer erodes into the mudstone. It is also approximately only 10cm thick, however in this case is rippled and contains sandstone pebbles with an average diameter of 4cm. A single palaeocurrent reading was recorded of 270°.

The following 1.5m thick, massive siltstone gradually grades into a silty mudstone, and contains lenticular, coarse grained, ripple-cross laminated sandstone layers, which contain quartz grains up to 5mm in diameter. The siltstone appears massive, is dark grey, and contains small chert-like concretions reaching 3cm diameter towards its top.

The silty mudstone is eroded by another unit of horizontally laminated silty mudstone. This mudstone forms the base of a second palaeosol profile in the sedimentary sequence. This blue-grey mudstone reaches a thickness of 1m, coarsens upwards, and shows invertebrate burrowing. A large circular section 20cm in diameter showed intense bioturbation totally destroying any sign of sedimentary structure. Soft-sediment deformation is also present throughout the layer. Fossilised roots are found 0.5m into the layer in the horizontal plane.

The second layer in the soil profile is a 60cm thick layer of massive siltstone. However the outcrop is situated directly adjacent a dolerite dyke resulting in the sediments being baked and making identification difficult. The siltstone is baked to a light grey colour and contains *Calamities* stems, and bone chips. There are also small areas of coarse grained pockets throughout the unit, and areas that are slickensided.

The sedimentary sequence is then interrupted by a 5m thick dolerite sill.

34m to 40m

The section continues with a medium grained, ripple cross-laminated sandstone reaching a thickness of 50cm and is too weathered for any palaeocurrent readings to be taken. The sandstone is baked to a whitish-grey colour. It is overlain by a 50cm thick greenish-grey siltstone, that appears massive and contains vertical and horizontal root impressions, and could form the base of a third soil profile. However, again there is another dolerite sill above which the soil does not continue.

The sequence continues 0.5m up with 40cm of horizontally laminated, fine grained sandstone which is light brown in colour. It is topped by a thin, 5cm thick band of very coarse grained, light brown sandstone, which is ripple cross-laminated, and forms the base of a 3m thick medium grained, light brown sandstone unit. The base of the unit, up to approximately the 1m mark, is dominated by ripple cross-laminated, micaceous sandstone that is extremely pebbly. These sandstone pebbles are flat in the horizontal plane and oval in shape, and average 1-2cm in length. Palaeocurrent readings from rib-and-furrow include 249°, 279°, 256°, and 291°.

The following 2m of the sandstone has no pebbles, and is dominated by trough cross-bedding and ripple cross-lamination, with the occasional massive area. The bedding is very fine for both the rippled and cross-bedded layers, with layers commonly showing soft-sediment deformation. At this stage there is a third disruption in the sequence, and the section is continued 0.5m higher in the stream.

40m to 44m

The following approximately 2.5m of the log is composed of four erosion-based units of silt/sand couplets. The first unit is 1.2m thick and shows the characteristic light and dark grey colour banding. The base of this unit is baked to a light grey colour and contains large fragments of fossilised plant remains. The top of this unit contains sandstone pebbles ranging in diameter from 1 to 7cm. Two complete ripple surfaces are exposed at the top of the unit. The first has a wavelength of 7cm, and an amplitude of 0.5cm, and the second has a wavelength of 8cm, and an amplitude of 0.5cm. Both are symmetrical ripples giving palaeocurrent readings of 216°-036°, and 196°-016° respectively, while readings taken from rib-and-furrow give 297°, 252°, 306°, 056°, and 074°.

The second unit, 40cm thick, fines upwards, and is based by a 10cm thick section of extreme bioturbation which destroys all structure. The rest of the unit shows invertebrate burrowing. A single palaeocurrent reading of 349° was measured.

The third couplet unit is approximately 50cm thick and also shows invertebrate burrowing. Towards the top of this unit are five well exposed ripple surfaces of symmetrical ripples directly overlying each other. Starting from the bottom surface -

1. wavelength = 4.5cm, current direction = 206°-026°;
2. wavelength = 7cm, current direction = 166°-346°;
3. wavelength = 4.5cm, current direction = 161°-341°;
4. wavelength = 4cm, current direction = 208°-028°; and
5. wavelength = 4cm, current direction = 193°-013°.

All had an amplitude of 0.5cm, and all the surfaces show invertebrate burrowing.

The fourth couplet unit shows a marked decrease in grain size as the sandstone component of the couplets decreases to a large extent. The top of this unit shows extreme bioturbation destroying most of the structure. This unit could possibly be the base of another palaeosol profile as it also contains fossilised roots in the vertical plane. This unit is topped by a 10cm thick layer of extremely carbonaceous, dark grey mudstone, containing fragments of fossilised plant remains. This organic rich layer is eroded by a thin layer of rippled siltstone.

Conformably overlying the siltstone is a 50cm thick unit of silty mudstone which shows a slight coarsening of grain size towards its top. It is horizontally laminated but gradually becomes wavy laminated as it coarsens. This mudstone is light and dark grey colour banded.

The following 70cm comprises hummock cross-laminated, fine grained, greyish-brown sandstone which shows an upward fining of grain size, becoming a siltstone at the top of the unit. Throughout the unit there are thin bands (reaching 4cm thickness) of massive, lenticular siltstone.

44m to 47m

The above unit is topped by another thin band of ripple cross-laminated sandstone which at its thickest is approximately 5cm thick. The sandstone is light grey and medium grained.

The above thin band of sandstone forms the base of a 1.5m unit of light grey, fine grained sandstone. It shows a variety of sedimentary structures throughout its thickness, starting with ripple cross-lamination, becoming hummock cross-lamination, horizontal cross-lamination, once again hummock, and ending with another small section of rippled sandstone. Soft-sediment deformation is apparent in the lower section of hummock bedding.

Conformably overlying this is a siltstone, 1.5m thick, which fines to a silty mudstone, and again coarsens to a dark grey siltstone horizontally laminated on a millimetre scale.

47 to 54m

Continuing the sequence is a 1m thick grey siltstone forming the base of another palaeosol profile. The first half of this unit is horizontally laminated, becoming on appearances massive with the advent of a fossilised root horizon. It is covered by a siltstone which rapidly fines into an organic rich mudstone containing coalified remnants of stem material. Approximately 35cm into this silty mudstone is an extremely thin layer of low grade coal, above which the mudstone coarsens into an approximately 2m thick unit of horizontally laminated silty mudstone, greyish-green in colour. Its top half contains numerous thin bands of fine grained sandstone most of which are no thicker than 10cm, occasionally reaching 20cm. These layers are boudinaged, and internally show a massive base with a rippled top. The first four and sixth bands are greenish-brown in colour, whilst the fifth and last bands (the thickest bands) are composed of silt-sand couplets and therefore light and dark grey in colour.

The last sandstone layer which tops the silty mudstone unit, reaches a thickness of 15cm. Its surface contains quartz and feldspar pebbles which are sub-rounded and range in diameter from 1mm to 2cm, and also shows invertebrate burrowing. A single complete ripple surface measured has a wavelength of 5cm, with a 0.5cm amplitude. The palaeocurrent direction measured 202° - 022° .

The overlying unit measures 80cm in thickness and is also composed of silt-sand couplets, however the sand component is less than that of the underlying unit making this unit more siltstone like in composition. The surface of the ripples shows invertebrate burrowing. The siltstone is micaceous and contains fossilised plant remains. It is topped by a 10cm thick, fine grained sandstone light grey in colour and ripple cross-laminated. Two palaeocurrent readings from rib-and-furrow structures both measured 262° .

The above forms the base of another sandstone unit composed of silt-sand couplets. It has been classified as a fine grained sandstone as the sandstone component is more abundant than the siltstone. There are thin, discontinuous bands of dark grey mudstone throughout the unit. These couplets are extremely bioturbated often destroying the sediment structure.

The burrow sizes are larger than seen in the earlier sediments with diameters reaching 1cm.

Above the couplet unit is a 1.5m sequence of fines. A horizontally laminated, silty mudstone fines into a massive mudstone layer which contains a pinch-and-swell coal layer at its centre. There is no plant material in the surrounding mudstone. The sequence continues with a slightly silty mudstone which also shows horizontal lamination on a millimetre scale. The siltstone shows invertebrate burrowing and contains vertical fossilised root impressions in its upper reaches. The mudstone is light and dark grey colour banded.

54m to 60m

The root horizon is eroded by a 3m thick coarse member unit which is based by a lag conglomerate. The lag contains mostly quartz grains which are rounded to sub-rounded and reach a length of 2cm. The sandstone matrix is light grey. Following the lag is a sandstone which grades from coarse grained to medium grained and is mostly trough cross-bedded. The troughs are extremely low angle and shallow, and are commonly based by rip-up clast conglomerates which reach 30cm in thickness. Towards the top of the unit, the sandstone of the individual crossbeds is coupled with a thin silt layer giving a light and dark grey banding effect of the crossbeds. The base of the unit contains large calcretised boulders reaching 3m in diameter.

The troughed unit is covered by a 1m thick, horizontally laminated, fine micaceous unit which grades from a silt to a mud. The base of this unit contains lenticular bands of light brown sandstone; and towards the top of the unit the dark grey mudstone is interbedded with fine green silty layers. The unit contains fragmented fossil plant material.

Eroding this mudstone is another fining upward layer which grades from a ripple cross-laminated, fine grained sandstone to a horizontally laminated siltstone. The sandstone lamination averages 2mm in thickness and appears colour banded by green and brown layering. The siltstone is laminated on a millimetre scale and shows green and grey colour banding. Both the brown and grey bands of the respective sections are an indication of the coarser component. The siltstone is micaceous and also contains fossilised plant fragments.

There follows a third, 35cm thick, fining upwards unit composed of a fine grained sandstone which grades into a siltstone. The unit is horizontally laminated, with layers averaging 1mm-2mm in thickness. Each individual layer coarsens upwards, and shows green and grey colour banding. This unit also contains very thin mats of fossilised plant material. It is topped by a 50cm thick, fine grained sandstone which is green in colour and ripple cross-laminated.

60m to 67.5m

There follows a fourth break in the sedimentary sequence with a 1m thick dolerite sill. Above this intrusion is a 50cm thick horizontally laminated sandstone. There is a slight indication of colour banding, alternating between light grey and a darker 'dirty' grey. There are sandstone pebbles at the surface of this layer, with diameters averaging 2cm.

There follows a second fine grained micaceous sandstone unit which is ripple cross-laminated and composed of silt/sand couplets. It is covered by a fining upwards unit of silt/sand couplets. Due to the minor sand component, the unit appears horizontally laminated (millimetre scale), eventually grading into a coarse siltstone as the number of sandstone layers dramatically decreases.

The thickness of the above unit varies from 50cm to 80cm as it has been eroded by a large coarse member unit. The first 1.3m of this unit is composed of medium grained sandstone, with sedimentary structures alternating between ripple cross-lamination and trough cross-bedding. The ripple cross-laminated sandstone is slightly finer grained. The rippled sandstone is light grey in colour and contains a few dark grey silt bands. The first rippled layer also contains sandstone pebbles reaching 8cm in length. Palaeocurrent directions from rib-and-furrow include 178°, 189°, 210°, and 212°. The trough-bedded sandstone is also light grey in colour, although has a 'dirty' appearance. The individual cross-beds measure 1cm thick, and the individual troughs are large and relatively shallow. The top of this unit contains a layer of large calcretised boulders reaching 4m in diameter.

The sandstone is covered by a discontinuous thin layer of horizontally laminated, dark grey

siltstone that contains fragments of fossilised plant material. Eroding the above sandstone and siltstone is a 2.7m thick sandstone unit which is based by a thin band of medium grained sandstone which contains sandstone pebbles ranging from 4-7cm in diameter, and rip-up clasts from the underlying siltstone. The first 1.5m of the sandstone is trough cross-bedded, medium grained and light grey in colour, with the troughs mostly filled by thin layers of ripple cross-laminated siltstone. The last 1.2m of the unit fines to a fine grained sandstone accompanied by the phasing out of the troughs, with the unit becoming wholly ripple cross-laminated and containing isolated pockets of horizontally laminated siltstone which show soft-sediment deformation. There is also a change in colour as the grey sandstone begins to alternate with a dirty brown, micaceous sandstone. Palaeocurrent directions from rib-and-furrow include 200°, 225°, 217°, 199°, and 218°.

There follows a third sandstone unit which fines into an organic-rich silty mudstone. This unit is based by a small section of micro-trough cross-bedding, followed by larger troughs filled by rippled sandstone. The sandstone is fine grained and greenish-brown in colour. Palaeocurrent directions measured from both troughs and ripples are chaotic, and include 343°, 322°, 201°, 298°, 184°, 201°, and 238°.

The sandstone fines into a massive, silty mudstone which contains a layer of fossilised root material, followed by a section containing excellent *Glossopteris* leaf impressions. This plant rich layer is eroded by a fine grained, grey and dirty grey banded sandstone unit which is ripple cross-laminated. The grey layers are finer in composition and show invertebrate burrowing. The dirt bands tend to contain fragmented fossil plant remains, with one dirt band yielding excellent impressions of *Glossopteris* leaves. Approximately 0.5m into the unit is a thin band of horizontally laminated, grey siltstone that is not bioturbated.

67.5m to end

The sequence continues with a 1m thick unit consisting of 0.5m siltstone grading into 0.5m of micaceous, olive green mudstone. The siltstone is grey, horizontally laminated and contains small circular calcrete concretions. As the siltstone grades into the mudstone the

internal structure becomes less noticeable and is finally destroyed by the presence of large, thick fossilised roots. The siltstone also contains fossilised roots and a covering layer containing *Glossopteris* leaf impressions, as well as small bone fragments.

A flat erosion surface separates the above mudstone from a second 70cm thick mudstone layer which is massive, grey, and contains fragmented fossilised plant remains. It has been eroded by a 30cm thick, light brown, fine grained sandstone, which is ripple cross-laminated on a millimetre scale and micaceous.

Overlying this is a 20cm band of horizontally laminated, grey, silty mudstone, which in turn is followed by another ripple cross-laminated, fine grained sandstone unit. This sandstone is also light brown in colour, micaceous, and its surface contains sandstone pebbles. These pebbles range in diameter from 4cm to 10cm. There is also fragmented fossilised plant material visible.

Conformably overlying the above is a light grey massive siltstone, followed by a unit of dark grey massive mudstone which coarsens to become a silty mudstone. The last 1cm of the unit is horizontally laminated, and is covered by another massive section of mudstone, which has weathered to an orange colour. This in turn is overlain by 35cm of horizontally laminated mudstone which shows light and dark grey colour banding.

The mudstone has been eroded by another unit of ripple cross-laminated, fine grained sandstone. The sandstone is micaceous, grey in colour, and its surface contains pebbles. There follows another massive layer of slightly silty mudstone, which contains small coalified pieces of fossilised plants. This layer is 20cm thick and grey in colour, and is topped by a thin clay-like band which is extremely fine grained and weathered orange.

Again, there is another unit of grey, massive siltstone, which is conformably topped by a fourth unit of fine grained, ripple cross-laminated sandstone. These individual layers are particularly thick, ranging from 1-5cm, and are interbedded with lenticular beds of mudstone. The sandstone is greyish-brown, micaceous, and contains fragmented plant

material.

The sandstone is topped by a 1.5m thick, olive green mudstone unit composed of 2-3cm thick layers which are made up of small coarsening upwards sequences. The internal structure of each layer shows a base of fine horizontal lamination, topped by a rippled surface showing invertebrate burrowing, with plant fragments separating the individual layers. Some of the surfaces contain millimetre sized grains. The top section of this mudstone contains a continuous layer of calcretised concretions, which reach a diameter of 2m, and is covered by a 20cm thick continuous layer of calcrete. This is followed by a 50cm thick olive green siltstone layer whose structure has been lost due to extreme bioturbation, and a second clay-like layer that is also weathered orange.

The sequence ends with a horizontally laminated, light grey siltstone unit containing fragmented fossilised plant material, vertebrate fossil remains, including a *Lystrosaurus* skull, ribs, and other disarticulated skeleton remains.

Appendix 3

Description of shoreline log

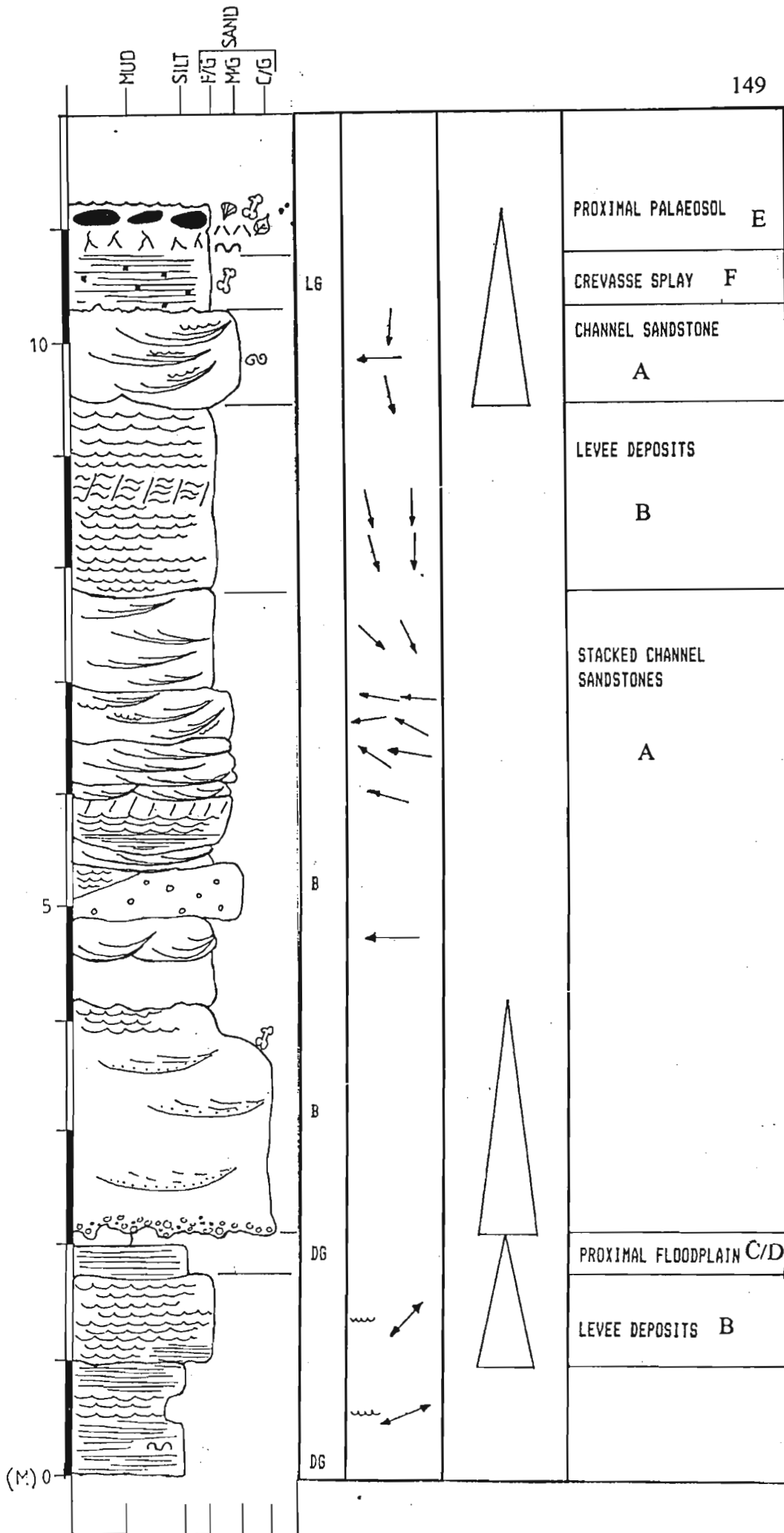
This log occurs stratigraphically just above the Kudu stream log, and contains a sequence of rippled shoreline sandstones which outcrop prominently in the area. This log is therefore known as the shoreline log, and was mapped in conjunction with Dr. R. Smith and Prof. T. Mason.

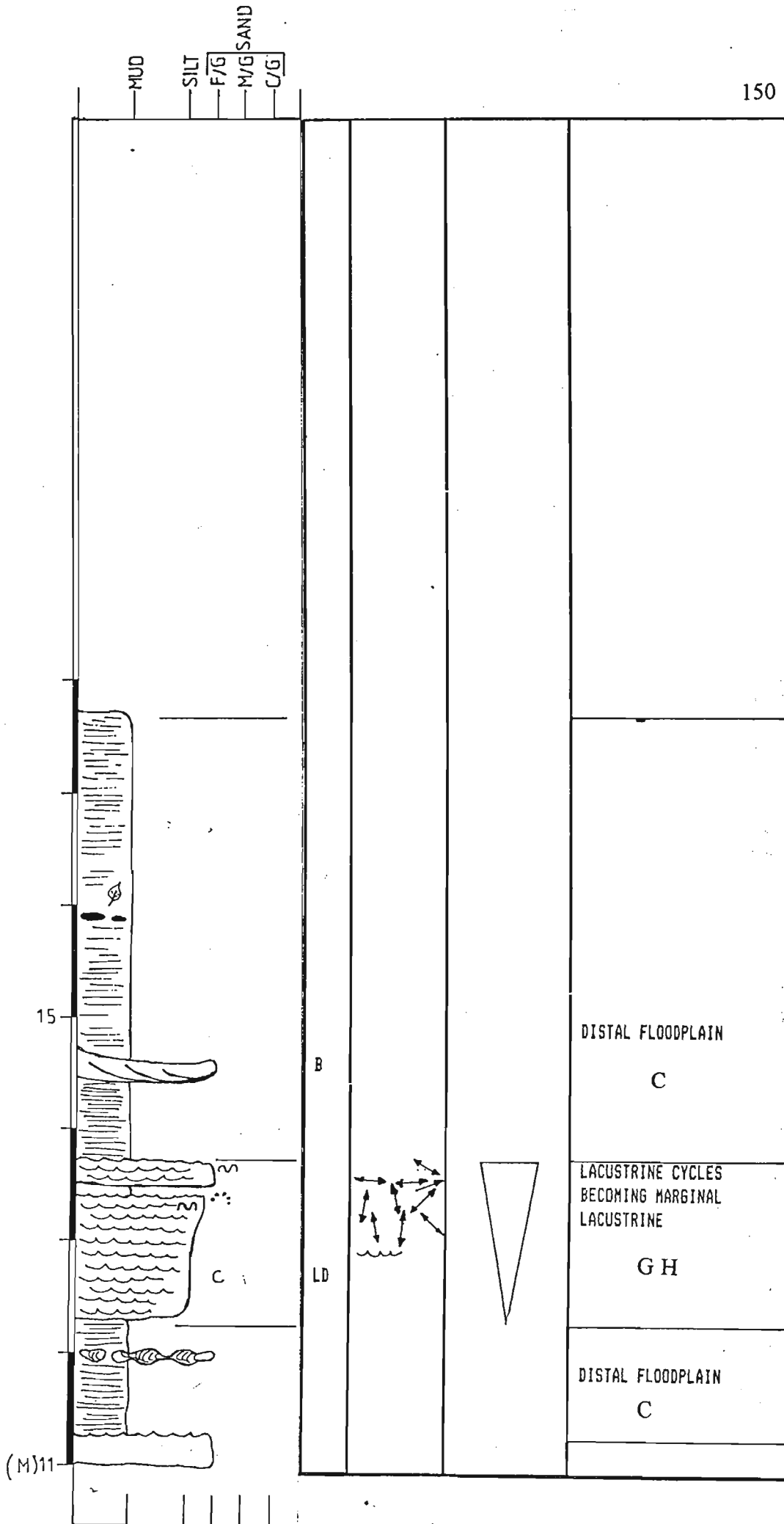
The shoreline log begins with a 1m thick dark grey siltstone which is finely laminated (<1mm), with a small degree of invertebrate burrowing. Halfway into the unit is a 20cm thick band of ripple cross-laminated silt/mud couplets, resulting in grey and dark grey colour banding. Palaeocurrent trend measures 068° - 248° .

The siltstone is overlain by 70cm of ripple cross-laminated, fine grained sandstone, the base of which shows lateral variation with horizontally laminated sandstone, and the top 5cm of the unit is massive. The outcrop is a vertical section with no rib-and-furrow structures present, however a general current trend was estimated from the crests and is approximately 044° - 224° . Amplitude measurements include 1cm, 1.2cm, 1.5cm, and 1.5cm. The sandstone terminates with a sharp contact followed by 28cm of horizontally laminated siltstone, and 12cm soft, carbonaceous mudstone.

The mudstone is eroded by a coarse lag conglomerate which forms the base of a 2m thick coarse grained sandstone unit. The lag contains quartz and feldspar pebbles ranging in size from 3mm to 5cm in diameter. The feldspar constitutes approximately 20% of the composition. This feldspathic sandstone is superficially massive with coarse grained partings or washes, indicating trough cross-bedding with fining upward fill, becoming fine grained sandstone. The clasts in the partings are angular to sub-rounded. Bone chips were seen in the uppermost reaches of the trough cross-bedded unit. The top of this sandstone unit fines to a fine grained, ripple cross-laminated sandstone (approximately 40cm) which becomes laterally massive.

There follows an erosive contact with an 80cm thick, fine grained sandstone which is divided into 40cm of massive sandstone followed by 40cm of trough cross-bedded





MUD

SILT

F/G

M/G SAND

C/G

15

B

LD

DISTAL FLOODPLAIN

C

LACUSTRINE CYCLES
BECOMING MARGINAL
LACUSTRINE

GH

DISTAL FLOODPLAIN

C

(M)11

sandstone. A single palaeocurrent reading from the troughs measures 270° . The troughs are overlain by 50cm of medium grained sandstone which is mostly massive but does show some lateral variation with ripple cross-lamination. It contains quartz and feldspar pebbles in the range of 2 to 4mm, and sandstone pebbles which reach 4.5cm in diameter.

The sandstone is overlain by 13cm of fine grained, "dirty" sandstone which has been eroded by a 1m wide trough of silty, micaceous sandstone. The trough is filled by 36cm of sandstone ranging from fine to medium grained. The scour fill begins with 14cm of centimetre thick, horizontally laminated sandstone, followed by 7cm ripple cross-laminated sandstone, topped by planar cross-bedding, which gives a palaeocurrent direction towards the east-southeast. The planar surfaces are eroded by a 11cm thick layer of troughs. A single trough measured 1m wide and gave a palaeocurrent reading of 286° .

Overlying the above troughs is a 34cm unit comprised of three stacked troughs of medium grained sandstone. The maximum depth of the troughs is 20cm, the widths are longer than 2m, and their lengths average 6 to 7m long. Palaeocurrent directions from the troughs include 304° and 280° , giving an average direction towards the west-northwest.

There follows another unit of trough cross-bedding. It measures 50cm thick, and the lower part of the foresets is rippled. Individual troughs range from 1 to 3m in length, and palaeocurrent readings taken include 262° , 298° , 280° , and 274° .

The sequence continues with a third unit of trough cross-bedded sandstone that is finer grained than the underlying units. The unit is 86cm thick, and comprised of large, shallow troughs which are greater than 5m in width. Palaeocurrent readings include 134° and 154° .

Conformably overlying the troughs is 166cm of ripple, and climbing-ripple cross-laminated, fine grained sandstone. Palaeocurrent directions from rib-and-furrow structures include 166° , 182° , 168° , and 180° . Towards the top of the unit the ripples become megaripples.

Topping the megaripples is another 80cm thick unit of trough cross-bedded, medium

grained sandstone. The troughs are filled with rippled sandstone which are in an oblique direction to the trough directions. There is a 020° diversion between the trough long axis and crest orientation of the ripples. The troughs are large and shallow, and the rippled layers show deformation. The size of the troughs range from 4m to 5m wide, and palaeocurrent directions measured include 168° , 268° , and 184° .

There follows an erosional contact with 80cm of horizontally laminated, fine grained sandstone. It is grey in colour and contains numerous mudchips and bone fragments. The last 20cm of the sandstone contains vertical roots and burrows. Fragments of *Calamities* and *Schizoneura* are found in the rooted horizon. The rooted horizon is topped by a layer of carbonate pods which range in size from 10 to 25cm in thickness. The pods contain bones and fish scales, and in places the surface is wave rippled with possible footprints. The surface of these pods are sharply defined, and their bases are gradational. These pods often coalesce to form thin sheets of calcrete.

The sequence continues with 1m of horizontally laminated mudstone which contains pinch-and-swell sandstone layers. The mudstone is conformably overlain by 1.5m unit of ripple cross-laminated sandstone and siltstone couplets. The unit shows a coarsening upwards trend as the grey siltstone component virtually disappears, and the sandstone component dominates. The base of this unit is almost totally composed of only grey siltstone topped by extremely thin layers of lighter sandstone. The thick siltstone layers appear massive.

The top of the unit is composed of sandstone layers which have an internal structure composed of a thin, basal clay veneer, followed by massive sandstone, topped by a ripple surface. The individual layers range from 1.5cm to 8cm in thickness, with no erosion of the successive layers occurring. The sandstone is brown in colour. The ripples are symmetrical and often bifurcated, and there are both sharp and flat crested ripples, with occasional ladderback ripples. The successive layers show varying current directions, and also varying wavelengths. Approximately 110cm into the unit is a surface which shows reworked footprints, and trampled areas. There are isolated vertical burrows and slump structures in the sandstone. Overlying this footprint surface is 9cm of mudstone. The

uppermost surface of the unit also shows trampling and horizontal burrowing. Wavelengths vary from 2.5cm to 9cm, and the amplitude is generally 1cm, or below.

Palaeocurrent trends include 350°-170°, 184°-004°, 314°-134°, 190°-010°, 348°-168°, 226°-046°, 236°-056°, 280°-100°, 250°-070°, 276°-096°, 268°-088°, 300°-120°, 330°-150°.

Overlying the trampled surface is approximately 4m of horizontally laminated, extremely fissile claystone. It contains *Glossopteris* and *Calamities* leaf impressions, and isolated carbonate nodules. Seventy centimetres into the unit is a 30cm thick layer composed of sandstone pods. The sandstone is fine grained and light brown in colour.

Appendix 4

Description of Fossil Dam Log

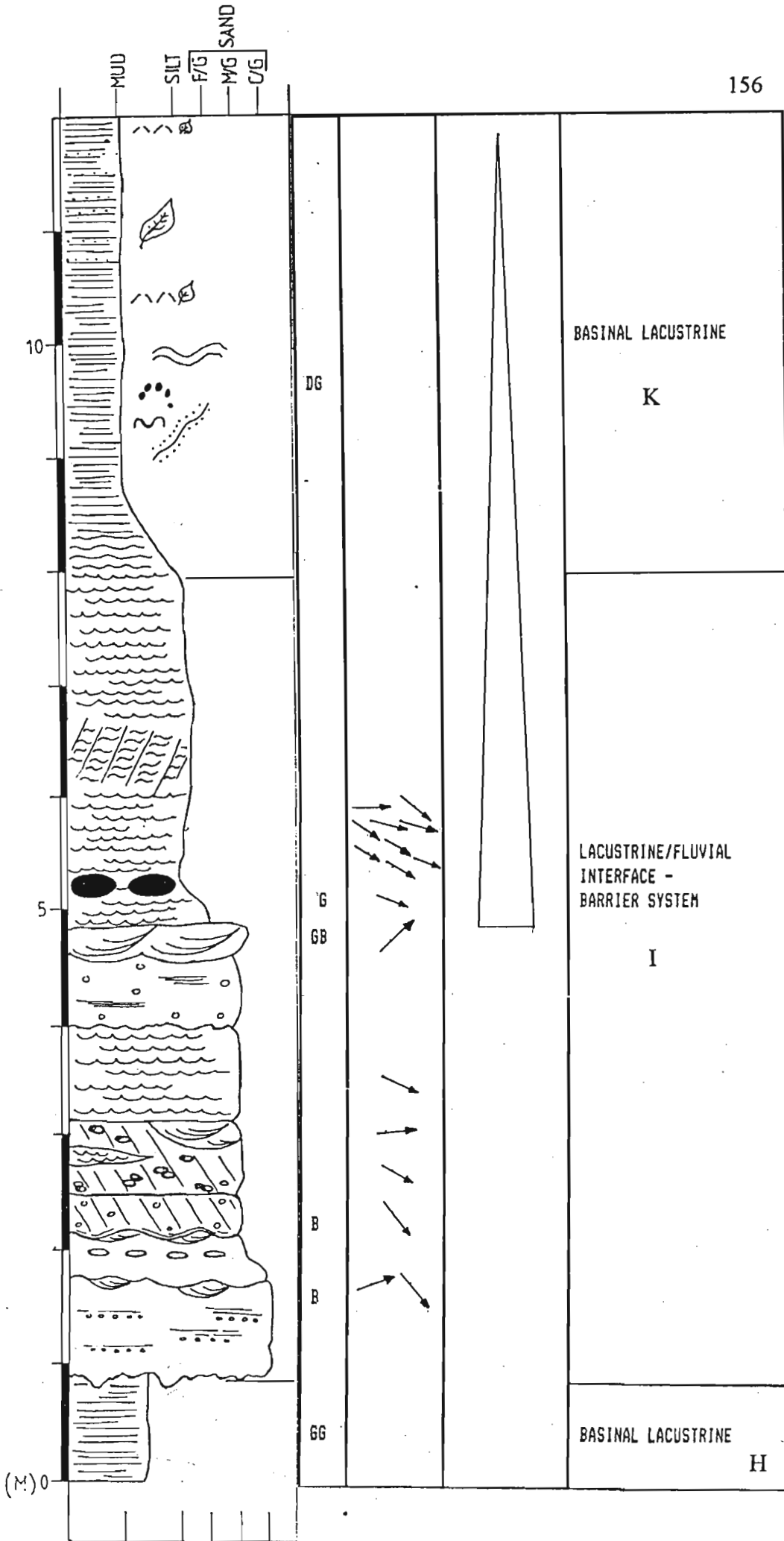
This log is mapped from the upper reaches of the Bedstead Stream, and therefore has lateral stratigraphic continuity with the Shoreline and Kudu stream logs. The section logged, measures only 16m thick, yet it is an extremely important sedimentary section as it yields rare findings of vertebrate trackways belonging to the mammal-like reptile group. This section was logged together with Dr. R. Smith and Prof. T. Mason.

The base of the section begins with approximately 90cm of horizontally laminated, silty mudstone that is thinly bedded with individual layers measuring 3-4mm, greenish-grey in colour, and displays blocky weathering.

The above is eroded by a coarse grained sandstone, the base of which shows high relief at the erosional contact, and can be divided into two units. The first massive unit is approximately 80cm thick, and is topped by a layer of shallow troughs. Palaeocurrent readings from the troughs include 070°, 140°, and 140°. This sandstone contains dark grey, silty mudstone partings which reach 3cm in thickness, and contain single pebble layers consisting of rounded quartz and feldspar grains which average in diameter from 3mm - 5mm.

The aforementioned shallow troughs separate the above sandstone from the second coarse grained sandstone unit. This second unit measures 40cm in thickness, and shows an upward fining in grain size. As with the above unit it is also massive, and topped by a series of shallow troughs. Halfway into the unit is a layer of concretions which are oblate and spherical in shape, and range in diameter from 4cm to 7cm.

A fine grained, scour sandstone parting separates the above sandstone from a series of medium grained sandstone units. The first unit is a planar cross-bedded sandstone measuring 40cm at its thickest, 6m in width and is a light yellowish-brown colour. There is a random distribution of sandstone pebbles throughout its thickness which range in size from 1.5cm to a large 15cm. The foresets measure 1 to 1.5cm in thickness, and the palaeocurrent direction measures 142°.



The second unit is also a planar cross-bedded set, and measures 54cm in thickness. Halfway into the unit is a small section of ripple cross-lamination, and towards the top of this unit is an isolated trough. The trough measures 2m wide and 0.5m deep, with a current direction towards 084°. There are sandstone concretions throughout the unit, which in some instances coalesce to form larger concretions. Again there is a large range in size from 1cm to 15cm. The individual foresets of this planar unit average 1cm in thickness, and the azimuth measured is towards 120°.

Overlying the above planar unit is a 85cm thick unit of ripple cross-laminated, medium grained sandstone. The average amplitude of the ripples centres around 1.5cm, and a compass reading taken from rib and furrow measures 076°. This unit is eroded by a fourth, medium grained sandstone unit which is similar in structure to the first two coarse grained units logged.

The fourth unit measures 80cm in thickness and appears massive, with thin lenses of silty material. It also contains sandstone pebbles throughout its thickness. Again, this massive unit is topped by a layer of shallow troughs. Two troughs measured both give a current direction towards 046°, and are respectively 20cm and 30cm deep.

Overlying the troughs is a thick, fine grained sequence which grades from a fine grained sandstone to a mudstone. This 11m thick sequence appears gradational, ranging from a fine grained, ripple cross-laminated greywacke to a horizontally laminated series of mudstone layers showing a great diversity of palaeobiology.

In the first approximately 20cm of the sequence, there is a gradation from a greenish-yellow fine grained sandstone, to a greener siltstone. At this gradational stage is a layer of large calcrete boulders which have weathered to a brown colour and show the same sedimentary structures as the surrounding sediment. Measurements taken from two of the concretions are 1.5m by 1.8m, and 2m by 1.1m. Lamination is on a millimetre scale, and a crest orientation reading, taken from the base of the sequence, measures 110°. Directions taken from ripples above the calcrete boulders include 120°, 110°, 122°, 118°, 124°, 104°, 106°,

090°, and 130°. Amplitude measurements range from 1.5cm to 2.2cm, and wavelength measurements taken include 9cm and 11cm.

Half-way into the ripple cross-laminated section is a section of climbing-ripple cross-lamination, climbing at approximately 025°. The ripple cross-laminated siltstone slowly grades into the horizontally laminated mudstone slabs at about the 8m mark. The palaeontology of the approximately following three metres of the section is known in some detail as many of the mudstone layers were studied individually in a large dam excavation. The first few meters is dominated by the presence of tetrapod trackways (Plate 8), and is followed by a 1m section dominated by a fossil plant mats. From the 11m mark to 16m mark, the mudstone contains isolated plant fragments. Also seen were arthropod trackways, beaded trails, fish trails, insect impressions and various meandering and zig-zag bioturbation. These fossils are described in detail in another section.

The individual mudstone slabs range in thickness from 1cm to 2cm and show internal, sub-millimetre scale lamination. The slabs are graded showing an upward fining from silty mudstone to mudstone. The base of these slabs often show load casts, and are occasionally lined by isolated quartz pebbles in single grain sand layers.

Appendix 5

Measuring trackways and their significance

The simplest trackways to measure are those left by bipedal animals, as they consist of only the hind feet, omitting the problem of distinguishing the pes from the manus (Lockley, 1991). Bipedal trackways are narrow as the animal walked erect, with one foot in front of another, and thereby resulting in a pace angulation of almost 180 degrees (Lockley, 1991).

Quadrupeds, on the other hand, leave trackways consisting of both the hind and fore feet, requiring that they be distinguished from each other to obtain correct measurements and information. However once a complete trackway with distinguishable pes and manus prints is found, examination offers a wealth of information on the causal organism.

Firstly, the manus prints on one side of the trackway are joined at corresponding points to form a line. The same is carried out on the opposite side of the trackway. The width between these two lines gives the trackway width of the manus. The same procedure is carried out for the pes prints. The width between the pes line on one side of the trackway, and a manus line on the opposite side, gives the standard trackway width.

A manus print on the left side of the trackway is then joined to the corresponding manus print on the right side. This is done up the entire length of the trackway, forming a zig-zag pattern. The angle formed between three of the joined prints corresponds to the pace angulation of the causal organism. This is done for both the manus prints and the pes prints.

Lines are then drawn from the prints to the midline. The distance between two points of alternate manus, or pes, footprints of the same limb gives the stride of the organism.

The distance between two points from corresponding manus, or pes, prints on either side of the trackway gives the pace of the animal. The pace is usually approximately half the stride length.

The approximate gleno-acetabular length of the animal, that is the length from the pectoral girdle to the pelvic girdle, can be obtained by measuring the distance from the centre of the

diagonal joining two corresponding manus prints, to the centre point joining the corresponding two pes prints. Unfortunately it is difficult to determine which pes set corresponds to a given manus set (Chestnut et al, 1994). Two likely possibilities exist:-

The first possibility is that there are no unoccupied footprints between the front and hind feet. This is gleno-acetabular distance type one.

The second possibility, Gleno-acetabular distance type two, occurs when there is one set of unoccupied footprints between the front and hind feet.

Also of interest when interpreting trackways, is the degree of overlap of the impression of the pes upon the manus (Sarjeant, 1975). Primary overlap is characteristic of animals in which the distance between the pectoral and pelvic girdles is not great. Tertiary overlap occurs only in extremely long bodied forms, for example salamanders, and in the fossil state is indicated by the wide interval between overlapping prints and a high, even obtuse, step angle (Sarjeant, 1975).

Trackway width helps to define the erectness of the causal animal (Lockley, 1991), that is, the narrower the trackway, the more erect the stance of the animal, and the more sprawled the animals gait, the wider the trackway. A wide trackway confers a stable animal, but one that is also not very maneuverable (King, 1991). Trackway width differs with varying speeds and length of leg (Lockley, 1991). The slower the animal is moving the more widely spaced are the feet, and the faster the animal moves the closer to the midline; this is for stability during the former, and a greater efficiency when moving forward in the latter (Lockley, 1991).

The trackway width combined with the animals stride further indicates how efficient the animal was during locomotion. A broad trackway combined with a short stride indicates an inefficient walker, whereas a narrow trackway and a long stride indicates an efficient

walker moving at an appreciable speed (Sarjeant, 1975). However manoeuvrable animals do sacrifice some stability for agility (King, 1991).

Pace angulation also helps in determining how the animal walked. The higher the pace angulation, the more erect the animal walked as the limbs were positioned under the body during locomotion, forming a trackway where one print is placed in front of another and not next to each other (Chestnut et al, 1994). Low pace angulation indicates a sprawling gait. However pace angulation is also affected by the speed of the animal (Lockley, 1991), and can therefore vary throughout the trackway.

The gleno-acetabular length is important to deduce the trunk length, and therefore the size, of the animal. However in some animals, notably amphibians, the body motion in locomotion is rather sinuous and the equivalence is therefore not quite exact (Sarjeant, 1975).

Having obtained the gleno-acetabular length of a quadrupedal trackmaker and the length of its stride, attempting the restoration of the animal becomes feasible. This interpretation is most readily done for reptiles and amphibians, where limb movement is essentially in phase, that is, the forelimb and hind limb movement of opposite sides occurs more or less simultaneously (Sarjeant, 1975).

The above measurements can indicate exactly how an animal walked, allowing for a partial determination of its way of life. Another important facet of these measurements is that an animal's speed can be calculated from them - a valuable tool used especially for calculating the speed of the dinosaurs. Footprints have also proved invaluable in dinosaur research as vast tracksites discovered show that the dinosaurs were indeed social creatures, and would evidently travel in herds. They also indicate that the predatory dinosaurs hunted in packs (Lemonick, 1993).

Appendix 6

Measuring trackway method.

The trackways were mapped using a 50cm square piece of card. This was used to draw 50cm squares onto the trackway surface using chalk. If the trackway was small, this was further divided up into 25cm squares, and again if the need arose. The footprints were then copied to scale onto graph paper.

Light conditions are a critical factor in footprint collecting, ideal conditions are late afternoon of summer days or sunny days in winter, when slanting sunlight creates long shadows and causes casts or moulds to stand out prominently (Sarjeant, 1975). The time for mapping was therefore mostly limited to the early morning and late afternoon - which also afforded excellent photographs. Due to these time constraints mapping was limited to only the best trackways found. For study purposes, it is important to have a series of footprints, that is a trackway usually consisting of a minimum of three sequential sets of impressions, so that the progressive motion (the gait) of the trackmaker can be determined (Sarjeant, 1975 and Lockley, 1991). The study of a single print has serious limitations; one cannot always be sure whether it is the track of a quadruped or biped, or even whether it represents manus or pes (Sarjeant, 1975). The surfaces which only held single or incomplete tracks were therefore discarded and due to circumstances considered a waste of time. Unfortunately, as Lockley, 1991, states - imperfect tracks tend to be the rule rather than the exception.

Appendix 7

Key to Tables :

SLP - Stride of left pes

SLM - Stride of left manus

SRP - Stride of right pes

SRM - Stride of right manus

PAP - Pace angulation of pes

PAM - Pace angulation of manus

P - Pace

PP - Pace of pes

PM - Pace of manus

GA1 - Gleno-acetabular distance type 1

GA2 - Gleno-acetabular distance type 2

TS - Standard trackway width

TMM - Manus trackway width

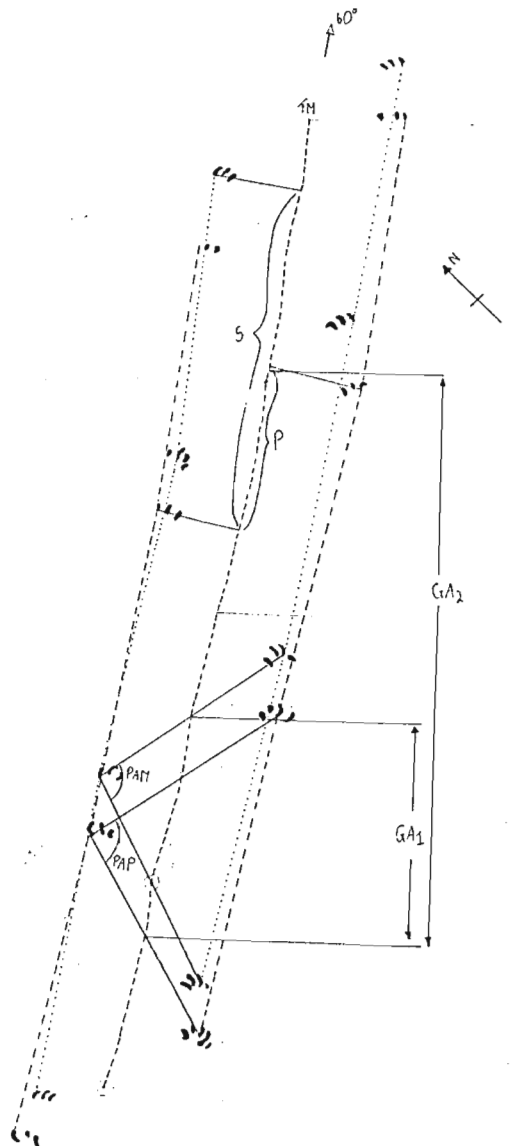
TP - Pes trackway width

Excavation 1
Surface 1 - Trackway 1

SLP	SLM	SRP	SRM	PAP	PAM	P	GA1	GA2	TS	TMM	TP
79	73	76	79	90	98	39	53	131	35	34	37
64	78	80	80	93	97	41	53	116	36	34	37
	68			93	94	38	46		37	36	38
				91	97	38			38	36	39
				71	82	41			38	35	40
				72	77	40			38	36	43
						39			38	33	44
						40			39	39	44
						25			40		
						28			42		
									43		

All readings in cm except for pace angulation

PAP	PP	TP	PAM	PM	TMM
71°	39	43	77°	28	39
72°	26	44	82°	40	36
90°		36	94°	38	35
91°	41	40	97°	40	34
93°	39	36	97°	41	35
93°	38	38	98°		33
Average pace	36.6cm			37.4cm	

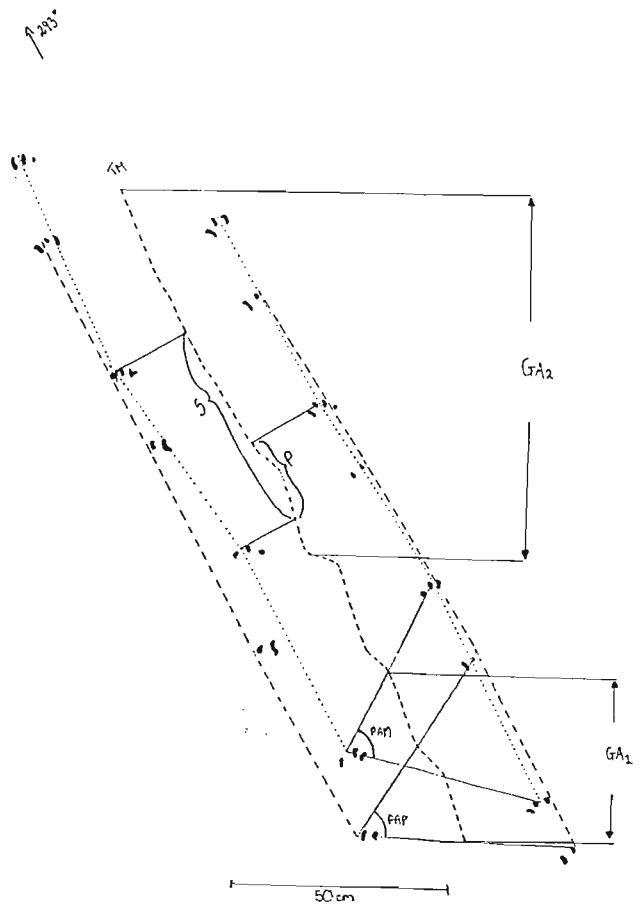


Excavation 1
Surface 1 - Trackway 2

SLP	SLM	SRP	SRM	PAP	PAM	P	GA1	GA2	TS	TMM	TP
51	54	50	56	60	77	31	44	95	43	36	45
54	51	48	49	57	72	26	45	95	44	36	46
53			51	60	73	26	43		38	34	44
				63	69	25			38	35	43
				59	65	27			44	38	41
				66	73	26			44	38	
						21			36		
						27			43		
						30			36		
						19			41		
						21			38		
						34			40		
									39		

All readings in cm except for pace angulation

PAP	PP	TP	PAM	PM	TMM
57°	26	26	65°	30	22
59°	30	24	69°	21	19
60°	25	25	72°	26	20
60°		25	73°	27	19
63°	26	24	73°	21	21
66°	19	23	77°	31	20
Average pace	25.2cm			26cm	

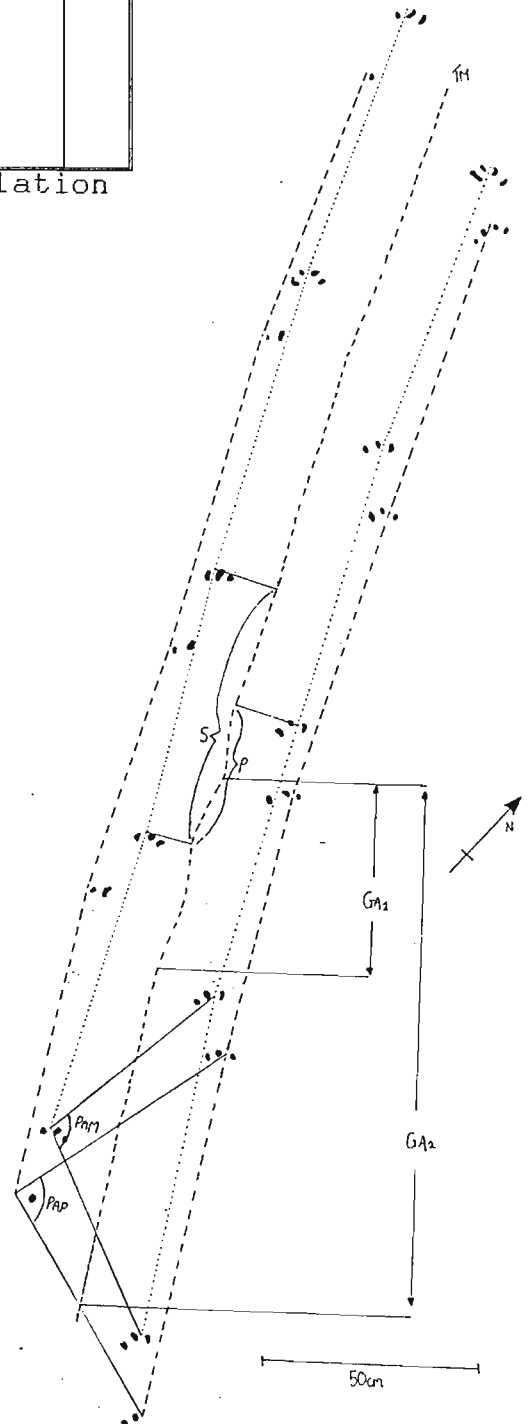


Excavation 1
Surface 1 - Trackway 3

SLP	SLM	SRP	SRM	PAP	PAM	P	GA1	GA2	TS	TMM	TP
75	73	65	81	94	105	41	59	128	36	30	41
60	65	71	68	85	107	43	48	114	36	28	41
75	71	71	69	76	102	40	51	123	35	28	40
64				76	98	31	51		34	30	39
				82	98	34			35	30	41
				85	102	34			31	31	41
				80	95	34			35		
				75	90	28			35		
						26			35		
						44			36		
						39					
						30					
						34					
						41					
						36					

All readings in cm except for pace angulation

PAP	PP	TP	PAM	PM	TM
75°	41	40	90°	36	31
76°	34	39	95°	34	31
76°	31	41	98°	34	28
80°	30	41	98°	28	29
82°	26	39	102°	41	29
85°	44	40	102°	34	26
85°	43	40	105°	40	31
			107°	39	28
Average pace	35.6cm			35.8cm	

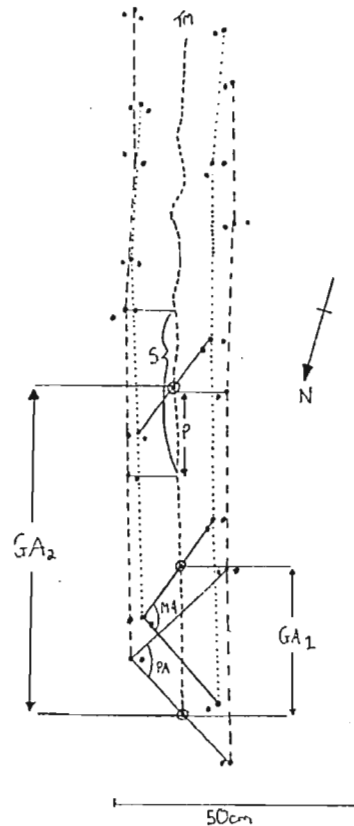


Excavation 1
Surface 2 - Trackway 1

SLP	SLM	SRP	SRM	PAP	PAM	P	GA1	GA2	TS	TMM	TP
37	38	40	37	86	101	15	29	66	18	15	21
34	36	36	37	83	103	13	28	64	20	15	21
31	31	35	35	78	103	18	29		18	16	21
35		29	28	78	98	18	25		19	17	21
				73	95	18			19	16	21
				71	89	20			20		
				72	80	18			18		
						11			18		
						19			18		
						16			18		
						19			18		
						18			18		
						21					
						18					

All readings in cm except for pace angulation

PAP	PP	TP	PAM	PM	TMM
71°	13	21	80°	11	15
72°	15	20	89°	21	15
73°	18	21	95°	18	16
78°	16	21	98°	19	16
78°	18	21	101°	18	15
83°	19	20	103°	18	15
86°	18	20	103°	20	15
Average pace	16.7cm			17.9cm	

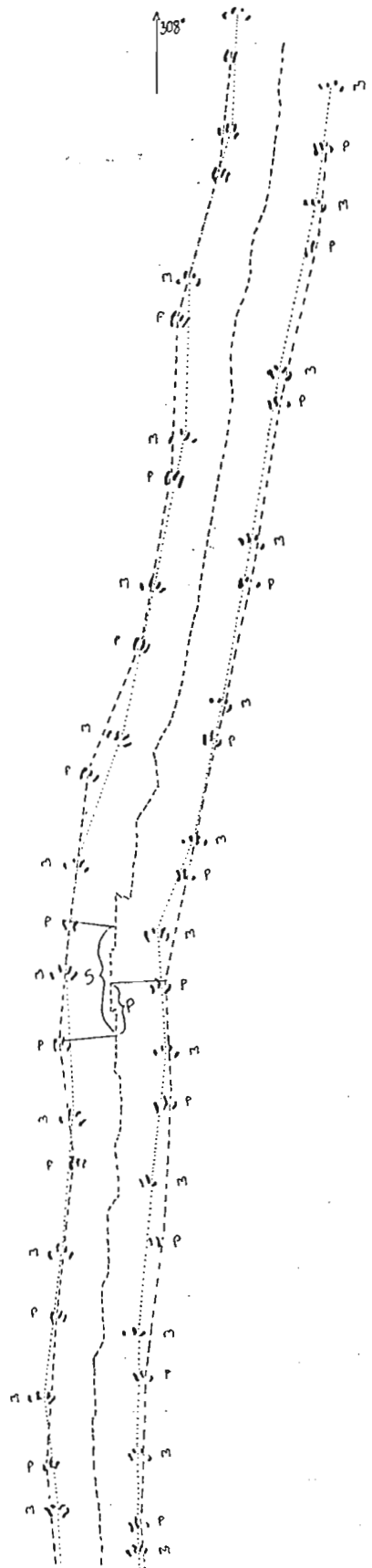
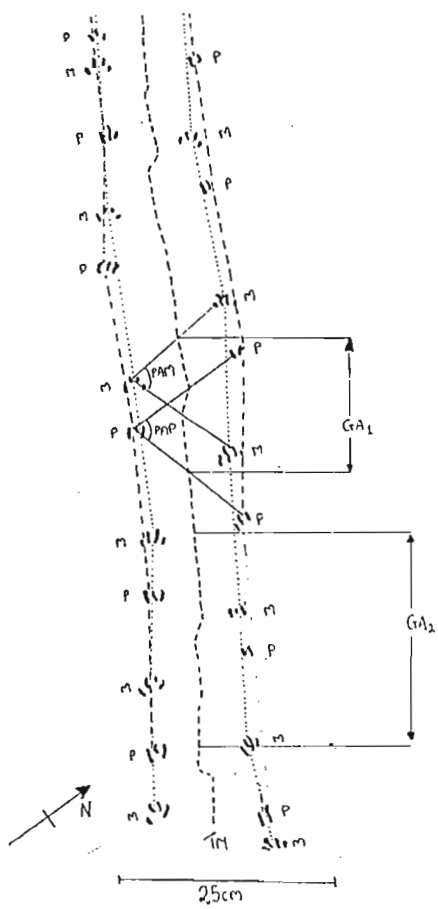


Excavation 1
Surface 3 - Trackway 1

SLP	SLM	SRP	SRM	PAP	PAM	P		GA1	GA2	TS	TMM	TP
19	16	13	16	72	53	8	9	15	33	13	11	13
20	17	16	19	75	67	11	8	15	34	12	10	12
20	19	20	18	70	70	8	9	16	35	11	11	14
15	20	18	19	76	78	9	10	16	34	11	11	14
13	18	15	19	74	88	11	9	16	29	11	11	12
17	15	13	13	66	83	9	8	16	31	11	11	12
19	15	19	16	68	78	11	11	17	36	12	13	13
20	18	18	20	62	74	8	8	17	34	13	11	13
16	18	18	17	66	75	8	9	16	33	13	12	13
14	18	15	14	55	79	8	9	16	29	12	11	14
20	21	16	15	57	86	4	6	13	31	13	12	15
16	19	18	17	74	70	8	7	14	34	11	13	13
23	21	21	21	73	85	9	8	16	38	11		14
21	16	20	22	76	62	11	8	16	37	13		15
18	19	21	22	69	64	7	10	15	32	12		
16	13	11	15	78	82	10	9	13		11		
				72	84	9	8			13		
				58	77	8	9			13		
				60	76	8	10			13		
				61	71	7	5			14		
				54	62	7	8			13		
				68	63	9	6			12		
				60	53	11	10			12		
				65	64	7	8			13		
				80	73	10	13			12		
				79	77	10	8			13		
				85	82	11	13			14		
				73	81	11	9					
				66	90	10	11					
				63	76	11	11					
				50	74	6	7					
				56	70	6	8					
					64	10						
					60	7						

All readings in cm except for pace angulation

PAP			PP			TP			PAM			PM			TMM		
50°	65°	73°	6	7	11	14	14	13	53°	70°	78°	6	7	9	13	13	10
54°	66°	74°	7	9	8	14	14	12	53°	71°	79°	7	10	9	13	12	10
55°	66°	74°	8	10	11	11	16	13	62°	73°	81°	5	8	13	12	12	11
56°	66°	75°	6	8	11	13	12	12	62°	74°	82°	8	11	8	11	12	11
57°	68°	76°	4	11	9	11	14	12	63°	74°	82°	8	11	10	11	14	11
58°	68°	76°	8	9	11	13	14	12	64°	75°	83°	8	8	9	12	11	10
60°	69°	78°	8	7	10	14	13	13	64°	76°	84°	10	11	9	13	12	11
60°	70°	79°	11	8	10	15	12	13	64°	76°	85°	8	9	7	12	11	11
61°	72°	80°	7	8	10	13	13	12	67°	77°	86°	9	8	9	11	11	10
62°	72°	85°	8	9	11	13	12	13	70°	77°	88°	6	13	10	10	12	9
63°	73°		11	9		15	13		70°	78°	90°	8	8	9	11	11	11
Average pace			8.8cm									8.8cm					

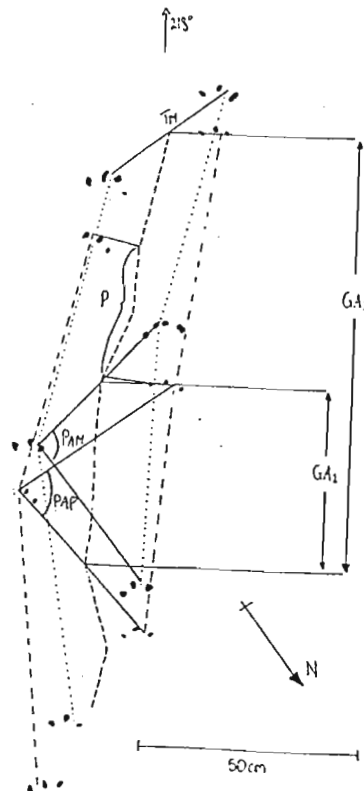


Excavation 1
Surface 3 - Trackway 2

SLP	SLM	SRP	SRM	PAP	PAM	P	GA1	GA2	TS	TMM	TP
64	66	60	63	103	114	29	43	104	29	20	29
		63		83	98	31	44		24	24	31
				97	117	33			30	25	31
				101	108	31			28	24	28
						29			28	21	26
						35			30	20	
						32			25	20	
									28		
									21		
									26		
									24		

All readings in cm except for pace angulation

PAP	PP	TP	PAM	PM	TMM
83°	29	33	98°	29	26
97°	31	29	108°	32	20
101°	33	25	114°		20
103°		28	117°	35	20
Average pace	31cm			32cm	

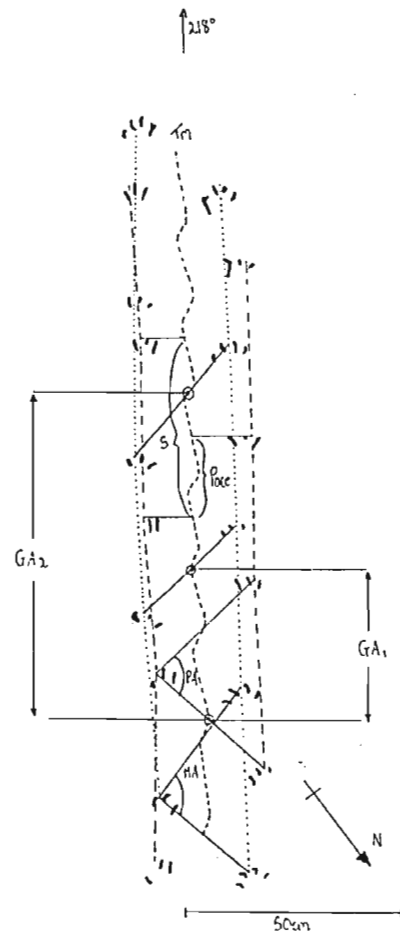


Excavation 1
Surface 3 - Trackway 3

SLP	SLM	SRP	SRM	PAP	PAM	P	GA1	GA2	TS	TMM	TP
38	43	44	39	66	76	24	36	76	23	23	25
43	37	35	44	69	78	19	36	73	21	23	24
36	37	41	40	72	79	20	34		21	21	25
41	40		36	77	81	17			22	23	26
				78	84	26			21	24	26
				80	90	11			21	21	26
				84	91	25			26	20	26
					91	23			26	20	
						23			28		
						16			28		
						19			26		
						24			26		
						18			20		
						18					

All readings in cm except for pace angulation

PAP	PP	TP	PAM	PM	TMM
66°	16	26	76°	26	23
69°	19	26	78°	18	23
72°	20	25	79°	11	21
77°	24	26	81°	18	23
78°	19	26	84°	18	24
80°		25	90°	25	21
84°	24	24	91°	23	20
			91°		20
Average pace	20.3cm			19.9cm	

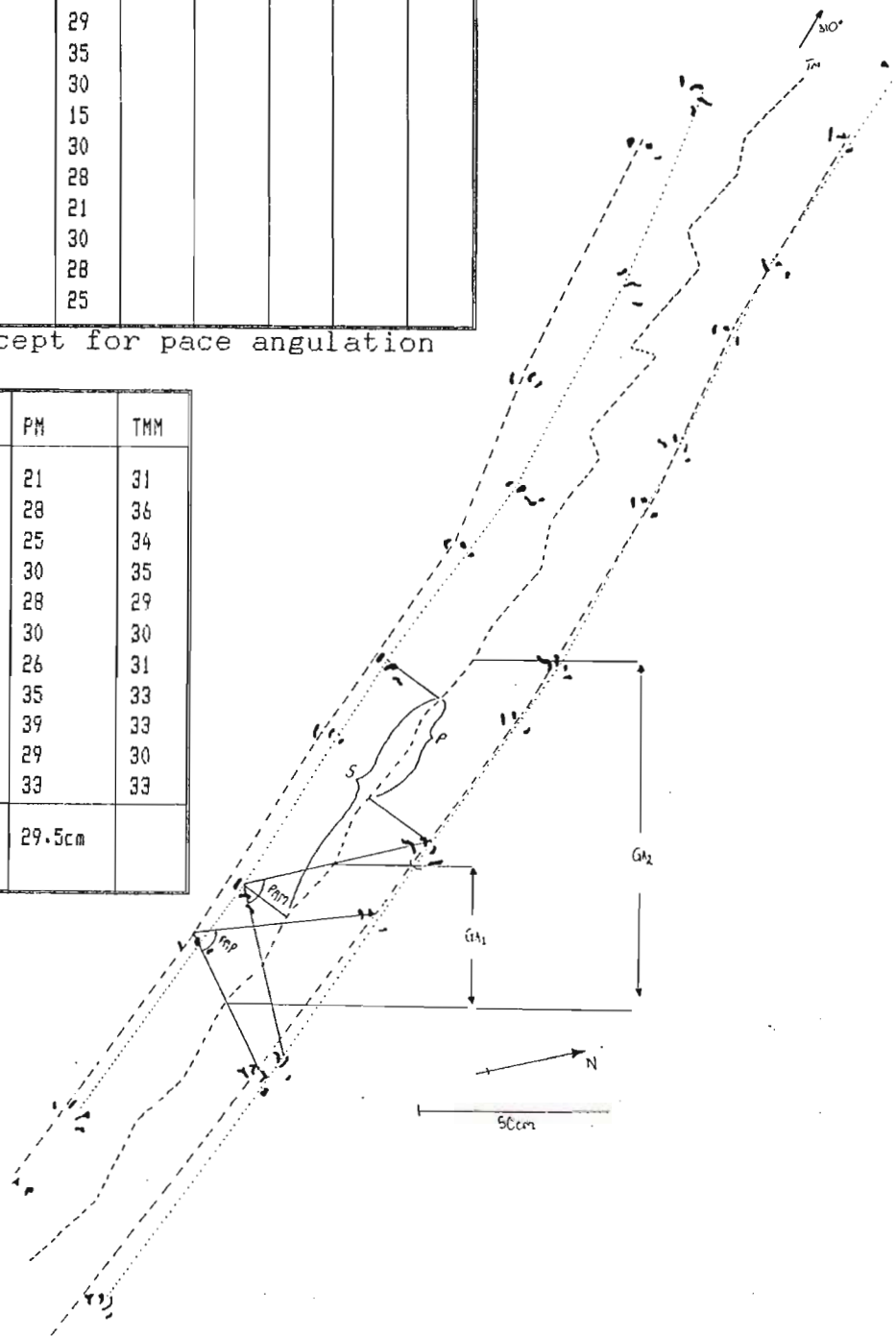


Excavation 1
Surface 4 - Trackway 1

SLP	SLM	SRP	SRM	PAP	PAM	P	GA1	GA2	TS	TMM	TP
71	66	85	73	104	96	33	56	121	35	33	31
63	65	46	63	88	90	55	43	103	29	33	33
53	54	60	55	70	90	39	49	106	35	33	36
49	59	61	61	83	90	16	49	103	30	34	36
60	49	48	49	78	78	26	49	100	36	30	40
		54	56	73	77	30	46		33	30	41
				82	91	35			38	30	41
				59	86	31			33		
				60	79	30			39		
				74	72	28			30		
				67	76	25			35		
						25					
						29					
						35					
						30					
						15					
						30					
						28					
						21					
						30					
						28					
						25					

All readings in cm except for pace angulation

PAP	PP	TP	PAM	PM	TMM
59°	35	41	72°	21	31
60°	15	41	76°	28	36
67°	30	41	77°	25	34
70°	16	33	78°	30	35
73°	28	38	79°	28	29
74°	30	40	85°	30	30
78°	31	36	90°	26	31
82°	25	38	90°	35	33
83°	30	35	90°	39	33
88°	55	31	91°	29	30
104°		31	96°	33	33
Average pace	29.5cm			29.5cm	

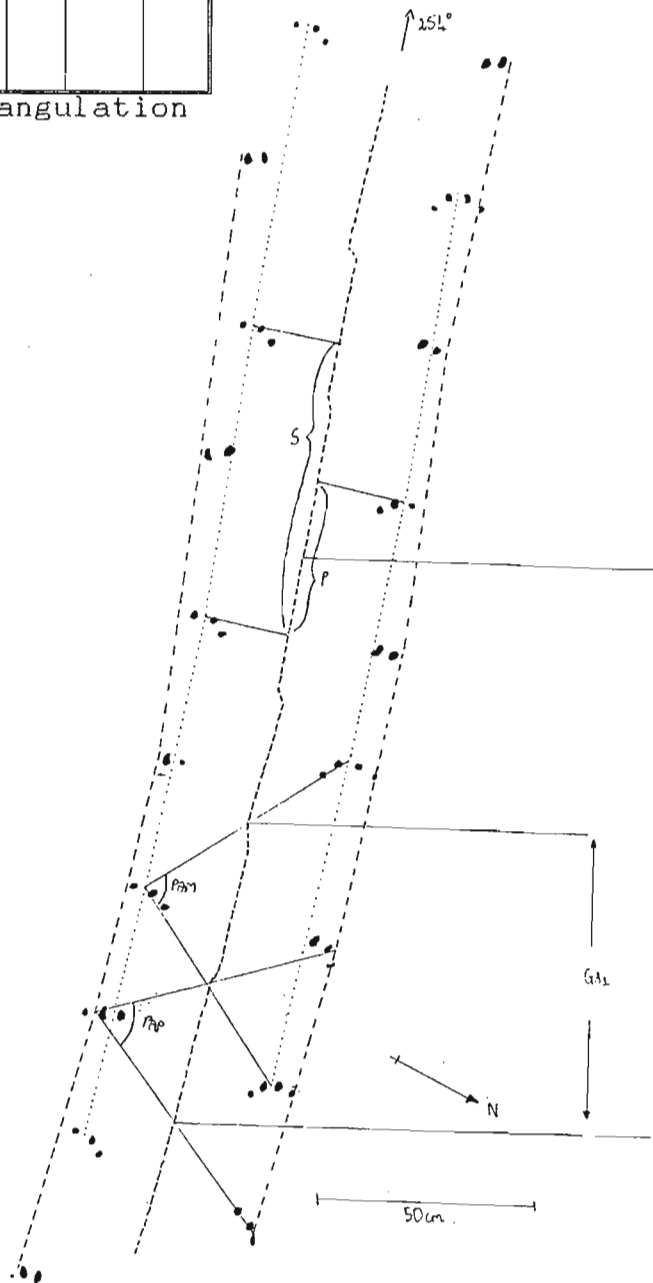


Excavation 1
Surface 5 - Trackway 1

SLP	SLM	SRP	SRM	PAP	PAM	P	GA1	GA2	TS	TMM	TP
51	58	69	78	63	72	19	71	135	45	39	50
64	66	70	63	69	90	29	70	140	44	39	50
73	69	71	70	64	77	38	70		47	40	51
70				72	75	35			44	40	53
				68	78	40			47	41	54
				69	81	35			48	42	54
				66	80	26			46	42	57
				61		36			51		
						38			48		
						33			44		
						34					
						39					
						36					
						44					

All readings in cm except for pace angulation

PAP	PP	TP	PAM	PM	TMM
61°	36	56	72°	19	39
63°		50	75°	26	40
64°	29	50	77°	40	40
66°	34	54	78°	36	41
68°	35	53	80°	38	41
69°	38	54	81°	33	41
69°	39	49	90°	44	39
72°	35	50			
Average pace	35.1cm			33.7cm	

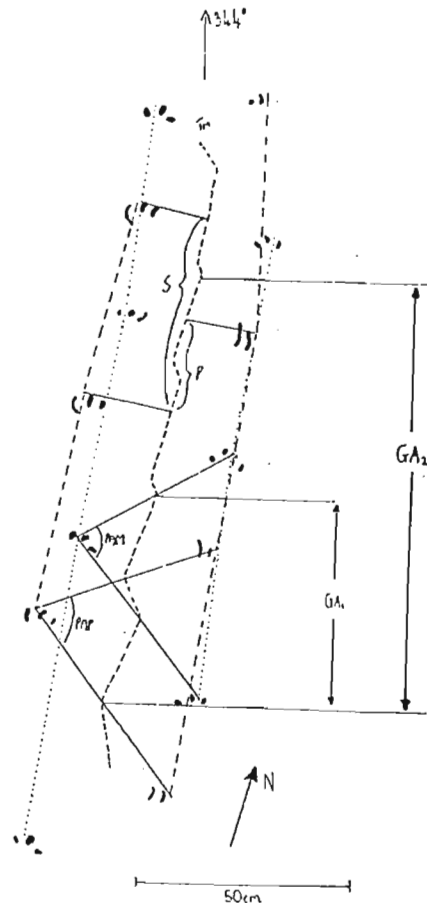


Excavation 1
Surface 5 - Trackway 2

SLP	SLM	SRP	SRM	PAP	PAM	P	GA1	GA2	TS	TMM	TP	
52	56	51	60	72	91	36	49	103	32	34	39	
46			52	68	82	24	48		32	33	38	
					70	83	29			32	32	37
					69	80	23			40	31	36
					88	74	24			38	30	33
							34			33		
							27			32		
							29			37		
							23			31		
										36		
										30		
										34		
							28					

All readings in cm except for pace angulation

PAP	PP	TP	PAM	PM	TMM
68°	23	35	75°	23	31
68°	24	38	80°	29	30
70°	29	36	82°	34	33
72°	36	39	82°	27	31
88°	24	30	83°		34
			91°		
Average pace	27.2cm			28.3cm	

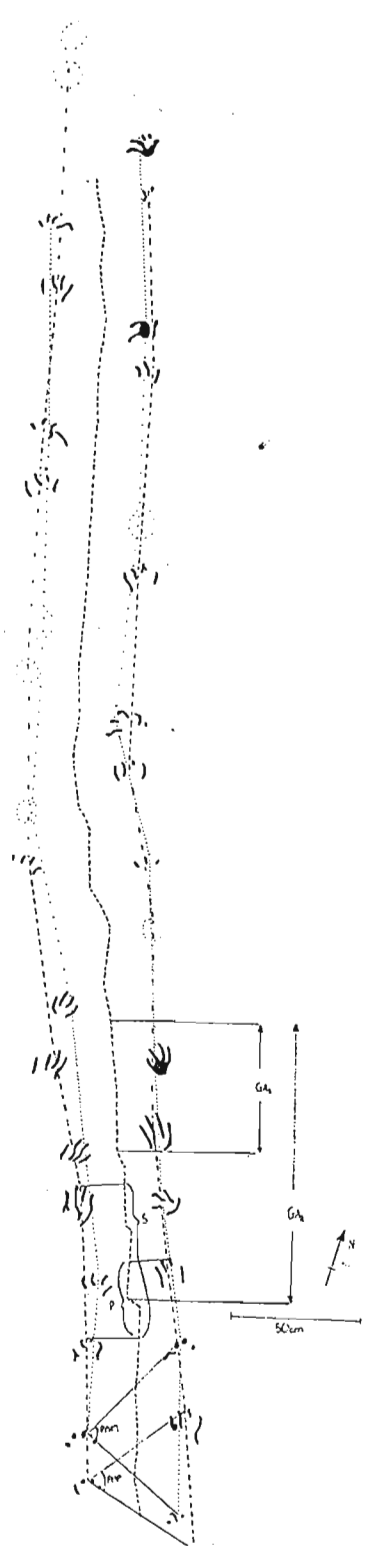


Excavation 1
Surface 5 - Trackway 3

SLP	SLM	SRP	SRM	PAP	PAM	P	GA1	GA2	TS	TMM	TP
56	61	59	66	69	87	26	50	111	36	35	40
60	53	56	56	72	84	29	56	109	36	34	36
56	59	79	58	81	91	29	50	118	38	30	34
78	80	66	75	84	84	30	66	133	38	29	31
79			54	84	86	25	50	125	29	30	35
				77	85	34	56	134	34	31	43
				86	91	44	58	133	33	33	46
				87	91	34	55		28	43	41
				86	87	30			35	40	41
						25			29	40	41
						31			41	31	36
						21			35	34	35
						35			48	38	
						23			40	38	
						40			41	38	
						40			38		
									36		
									36		
									39		
									38		
									39		
									38		
									41		
									40		
									33		

All readings in cm except for pace angulation

PAP	PP	TP	PAM	PM	TMM
69°		40	84°	30	34
72°	26	39	84°	31	28
77°	25	34	85°	35	31
81°	29	35	86°	21	29
84°	29	33	87°	40	36
84°	30	31	87°		36
86°	34	41	91°	23	33
86°	34	36	91°	25	29
87°	44	40	91°	40	38
Average pace	31.4cm			30.6cm	

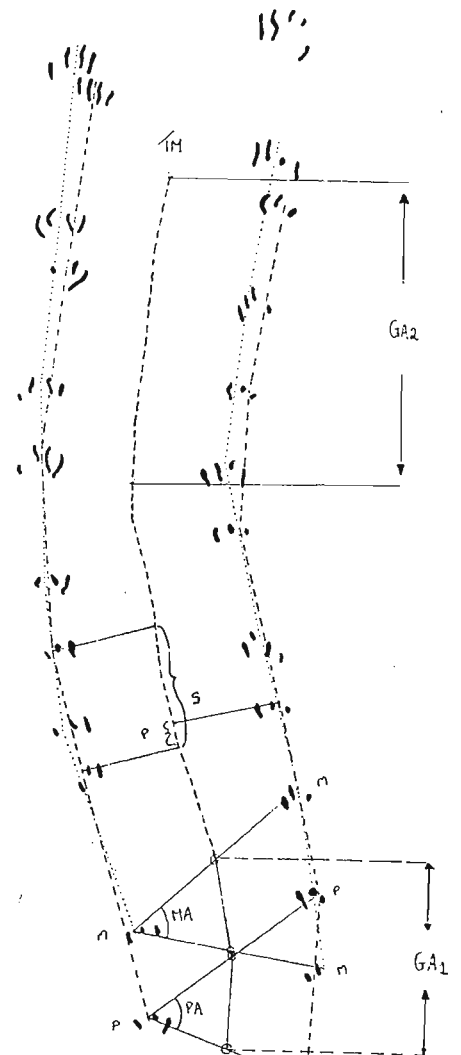


Excavation 1
Surface 6 - Trackway 1

SLP	SLM	SRP	SRM	PAP	PAM	P	GA1	GA2	TS	TMM	TP
58	51	44	43	57	51	25	44	88	44	49	48
30	35	47	38	62	57	34	39	76	44	49	47
48	48	43	38	47	41	6	36	80	44	46	48
43	38	34	40	32	41	23	35	73	44	46	48
43	40	33	41	46	47	19	34		44	46	48
				54	56	24			45	46	48
				40	47	20			48	45	49
				53	45	23			48	50	49
				50	40	23			48	49	44
				46	43	15			49		
						23			49		
						28			49		
						10			49		
						20			47		
						26			51		
						19			51		
						25			50		
						11					

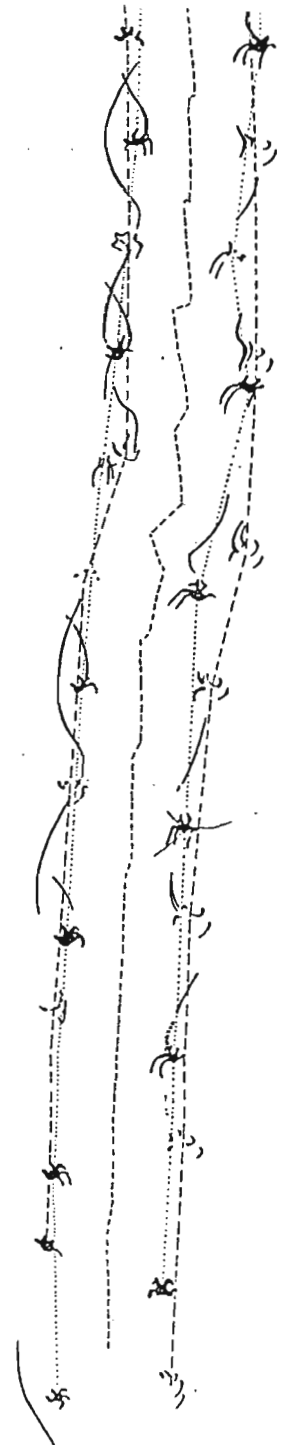
All readings in cm except for pace angulation.

PAP	PP	TP	PAM	PM	TMM
32°	6	49	40°	11	46
40°	24	48	41°	10	49
46°	23	48	41°	28	50
46°	23	49	43°		49
47°	34	49	45°	25	46
50°	23	48	47°	19	45
53°	20	46	47°	20	48
54°	19	45	51°	15	43
57°		38	56°	26	43
62°	25	46	57°	23	46
Average pace	21.9cm			19.7cm	



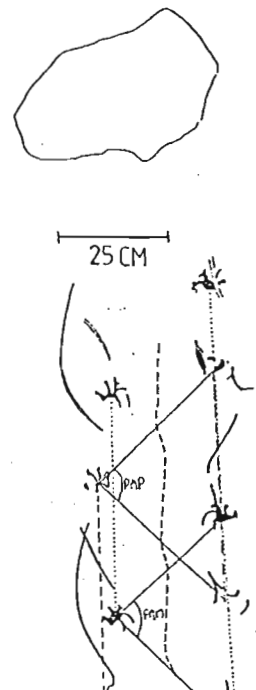
Excavation 2
Surface 5 - Trackway 1

SLP	SLM	SRP	SRM	PAP	PAM	P	GA1	GA2	TS	TMM	TP
54	51	53	56	87	87	24	48	103	30	26	29
53	56	54	55	87	92	26	46	104	29	28	29
51	59	54	56	85	95	29	46	103	25	26	30
30	51	33	49	83	95	26	48	103	29	25	31
48	28	44	29	82	92	26	46	101	25	28	30
48	49	48	50	82	92	25	50	89	24	31	31
50	46	48	49	83	91	29	51	78	26	26	34
				77	98	29	50	84	28	26	34
				51	93	28	49	94	29	26	29
				50	90	24	46	96	28	26	29
				70	80	28	45	95	29	26	29
				78	44	29	48	96	26	25	30
				80	53	33	48		33	24	
				79	89	26	50		34		
				81	90	24	48		26		
				80	78	25	49		25		
				77	83	28			28		
					86	8			31		
						23			25		
						21			21		
						21					
						8					
						26					
						23					
						28					
						23					
						26					
						24					
						23					
						21					
						29					
						26					



All readings in cm except for pace angulation

PAP		PP		TP		PAM		PM		TMM	
50°	82°	8	29	34	31	44°	92°	23	26	33	26
51°	83°	25	25	35	31	53°	92°	8	26	31	26
70°	83°	21	29	29	30	78°	92°	23	24	28	25
77°	85°	26		31	30	80°	93°	28	33	29	26
77°	87°	29	26	30	28	83°	95°	26		28	25
78°	87°	21		30	29	86°	95°	26	29	26	24
79°		21		30		87°	98°		28	26	26
80°		26		30		89°		23		25	
80°		21		29		90°		24		25	
81°		28		29		90°		24		25	
82°		24		30		91°		28		26	
Average pace		23.9cm						25.1cm			

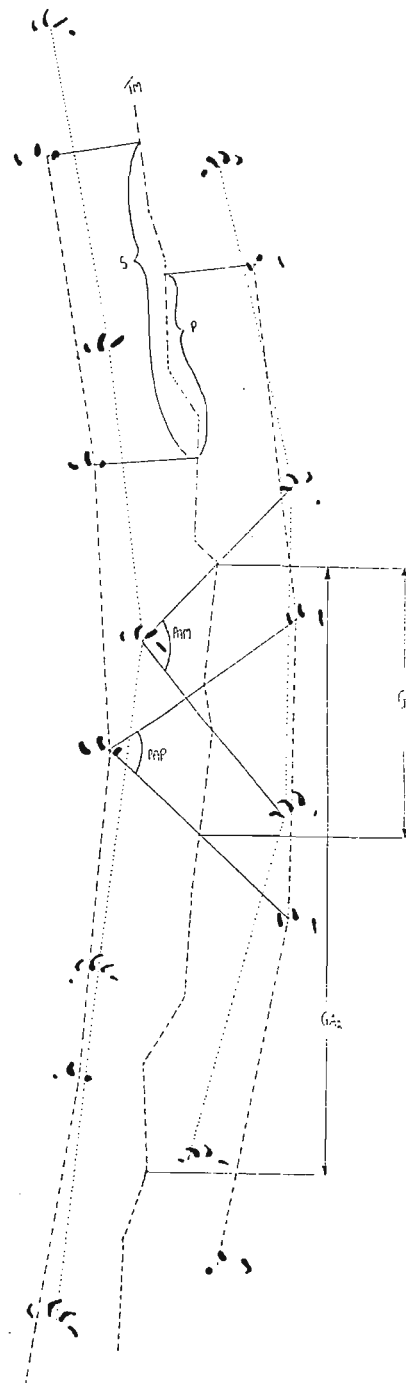


Excavation 2
Surface 6 - Trackway 1

SLP	SLM	SRP	SRM	PAP	PAM	P	GA1	GA2	TS	TMM	TP
111	112	115	118	90	103	56	94	206	51	40	56
99	113	94	101	79	96	51	91	200	56	49	59
105	101	112	100	87	94	55	89	191	58	52	64
				93	114	65	89	190	53	51	61
				80	91	63	86	193	51	53	64
				72	82	47	93		51	48	61
				79	96	48			43		62
						46			51		
						54			58		
						51			60		
						48			65		
						61			60		
						51			56		
						44					

All readings in cm except for pace angulation

PAP	PP	TP	PAM	PM	TMM
72°	46	64	82°	54	55
79°	47	61	91°	65	55
79°	61	63	94°	48	50
80°	63	64	96°	51	48
87°	51	61	96°	48	49
90°	51	58	103°	55	46
			114°	56	36
Average pace	53.2cm			53.9cm	



Acknowledgements

I would like to thank Mr. and Mrs. Green for allowing me to carry out field work on their farm.

I would also like to thank Prof. T. Mason for initiating this project and for providing funding to carry out the work. Thanks also to Prof. M.K. Watkeys and Dr. R. Smith for editing my thesis and showing the path to brevity.

A special thanks goes to Les Nutting who chauffeured me to, and accompanied me on, all the field trips, and who also virtually dug the Fossil dam single handedly.

Thanks to Prof. Raubenheimer for the analysis on the mammal-like reptile tusks.

References

- Alexander, R.McN. (1976). Estimates of speeds of dinosaurs. *Nature*, **261**, 129-130.
- Allen and Collinson (1978). Lakes. 60. In: Reading, H.G., Ed., *Sedimentary Environments and Facies*. Blackwell Scientific Publications, Oxford. 557pp.
- Anderson, J.M. and Anderson, H.M. (1985). *Palaeoflora of southern Africa - Prodrum of South African Megaflores, Devonian to lower Cretaceous*. AA Balkema, Rotterdam. 423pp.
- Botha, B.J.V. and Linstrom, W. (1978). A note on the stratigraphy of the Beaufort Group in north-western Natal. *Trans.geol.Soc.S.Afr.*, **81**, 35-40.
- Bromley, R. and Asgaard, U. (1979). Triassic freshwater ichnocoenoses from Carlsberg Fjord, East Greenland. *Palaeogeog., Palaeoclimatol., Palaeoecol.*, **28**, 39-80.
- Chesnut, D.R., Baird, D., Smith, J.H. and Lewis, Sr., R.Q. (1994). Reptile trackway from the Lee Formation (Lower Pennsylvanian) of South-Central Kentucky. *J.Palaeont.*, **68**(1), 154-158.
- Claoue-Long, J.C. *et al.* (1991). The age of the Permian-Triassic boundary. *Earth.Plane.Sci.Lett.*, **105**, 182-190.
- Collinson, J.D. (1978). Alluvial sediments. 15-60. In: Reading, H.G., Ed., *Sedimentary Environments and Facies*. Blackwell Scientific Publications, Oxford. 557pp.
- Erwin, D.H. (1994). The Permo-Triassic extinction. *Nature*, **367**, 231-235.
- Erwin, D.H. and Vogel, T.A. (1992). Testing for causal relationships between large pyroclastic volcanic eruptions and mass extinctions. *Geophy.Res.Lett.*, **19**, 893-896.

- Frey, R.W. and Pemberton, S.G. (1979). Trace fossil facies models. *In: Walker, R.G., Ed., Facies Models. Geosci.Can.Report.Series 1, 211pp.*
- Halstead, L.B. (1974). *Vertebrate Hard Tissues*. Wykeham Publications (London) Ltd, 179pp.
- Hiller, N. and Stavrakis, N. (1984). Permo-Triassic fluvial systems in the south eastern Karoo Basin, South Africa. *Palaeogeog., Palaeoclim., Palaeoecol.*, **45**, 1-21.
- Hobday, D.K. (1978). Fluvial Deposits of the Ecca and Beaufort Groups in the eastern Karoo Basin, southern Africa. 413-430. *In: Miall, A.D., Ed., Fluvial Sedimentology. Canadian Society of Petroleum Geologists, Calgary, Alberta, Canada. 859pp.*
- Hotton, N. (1986). Dicynodonts and their role as primary consumers. 71-82. *In: Hotton, N., Maclean, P.D., Roth, J.J. and Roth, E.C., Eds., The Ecology and Biology of Mammal-Like Reptiles. Smithsonian Institution Press, Washington and London, 325pp.*
- Kemp, T.S. (1982). *Mammal-like reptiles and the origin of mammals*. Academic Press.
- King, G. (1991). *The Dicynodonts - a study in palaeobiology*. Chapman and Hall, London, 227pp.
- Kovacs-Endrody, E. (1991). On the Late Permian age of Ecca *Glossopteris* floras in the Transvaal Province with a key to and description of 25 *Glossopteris* species. *Memoir of the Geological Survey*, **77**, 1-111.
- Lacey, W.S., van Dijk, D.E. and Gordon-Gray, K.D. (1975). Fossil plants from the Upper Permian in the Mooi River district of Natal, South Africa. *Ann.Natal Mus.*, **22**, 349-420.

- Le Roux, J.P. (1992). Palaeoenvironmental interpretation of tabular sandstones in the Beaufort Group of the Karoo Basin, South Africa. *S.Afr.J.Geol.*,**95**,171-180.
- Lockley, M. (1991). *Tracking dinosaurs*. Cambridge University Press, 238pp.
- MacRae, C.S. (1990). Fossil vertebrate tracks near Murraysburg, Cape Province. *Palaeont.afr.*,**27**,83-88.
- Maxwell, W.D. (1992). Permian and Early Triassic extinction of non-marine tetrapods. *Palaeontology*,**35**,571-583.
- Miall, A.D. (1977). A review of the braided river depositional environment. *Earth Sci.Rev.*,**13**, 1-62.
- Miall, A.D. (1984). *Principles of Sedimentary Basin Analysis*. Springer-Verlag New York, 490pp.
- Osborne, J.W. (Ed). *Dental anatomy and embryology*. Blackwell Scientific Publications, Oxford, 447pp.
- Picard, M.D. and High, Jr., L.R., (1979). Lacustrine stratigraphic relations.1-21. In: Anderson, A.M. and van Biljon, W.J., Eds., *Some sedimentary basins and associated ore deposits of South Africa*. GeoKongres :Geol.Soc.S.Afr.Spec.Publ.**6**. 228pp
- Pitrat, C.W., (1973). Vertebrates and the Permo-Triassic extinction. *Palaeogeog.,Palaeoclimatol.,Palaeoecol.*,**14**,249-264.
- Rayner, R.J. (1992). *Phyllotheca*: The pastures of the Late Permian. *Palaeogeogr., Palaeoclimatol.,Palaeoecol.*,**92**, 31-40.

- Riek, E.F. (1973). Fossil insects from the Upper Permian of Natal, South Africa. *Ann.Natal Mus.*,**21**, 513-532.
- Rubidge, B.R. (1995). Biostratigraphy of the *Eodicynodon* Assemblage Zone. In: B.R. Rubidge (Editor), *Biostratigraphy of the Beaufort Group (Karoo Supergroup)*, *South Africa*. S.Afr.Comm.Strat.
- Sarjeant W.A.S. (1975). Fossil tracks and impressions of vertebrates. 283-324. In: Frey. R.W., Ed., *The study of trace fossils*. Springer-Verlag, Berlin, 562pp.
- Simpson S. (1975). Classification of trace fossils. 39-54. In: Frey. R.W., Ed., *The study of trace fossils*. Springer- Verlag, Berlin, 562pp.
- Smith, R.M.H. (1980). The lithology, sedimentology and taphonomy of flood plain deposits of the Lower Beaufort (Adelaide Subgroup) strata near Beaufort West. *Trans.geol.Soc.S.Afr.*,**83**, 399-413.
- Smith, R.M.H. (1990b). Alluvial paleosols and pedofacies sequences in the Permian lower Beaufort of the southern Karoo Basin, South Africa. *J.Sed.Pet.*,**60**, 258-276.
- Smith, R.M.H. (1990a). A review of stratigraphy and sedimentary environments of the Karoo Basin of South Africa. *J.Afr.Earth Sci.*,**10**, 117-137.
- Smith, R.M.H. (1993a). Sedimentology and ichnology of floodplain palaeosurfaces in the Beaufort Group (Late Permian), Karoo Sequence, South Africa. *Palaios.*,**8**,339- 357.
- Smith, R.M.H. (1993b). Vertebrate taphonomy of Late Permian floodplain deposits in the southwestern Karoo Basin of South Africa. *Palaios.*,**8**,45-67.

- Smith, R.M.H., Eriksson, P.G., and Botha, W.J. (1993). A review of the stratigraphy and sedimentary environments of the Karoo-aged basins of southern Africa. *J.Afr.Earth Sci.*, **16**, 143-169.
- Smith, R.M.H. (1995). Changing fluvial environments across the Permian-Triassic boundary in the Karoo Basin, South Africa and possible causes of tetrapod extinctions. *Palaeogeog., Palaeoclimat., Palaeoecol.*, **117**, 81-104.
- The South African Committee for Stratigraphy (SACS). (1980). Stratigraphy of South Africa. Part 1. Comp.L.E. Kent. Lithostratigraphy of the Republic of South Africa, South West Africa/Namibia and the Republics of Bophuthatswana, Transkei and Venda. *Handb.geol.surv.S.Afr.*, **8**, 690pp.
- Stear, W.M. (1978). Sedimentary structures related to fluctuating hydrodynamic conditions in flood plain deposits of the Beaufort Group near Beaufort West, Cape. *Trans. geol. Soc. S. Afr.*, **81**, 393-399.
- Stear, W.M. (1980). Channel sandstone and bar morphology of the Beaufort Group Uranium District near Beaufort West. *Trans.geol.Soc.S.Afr.*, **83**, 391-398.
- Tucker, M.E. and Benton, M.J. (1982). Triassic environments, climates and reptile evolution. *Palaeogeog., Palaeoclimatol., Palaeoecol.*, **40**, 361-379.
- Turner, B.R. (1981). Possible origin of low angle cross-strata and horizontal lamination in Beaufort Group sandstones of the southern Karoo Basin. *Trans.geol.Soc.S.Afr.*, **84**, 193-197.
- Turner, B.R. (1986). Tectonic and climatic controls on continental depositional facies in the Karoo Basin of northern Natal, South Africa. *Sed. Geol.*, **46**, 231-257.

- Turner, B.R. (1993). Palaeosols in Permo-Triassic continental sediments from Prydz Bay, East Antarctica. *Sed.Pet.*, **63**, 694-706.
- Visser, J.N.J. and Dukas, B.A. (1979). Upward-fining fluvial megacycles in the Beaufort Group, north of Graaf-Reinet, Cape Province. *Trans.geol.Soc.S.Afr.*, **82**, 149-154.
- Wang, K., Geldsetzer, H.H.J., and Krouse, H.R., (1994). Permian-Triassic extinction: Organic C¹³ evidence from British Columbia, Canada. *Geology*, **22**, 580-584.
- Wignall, P. (1992). The day the world nearly died. *New Sci.*, **25**, 51-55.
- Wignall, P.B. and Hallam, A. (1992). Anoxia as a cause of the Permian/Triassic mass extinction: facies evidence from northern Italy and the western United States. *Palaeogeog., Palaeoclimatol., Palaeoecol.*, **93**, 21-46.
- Wignall, P.B. and Hallam, A. (1993). Griesbachian (Earliest Triassic) palaeoenvironmental changes in the Salt Range, Pakistan and southeast China and their bearing on the Permo-Triassic mass extinction. *Palaeogeog., Palaeoclimatol., Palaeoecol.*, **102**, 215-237.
- Yemane, K. and Kelts, K. (1990). A short review of palaeoenvironments for Lower Beaufort (Upper Permian) Karoo sequences from southern to central Africa : A major Gondwana lacustrine episode. *J.Afr.Earth Sci.*, **10**, 169-185.
- Yemane, K., Siegenthaler, C., and Kelts, K. (1989). Lacustrine environments during Lower Beaufort (Upper Permian) Gondwana deposition, northern Malawi. *Palaeogeog., Palaeoclimatol., Palaeoecol.*, **70**, 165-178.
- Zhou, L. and Kyte, F.T. (1988). The Permian-Triassic boundary event: a geochemical study of three Chinese sections. *Earth Plan.Sci.Lett.*, **90**, 411-421.